

DESIGN AND MODELING ELASTOMERIC VIBRATION ISOLATORS USING FINITE ELEMENT
METHOD

A THESIS SUBMITTED TO
THE GRADUATE SCHOOL OF NATURAL AND APPLIED SCIENCES
OF
MIDDLE EAST TECHNICAL UNIVERSITY

BY

HALİL ARDIÇ

IN PARTIAL FULFILLMENT OF THE REQUIREMENTS
FOR
THE DEGREE OF MASTER OF SCIENCE
IN
MECHANICAL ENGINEERING

FEBRUARY 2013

Approval of the thesis:

DESIGN AND MODELING ELASTOMERIC VIBRATION ISOLATORS USING FINITE ELEMENT METHOD

submitted by **HALİL ARDIÇ** in partial fulfillment of the requirements for the degree of **Master of Science in Mechanical Engineering Department, Middle East Technical University** by,

Prof. Dr. Canan Özgen
Dean, Graduate School of **Natural and Applied Sciences**

Prof. Dr. Suha Oral
Head of Department, **Mechanical Engineering**

Asst. Prof. Dr. Gökhan O. Özgen
Supervisor, **Mechanical Engineering Dept., METU**

Sami Samet Özkan, M. Sc.
Co-Supervisor, **ROKETSAN A.Ş.**

Examining Committee Members:

Prof. Dr. Y. Samim Ünlüsoy
Mechanical Engineering Dept., METU

Asst. Prof. Dr. Gökhan O. Özgen
Mechanical Engineering Dept., METU

Prof. Dr. Y. Mehmet Çalışkan
Mechanical Engineering Dept., METU

Sami Samet Özkan, M. Sc.
Mechanical Engineer, ROKETSAN A.Ş.

Asst. Prof. Dr. Çağlar Başlamışlı
Mechanical Engineering Dept., Hacettepe University

Date: 01.02.2013

I hereby declare that all information in this document has been obtained and presented in accordance with academic rules and ethical conduct. I also declare that, as required by these rules and conduct, I have fully cited and referenced all material and results that are not original to this work.

Name, Last name: Halil Ardıç

Signature :

ABSTRACT

DESIGN AND MODELING ELASTOMERIC VIBRATION ISOLATORS USING FINITE ELEMENT METHOD

Ardıç, Halil

M.S., Department of Mechanical Engineering

Supervisor: Asst. Prof. Dr. Gökhan O. Özgen

Co-Supervisor: Sami Samet Özkan, M. Sc.

February 2013, 91 pages

In this thesis, a process is developed for designing elastomeric vibration isolators in order to provide vibration isolation for sensitive equipment being used in ROKETSAN A.Ş.'s products. For this purpose, first of all, similar isolators are examined in the market. After that, appropriate elastomeric materials are selected and their temperature and frequency dependent dynamic properties are experimentally obtained. Parametric finite element model of the isolator is then constituted in ANSYS APDL using the properties of elastomeric materials and the conceptual design of the isolator. Then, according to design requirements, final design parameters of the vibration isolator are determined at the end of design iterations. In the next step, vibration isolator that was designed is manufactured using the elastomeric material chosen, by a local rubber company. Finally, design process is verified by comparing analysis and test results.

Keywords: Vibration isolator, elastomeric isolator design, finite element analysis, ANSYS APDL, dynamic properties of elastomers

ÖZ

ELASTOMER TİTREŞİM TAKOZLARININ SONLU ELEMANLAR YÖNTEMİ KULLANILARAK TASARLANMASI VE MODELLENMESİ

Ardıç, Halil
Yüksek Lisans, Makina Mühendisliği Bölümü
Tez Yöneticisi: Y. Doç. Dr. Gökhan O. Özgen
Ortak Tez Yöneticisi: Yük. Müh. Sami Samet Özkan
Şubat 2013, 91 sayfa

Bu tez kapsamında, ROKETSAN A.Ş.'nin ürünlerinde kullanılan hassas donanımların titreşim yalıtımını sağlamak için kullanılacak elastomer titreşim takozlarının tasarımı için bir süreç geliştirilmiştir. Bu amaçla, ilk önce, piyasadaki benzer ticari takozlar incelenmiştir. Daha sonra, uygun elastomer malzemeler seçilmiş ve malzemelerin sıcaklık ve frekansa bağlı dinamik özellikleri testlerle elde edilmiştir. Elastomer malzemelerin özellikleri ve takozun kavramsal tasarımı kullanılarak, takozun parametrik sonlu elemanlar modeli ANSYS APDL'de oluşturulmuştur. Sonra, tasarım gereksinimlerine göre, tasarım iterasyonları sonrasında, titreşim takozunun nihai tasarımı belirlenmiştir. Bir sonraki aşamada, tasarlanan titreşim takozu, tasarım iterasyonu sonrasında belirlenen elastomer malzeme ile yerli bir kauçuk firmasında üretilmiştir. Son olarak analiz ve test sonuçları karşılaştırılarak tasarım süreci doğrulanmıştır.

Anahtar Kelimeler: Titreşim takozları, Elastomer takoz tasarımı, sonlu elemanlar analizi, ANSYS APDL, elastomerlerin dinamik özellikleri

ACKNOWLEDGMENTS

I am extremely grateful to my supervisor Asst. Prof. Dr. Gökhan O. Özgen and my co-supervisor Sami Samet Özkan for their professional support, guidance and encouragement throughout the completion of this thesis work.

I would also like to express my sincere appreciation to Bayındır Kuran who is a system administrator in ROKETSAN A.Ş. for his studies related to analytical modeling of vibration isolation system using Matlab.

I am also indebted to Bülent Acar, managing engineer in ROKETSAN A.Ş. for always making time to listen to my ideas, for his enthusiasm and encouragement.

Love and thanks to my darling, my family and my friends for their never-ending patience, support and encouragement.

The work presented in this thesis could not have been accomplished without the support from many individuals. Finally, my thanks go to all those who are not specifically mentioned here.

Ankara, 10 January 2013 Halil Ardıç

TABLE OF CONTENTS

ABSTRACT.....	v
ÖZ.....	vi
ACKNOWLEDGMENTS.....	vii
TABLE OF CONTENTS.....	viii
LIST OF TABLES	x
LIST OF FIGURES	xi
CHAPTERS	
1 INTRODUCTION.....	1
1.1 OBJECTIVE OF THE THESIS	1
1.2 MOTIVATION OF THE THESIS.....	2
1.3 ORGANIZATION OF THE THESIS	2
2 LITERATURE SURVEY	5
2.1 ELASTOMERIC VIBRATION ISOLATORS AND THEIR GENERAL PROPERTIES.....	5
2.2 MODELING VISCOELASTIC MATERIAL BEHAVIOR IN FREQUENCY DOMAIN	7
2.3 FAILURE CRITERIA OF ELASTOMERIC MATERIALS.....	11
2.4 FINITE ELEMENT MODELING OF ISOLATORS	12
3 TECHNICAL REQUIREMENTS OF THE ISOLATOR.....	13
3.1 AREA OF APPLICATION.....	13
3.2 DESIGN REQUIREMENTS OF THE VIBRATION ISOLATOR TO BE DESIGNED...	14
3.3 PERFORMANCE MEASUREMENTS OF VIBRATION ISOLATORS.....	16
4 CONCEPTUAL DESIGN OF VIBRATION ISOLATOR	19
4.1 VIBRATION ISOLATORS USED IN LITERATURE.....	19
4.1.1 Lord Brand Isolators	19
4.1.2 Barry Brand Isolators	20
4.1.3 Laspar Brand Isolators	21
4.2 VIBRATION ISOLATORS USED IN SIMILAR APPLICATIONS.....	21
4.2.1 Properties of Vibration Isolator	21
4.2.2 Tests Conducted on Vibration Isolators.....	21
4.3 DETERMINATION OF ISOLATOR'S CONCEPTUAL DESIGN	25
5 ELASTOMERIC MATERIALS AND CHARACTERIZATION TESTS	27
5.1 DESIRED PROPERTIES OF ELASTOMERS IN THE ISOLATOR DESIGN.....	27
5.2 SELECTION OF ELASTOMER SPECIMENS FOR DYNAMIC CHARACTERIZATION	27
6 PARAMETRIC FEM GENERATION OF THE ISOLATOR	31
6.1 INTRODUCTION.....	31
6.2 GENERATION OF VIBRATION ISOLATOR PARAMETRIC MODEL	32
6.3 BOUNDARY/LOADING CONDITIONS OF THE ANALYSES	35
6.3.1 Modal Analysis	36
6.3.2 Static Analysis	36
6.3.2.1 Axial Static Analysis	36

6.3.2.2	Radial Static Analysis	37
6.3.3	Harmonic Analysis	38
6.3.3.1	Axial Harmonic Analysis.....	38
6.3.3.2	Radial Harmonic Analysis.....	39
7	CONVERGENCE STUDIES AND ANALYSES RESULTS.....	41
7.1	CONVERGENCE ANALYSES	41
7.1.1	Convergence of Axial Analyses.....	41
7.1.2	Convergence of Radial Analyses.....	45
7.2	SAVING INPUTS AND OUTPUTS OF ANALYSES	49
8	FINALIZATION OF THE DETAILED DESIGN	51
8.1	DESIGN ITERATIONS.....	51
8.1.1	First Design Iteration	53
8.1.1.1	Static Analysis	53
8.1.1.2	Modal Analysis.....	55
8.1.1.3	Harmonic Analysis	56
8.1.2	Second Design Iteration	63
8.1.2.1	Static Analysis	63
8.1.2.2	Modal Analysis.....	64
8.1.2.3	Harmonic Analysis	65
8.1.3	Third Iteration.....	67
8.1.3.1	Static Analysis	67
8.1.3.2	Modal Analysis.....	68
8.1.3.3	Harmonic Analysis	69
8.2	PRODUCTION OF THE PROTOTYPES AND VERIFICATION OF THE DESIGN PROCESS.....	71
9	SUMMARY AND CONCLUSIONS.....	79
9.1	GENERAL CONCLUSIONS	79
9.2	FUTURE WORK	80
	REFERENCES	82
APPENDICES		
A	ELASTOMER MATERIAL PROPERTIES.....	85
A.1	PROPERTIES OF THE TESTED ELASTOMERS FOUND IN THE LITERATURE.....	85
A.2	MASTER CURVES OF SELECTED ELASTOMERS.....	86

LIST OF TABLES

TABLES

Table 7.1 Stiffness values with different element sizes and percentage differences with the stiffness value obtained with 0.05 element size	42
Table 7.2 von Mises stress values with different element sizes and percentage differences with the stress values obtained with 0.05 element size	43
Table 7.3 First 3 axial natural frequencies with different element sizes and percentage differences with the natural frequencies obtained with 0.05 element size	44
Table 7.4 Stiffness values with different element sizes and percentage differences with the stiffness value obtained with high quality mesh.....	46
Table 7.5 Von Mises stress values with different element sizes and percentage differences with the stress values obtained with higher quality mesh	47
Table 7.6 First 5 axial natural frequencies with different element sizes and percentage differences with the natural frequencies obtained with high quality mesh	48
Table 8.1 Geometric parameter values for 3 iterations.....	51
Table 8.2 Axial and radial static stiffness values with different materials (1 st parameter set)	54
Table 8.3 First five natural frequencies of the isolator with fixed – free boundary condition	56
Table 8.4 First five natural frequencies of the isolator with free – free boundary condition	56
Table 8.5 System natural frequency and output g_{rms} value at 25 °C	62
Table 8.6 System natural frequency and output g_{rms} value at -30 °C	63
Table 8.7 System natural frequency and output g_{rms} value at 65 °C	63
Table 8.8 Axial and radial static stiffness values with EPDM 50 ShA (2 nd parameter set)	64
Table 8.9 First five natural frequencies of the isolator with EPDM 50ShA for fixed – free and free – free boundary conditions (2 nd parameter set)	65
Table 8.10 System natural frequencies and output grms values at -30, 25 and 65 °C (2 nd iteration)	67
Table 8.11 Axial and radial static stiffness values with EPDM 50 ShA (3 rd parameter set) ...	68
Table 8.12 First five natural frequencies of the isolator with EPDM 50ShA for fixed – free and free – free boundary conditions (3 rd parameter set)	69
Table 8.13 System natural frequencies and output grms values at -30, 25 and 65 °C (3 rd iteration)	70
Table A.1 Silicone rubber sheet mechanical properties [6]	85
Table A.2 Commercial EPDM sheet mechanical properties [6]	85
Table A.3 Commercial Neoprene sheet mechanical properties [6]	85

LIST OF FIGURES

FIGURES

Figure 2.1 Representative conical vibration isolator	6
Figure 2.2 Factors effecting the characterization of elastomer vibration isolators.....	6
Figure 2.3 Effect of temperature on elastomer material's complex modulus behavior (adapted from [1])	8
Figure 2.4 Effect of temperature on elastomer material's complex modulus behavior (adapted from [1])	9
Figure 2.5 Maxwell model	10
Figure 2.6 Schematic representation of Kelvin-Voigt model.	10
Figure 2.7 Standard Linear Solid Model.	11
Figure 2.8 Generalized Maxwell Model or Maxwell-Wiechert Model.....	11
Figure 3.1 Height and base diameter of vibration isolator	14
Figure 3.2 Random vibration profile in axial direction that will affect the equipment.....	15
Figure 3.3 Test configuration for the vibration isolators	15
Figure 3.4 Axial (left) and radial (right) test configurations	16
Figure 4.1 Generic structure of a conical vibration isolator	19
Figure 4.2 A sample conical vibration isolator by Lord Company	20
Figure 4.3 Section view of AM005 series vibration isolator	21
Figure 4.4 MTS test system in Bayrak Plastik	22
Figure 4.5 Axial (left) and radial (right) test configurations	23
Figure 4.6 Frequency Dependent Axial Dynamic Stiffness of AM-005-2 Isolator.....	23
Figure 4.7 Frequency Dependent Axial Loss Factor of AM-005-2 Isolator	24
Figure 4.8 Frequency Dependent Radial Dynamic Stiffness of AM-005-2 Isolator.....	24
Figure 4.9 Frequency Dependent Radial Loss Factor of AM-005-2 Isolator	25
Figure 4.10 Generic geometry (conceptual design) of the isolator.....	26
Figure 5.1 Elastomer material dynamic characterization test system	28
Figure 5.2 Tensile elastomer material specimen and force transducer, accelerometers, thermocouples locations.....	29
Figure 6.1 Geometrical parameters determined on the final conceptual design of the isolator	32
Figure 6.2 Getting geometric parameters into the ANSYS.....	33
Figure 6.3 Areas for each component of the vibration isolator	34
Figure 6.4 2-D surface model (left) and 3-D solid model (right).....	34
Figure 6.5 Finite element models with different element sizes	35
Figure 6.6 Fixed – free boundary condition for modal analysis.....	36
Figure 6.7 Boundary and loading conditions for axial static analysis	37
Figure 6.8 Boundary and loading conditions for radial static analysis.....	38
Figure 6.9 RBE2 connections, boundary and loading conditions for 2-D axisymmetric model	39
Figure 6.10 RBE2 connections, boundary and loading conditions for 3-D model	40
Figure 7.1 2-D axisymmetric models with different element sizes	42
Figure 7.2 Von Mises stress distribution of the EPDM 50 ShA (2-D).....	43
Figure 7.3 First 3 mode shapes of 2-D axisymmetric analysis model	44

Figure 7.4 3-D models with different element sizes	45
Figure 7.5 3-D finite element model with high density mesh (Reference model)	46
Figure 7.6 Von Mises stress distribution of the EPDM 50 ShA (3-D).....	47
Figure 7.7 First 5 mode shapes of 3-D analysis model	48
Figure 8.1 Geometrical parameters of the isolator, detailed design of which was be determined	52
Figure 8.2 Geometric structure of the isolator at the first iteration	53
Figure 8.3 Von Mises stress distributions on different elastomeric materials as a result of maximum axial static loading.....	54
Figure 8.4 Von Mises stress distributions on different elastomeric materials as a result of maximum radial static loading	55
Figure 8.5 Frequency dependent dynamic stiffness of the isolator with EPDM 50ShA at different temperatures (1 st design iteration).....	57
Figure 8.6 Frequency dependent loss factor of the isolator with EPDM 50ShA at different temperatures (1 st design iteration).....	57
Figure 8.7 Frequency dependent dynamic stiffness of the isolator with EPDM 80ShA at different temperatures (1 st design iteration).....	58
Figure 8.8 Frequency dependent loss factor of the isolator with EPDM 80ShA at different temperatures (1 st design iteration).....	58
Figure 8.9 Frequency dependent dynamic stiffness of the isolator with Neoprene 50ShA at different temperatures (1 st design iteration).....	59
Figure 8.10 Frequency dependent loss factor of the isolator with Neoprene 50ShA at different temperatures (1 st design iteration).....	59
Figure 8.11 Frequency dependent dynamic stiffness of the isolator with Silicone 50ShA at different temperatures (1 st design iteration).....	60
Figure 8.12 Frequency dependent loss factor of the isolator with Silicone 50ShA at different temperatures (1 st design iteration).....	60
Figure 8.13 Frequency dependent dynamic stiffness of the isolator with Silicone 80ShA at different temperatures (1 st design iteration).....	61
Figure 8.14 Frequency dependent loss factor of the isolator with Silicone 80ShA at different temperatures (1 st design iteration).....	61
Figure 8.15 Output PSD using EPDM 50ShA dynamic properties at 25 °C	62
Figure 8.16 Geometric structure of the isolator at the second iteration.....	64
Figure 8.17 Von Mises stress distributions on EPDM 50ShA due to axial (left) and radial (right) static loadings with 2 nd parameter set	64
Figure 8.18 Frequency dependent dynamic stiffness of the isolator with EPDM 50ShA at different temperatures (2 nd design iteration)	66
Figure 8.19 Frequency dependent loss factor of the isolator with EPDM 50ShA at different temperatures (2 nd design iteration)	66
Figure 8.20 Using 2 nd parameter set, axial and radial stiffness of the isolator with EPDM 50ShA at 25 °C	67
Figure 8.21 Geometric structure of the isolator at the third iteration	68
Figure 8.22 Von Mises stress distributions on EPDM 50ShA due to axial (left) and radial (right) static loadings with 3 rd parameter set.....	68
Figure 8.23 Frequency dependent dynamic stiffness of the isolator with EPDM 50ShA at different temperatures (3 rd design iteration)	69
Figure 8.24 Frequency dependent loss factor of the isolator with EPDM 50ShA at different temperatures (3 rd design iteration).....	70
Figure 8.25 Using 3 rd parameter set, axial and radial stiffness of the isolator with EPDM 50ShA at 25 °C	71
Figure 8.26 Solid model of final vibration isolator design.....	72
Figure 8.27 Final isolator design with flanges.....	72
Figure 8.28 Photographs of a prototype	73
Figure 8.29 Axial (left) and radial (right) test configurations of the prototypes.....	73
Figure 8.30 Tested axial dynamic stiffness of the prototypes and analysis result	74

Figure 8.31 Tested axial loss factor of the prototypes and analysis result	74
Figure 8.32 Tested radial dynamic stiffness of the prototypes and analysis result.....	75
Figure 8.33 Tested radial loss factor of the prototypes and analysis result.....	75
Figure 8.34 Axial dynamic stiffness average of the prototypes and analysis result	76
Figure 8.35 Axial loss factor average of the prototypes and analysis result	76
Figure 8.36 Radial dynamic stiffness average of the prototypes and analysis result	77
Figure 8.37 Radial loss factor average of the prototypes and analysis result	77
Figure A.1 Master curves of EPDM 50ShA shear sample.....	86
Figure A.2 Master curves of EPDM 50ShA tensile sample	87
Figure A.3 Master curves of EPDM 80ShA tensile sample	88
Figure A.4 Master curves of Neoprene 50ShA tensile sample.....	89
Figure A.5 Master curves of Silicone 50ShA tensile sample.....	90
Figure A.6 Master curves of Silicone 80 ShA tensile sample.....	91

CHAPTER 1

INTRODUCTION

Electronic equipment like missile computer, telemetry, inertial measurement unit, power supply unit are exposed to aerodynamic forces and random vibrations coming from missile engine during the free flight of a missile. In order for a missile to successfully complete its mission, electronic equipment found in the missile should carry out their functionality successfully under the vibration excitation. This can only be achieved when structural vibrations transmitted to the equipment are attenuated, for which vibration isolators are used widely. In this vibration isolation activity, passive vibration isolators are placed between vibrating panel and electronic equipment decoupling their dynamic responses.

In this thesis, an elastomeric vibration isolator will be designed, produced and validated for a missile vibration isolation application. As part of this thesis work, first all technical requirements for the isolator to be designed (geometric constraints, vibration isolation performance, temperature range, etc.) will be determined for a sample missile application in ROKETSAN A.Ş. Next, a few candidate elastomer materials will be selected and their specimens will be supplied. Dynamic characterizations of these materials will be accomplished at elastomer material dynamic characterization test setup, in ROKETSAN A.Ş. In the following step, conceptual design (geometrical layout and shapes of the elastomer and metal parts) of elastomer vibration isolator will be decided. Next, parametric finite element model of representing the conceptual design of the elastomer vibration isolator will be developed. Elastomer material characterization results (frequency dependent dynamic elastic modulus and loss factor) will be used as an input in parametric finite element model. Final detailed design of vibration isolator will be obtained using design iterations where performance of the isolator is estimated using finite element simulations. Then, prototypes will be manufactured with obtained final design of vibration isolator. Lastly, design process of the vibration isolator will be validated by dynamic test results of prototypes.

1.1 OBJECTIVE OF THE THESIS

Main objectives of this thesis are to develop a process for designing and manufacturing vibration isolators with the desired vibration isolation performance, which will be used for the vibration isolation of sensitive electronic equipment used in products designed by ROKETSAN A.Ş., and to validate this design process for a sample vibration isolator. Phases of the design and manufacture processes of the sample isolator are as follows: 1) Selecting appropriate elastomer material for the vibration isolator to be designed; 2) Characterizing elastic and damping properties of the elastomer material with respect to temperature and frequency; 3) Generating detailed design of vibration isolators (dimension, size etc.) that will satisfy vibration isolation performance requirements of the target application utilizing finite element analysis; 4) Having the vibration isolator produced by a local rubber company; 5) Validating design and manufacturing process by comparing measured properties of the designed vibration isolator with finite element simulations.

With the know-how developed with this thesis study, all vibration isolators that will be used for special or general applications may be designed with desired properties in ROKETSAN A.Ş. and they can be produced by local rubber companies. By this way, vibration isolation required for all defense industry applications in ROKETSAN A.Ş. may be met effectively.

1.2 MOTIVATION OF THE THESIS

There are some difficulties for procuring elastomer vibration isolators from national companies to meet the design performance needs ROKETSAN A.Ş. products. Elastomer vibration isolators that are being used in the products ROKETSAN A.Ş. are expected have stiffness values both in axial and radial directions as chosen during the design process and these values are also expected to be quite stable with very little uncertainty. They should operate effectively in large temperature ranges which are typical in defense applications. Their dynamic properties should be determined by tests and they should also be documented well. Lastly, damping values of elastomer vibration isolators should be high enough in order to achieve desired vibration isolation performance. National companies currently do not have vibration isolators that can fully meet these specific needs among their standard products. Actually, there are companies that can design a vibration isolator with desired properties; however, engineering development cost of this would be very high. Thus, economically limited number of orders, which is typical in defense products, is not economically viable.

Because of these reasons mentioned above, currently ROKETSAN A.Ş. procures appropriate vibration isolators from available catalog products of known international companies. Because of the fact that these products will have to be exported for defense applications, it brings up supplier country restrictions like subjects related to export license and end user of the products and shipping duration of vibration isolators can be delayed. Moreover, in some cases, problems related to supplying sufficient amount of vibration isolators are encountered. It is possible to experience bottlenecks related to supply in the future. The purpose of this thesis study is to develop and verify the design procedure for an elastomer vibration isolator with target stiffness and damping values in ROKETSAN A.Ş. and overcome these procurement bottlenecks.

1.3 ORGANIZATION OF THE THESIS

In this thesis, first of all literature was reviewed. General properties and dynamic characteristics of vibration isolators are studied. After getting sufficient information about isolators, technical requirements of a sample application were determined. After that, generic geometry of vibration isolator was established. Then, some standard elastomer materials were selected and their material characterization tests were conducted. In parallel with this, finite element model of vibration isolator was generated parametrically. Next, static and dynamic analyses of a generic vibration isolator were run. After that, through design iterations, vibration isolator's detailed design was finalized. Then performance of the designed isolator was obtained with characterization tests. Finally, design process of the vibration isolator was validated by comparing measured properties of the isolator with finite element simulations.

In *Chapter 1*, which is the current chapter, introduction was given for the thesis. Objective and motivation of the thesis were explained elaborately. Finally, organization of the thesis is provided.

Chapter 2 is about literature review about vibration isolators and studies related to vibration isolator design. In this chapter, general properties of elastomer vibration isolator are given. Important dynamic properties and how they are affected by various parameters are

comprehensively explained. Viscoelastic material models and their formulations are described. Design parameters and some studies related to vibration isolator design using finite element analysis are also given.

In *Chapter 3*, design requirements of vibration isolator for sample application are determined. Geometrical and functional requirements of vibration isolators were explained. Additionally, measurement of performance of vibration isolators is explained in this chapter.

In *Chapter 4*, conceptual design of vibration isolator is determined by analyzing commercially available vibration isolators. Vibration isolator designs in similar applications are also examined. Additionally, in order to maintain an opinion about the performance of a low profile avionic vibration isolators already being used in ROKESAN A.Ş. products, sample isolators are tested dynamically and results of these tests are given in this chapter. Finally, conceptual design of isolator is finalized and presented.

In *Chapter 5*, general information is given for standard elastomer materials used in commercial applications. Among them, several elastomer material candidates are chosen and their mechanical properties are experimentally obtained using a test system that is present in ROKETSAN A.Ş.

In *Chapter 6*, process for the generation a parametric finite element model of the vibration isolator to be designed is explained. Brief information related to parametric modeling in ANSYS environment is also given. Then, how vibration isolator's parametric modeling is constituted is described comprehensively. Finally, boundary and load conditions are given for the analysis to be conducted for making final design decisions for the vibration isolator being designed in this thesis work.

In *Chapter 7*, the process related to getting dynamic properties (frequency dependent dynamic stiffness and loss factor) and strength characteristics of vibration isolators using finite element based dynamic and static analysis is developed and explained in detail.

In *Chapter 8*, detailed design of elastomer vibration isolator is finalized according to design iterations. Final isolator design satisfies the design requirements that are designated in chapter 3. Vibration isolator prototype is manufactured in a local rubber company according final design.

CHAPTER 2

LITERATURE SURVEY

Literature survey begins with vibration isolators and their general properties. Different isolator types and their uses are explained. Basic properties of conical elastomer vibration isolators are given in the first subsection of this chapter. Then, main factors (temperature, frequency and dynamic amplitude) affecting the dynamic properties of elastomer vibration isolators and how they change the dynamic stiffness and loss factor are described. Third subsection is about viscoelastic materials and their models. The difference between elastic and viscoelastic behavior is clarified in this subsection. Then, information about dynamic modulus, classical viscoelastic models and fractional derivative models for viscoelastic material behavior are given. In the fourth subsection, failure criteria of elastomer materials are defined. Studies in literature related to vibration isolator design using finite element analysis are given in the last subsection. Overall, this chapter contains useful information on elastomer material behavior and elastomer vibration isolator design and modeling. Therefore, it will be benefitted for the other chapters.

2.1 ELASTOMERIC VIBRATION ISOLATORS AND THEIR GENERAL PROPERTIES

In order to control and isolate vibrations in structures and machines, vibration isolators of different sizes and configurations are used. Vibration isolators are used for two cases: to decrease transmission of vibration to the surrounding structures due to rotational motion of components in a machine or equipment and to protect a machine or equipment from vibration effects transmitted from supporting foundation structure.

Vibration isolators, selected or designed, are expected to fulfill some functions mentioned below:

- Supporting the dead-weight of the structure that is isolated without failing and creeping.
- Having sufficient stiffness in order to protect vibration transmission from foundation structure to machine or machine to foundation structure.
- Having appropriate damping performance. **[1]**

Elastomer materials are polymeric materials which have mechanical properties similar to natural rubber. Manufacturing in any kind of shape, having different stiffness values from low to high, having damping behavior more than metals, fulfilling the minimum mass and volume requirements, binding to metals effectively are important properties of elastomers for being used in vibration isolators commonly. Elastomer vibration isolators can sustain large deformations and can recover to their original state without any permanent deformation.

Elastomer isolators may be used with different types of loading. These are compression, shear, tension, or buckling, or any combination of those [2]. In most aerospace applications, conical elastomer vibration isolators are used because their stiffness characteristics can be arranged to be very close in all directions (iso-elastic [3]). They also occupy very little space in the axial direction which is a positive thing for applications which leave you very little space to position vibration isolators. Conical elastomer vibration isolators are used commonly in order to isolate vibrations in both axial and radial directions. In Figure 2.1, geometrical details of a typical conical elastomeric vibration isolator are given. With this configuration, dynamic stiffness and loss factor of a vibration isolator in axial and radial directions can be close to each other.

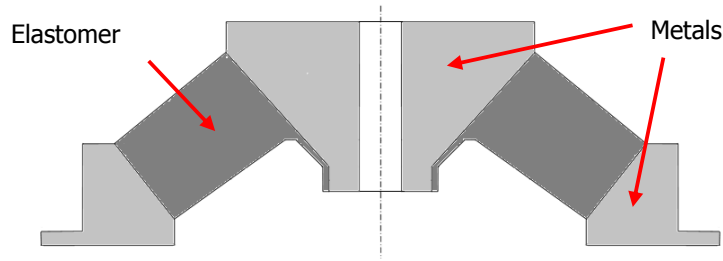


Figure 2.1 Representative conical vibration isolator

Most important parameters for the dynamic characterization of elastomer vibration isolators are dynamic stiffness and loss factor. Characterization of a vibration isolator can be completed if these parameters obtained in three axes. Elastomer materials used in vibration isolators are viscoelastic materials. Complex modulus value of viscoelastic materials depends on temperature, frequency, applied static preload and dynamic amplitude. Hence, stiffness and loss factor of a vibration isolator rely on type of viscoelastic material, operating temperature and frequency, static load, dynamic amplitude, and finally geometry of vibration isolator (Figure 2.2).

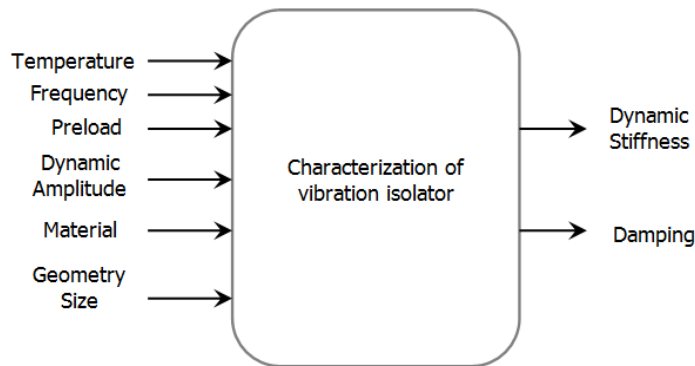


Figure 2.2 Factors effecting the characterization of elastomer vibration isolators

Dynamic properties of elastomer vibration isolator change with temperature, frequency, static preload and dynamic operating amplitude. Among these, the most important factor affecting the dynamic properties of vibration isolators is the temperature. Elastomer

materials used in vibration isolator and geometry and size of the isolator determine the degree and characteristics of other factors.

2.2 MODELING VISCOELASTIC MATERIAL BEHAVIOR IN FREQUENCY DOMAIN

Viscoelastic material behavior manifests itself as a stress-strain relationship that is somewhere in between pure viscous and pure elastic behaviors. Time-domain modeling of linear viscoelastic material behavior can be defined in terms of identified creep or relaxation parameters where stress and strain constitutive relation would be a linear ordinary differential equation including higher order derivative terms of both stress and strain. In the frequency domain, harmonic loads can be considered for representing stress-strain relationship. For uniaxial loading of a viscoelastic material specimen, the relation between harmonic amplitudes of stress and strain can be written in terms of a complex frequency dependent modulus $\tilde{E}^*(i\omega)$, which is defined as:

$$\sigma_0 = \tilde{E}^*(i\omega) \cdot \varepsilon_0 = (E'(\omega) + i \cdot E''(\omega)) \cdot \varepsilon_0 \quad (2.1)$$

where, ω is the frequency in rad/s, $E'(\omega)$ is the storage modulus, $E''(\omega)$ the loss modulus harmonic stress and strain are defined as:

$$\sigma(t) = \sigma_0 e^{i\omega t} \quad (2.2)$$

$$\varepsilon(t) = \varepsilon_0 e^{i\omega t} \quad (2.3)$$

Complex modulus can be written in another form:

$$\tilde{E}^*(i\omega) = E'(\omega)[1 + i\eta(\omega)] \quad (2.4)$$

where a loss factor term $\eta(\omega)$ is defined as:

$$\eta(\omega) = \frac{E''(\omega)}{E'(\omega)} \quad (2.5)$$

Loss factor $\eta(\omega)$ is a direct measure of a damping capacity of a material.

Real part of the complex modulus is called the storage modulus $E'(\omega)$ and imaginary part is called the loss modulus. For metals storage modulus (E') is constant over the frequency domain and loss modulus $E''(\omega)$ is a weak function of frequency. Loss factors are very low, i.e. 0.0001 - 0.001. For viscoelastic materials, both moduli are functions of frequency. They can achieve very high loss factors i.e. 0.1 - 1.5. For most viscoelastic materials, complex modulus has also strong temperature dependence.

The existence of an imaginary part in the modulus means that there is going to be a phase difference between stress and strain when the input is harmonic. When for harmonic or cyclic input-response case, stress versus strain plot is investigated a hysteresis loop will be observed due to the phase difference. The area of this loop is also a measure of the amount of energy lost (as heat) in a loading and unloading cycle [6] [7].

Frequency dependence of storage modulus and loss factor for typical viscoelastic materials can be investigated in constant temperature plots given in Figure 2.3. Three regions exist in these frequency plots. For most viscoelastic materials (elastomers, rubber, plastics, pressure

sensitive adhesives), loss factor is generally between 0.1 to 0.3 in the “Rubbery region” while modulus values could be as low as 2-3 MPa. In the Transition region, modulus values are very sensitive to frequency change and increases drastically with increasing frequency until the third and next (Glassy) region is reached. In the Glassy region, loss factor is usually below 10^{-2} , while modulus values are relatively stable with changing frequency and could be as high as 20000 Mpa.

Complex modulus also has strong temperature dependence. Temperature plots are mirror images of frequency plots of storage modulus and loss factor. Increasing frequency have a similar effect as lowering temperature (see Figure 2.4). Decreasing frequency has a similar effect as increasing temperature. Temperature-frequency equivalence is modeled by a term called the shift factor which enables modeling of complex modulus as a function of both frequency and temperature [1].

In order to use elastomer materials in isolation applications, complex modulus behavior of elastomer materials should be known for wide range of temperature and frequency.

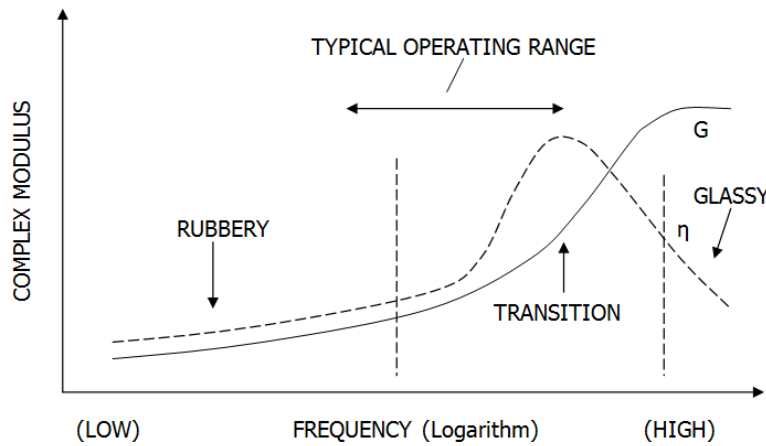


Figure 2.3 Effect of temperature on elastomer material’s complex modulus behavior (adapted from [1])

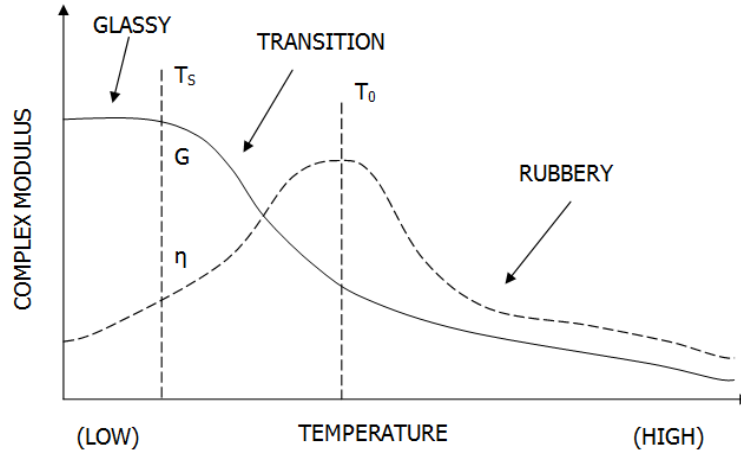


Figure 2.4 Effect of temperature on elastomer material's complex modulus behavior (adapted from [1])

Commonly known mathematical models for viscoelastic material behavior are Maxwell model, Kelvin-Voigt model, and Standard Linear Solid Model. In these models overall viscoelastic behavior are modeled using various combinations of simple elastic and viscous components (springs and dashpots, respectively).

In the Maxwell model [4], a purely viscous damper and a purely elastic spring is connected in series as shown in Figure 2.5. Time domain stress-strain the constitutive equation for this model can be represented by the following equation (2.6):

$$\frac{d\varepsilon}{dt} = \frac{\sigma}{\eta} + \frac{1}{E} \frac{d\sigma}{dt} \quad (2.6)$$

where σ is the stress, η is the viscosity of the material, and $\frac{d\varepsilon}{dt}$ is the time derivative of strain.

Complex modulus expression for the Maxwell model is as follows [8]:

$$E^*(\omega) = \frac{E\eta^2\omega^2 + i\omega E^2\eta}{\eta^2\omega^2 + E^2} \quad (2.7)$$

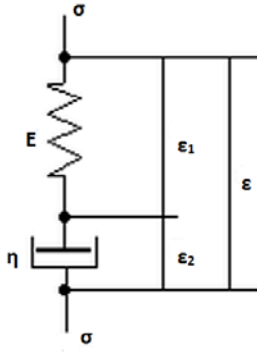


Figure 2.5 Maxwell model

The Kelvin-Voigt model is formed by connecting a viscous damper and a spring in parallel configuration as shown in Figure 2.6.

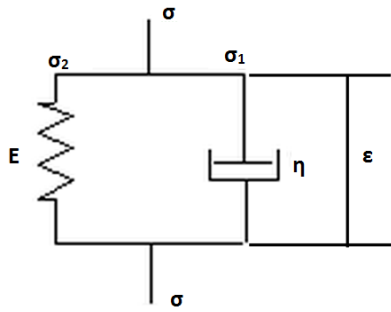


Figure 2.6 Schematic representation of Kelvin-Voigt model.

Time domain stress-strain constitutive equation for the Kelvin-Voigt model derived as follows [4]:

$$\sigma(t) = E\varepsilon(t) + \eta \frac{d\varepsilon(t)}{dt} \quad (2.8)$$

Complex modulus expression for the Kelvin-Voigt model is as follows:

$$E^*(\omega) = E + i\eta\omega \quad (2.9)$$

The Standard Linear Model is formed combining a Maxwell Model and a spring in parallel as shown in Figure 2.7.

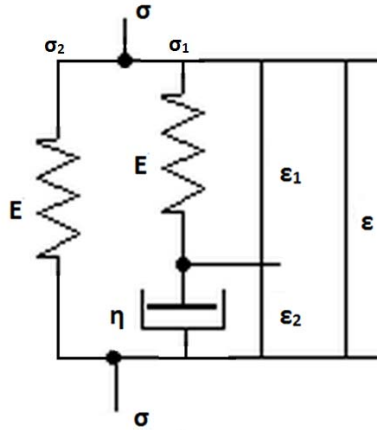


Figure 2.7 Standard Linear Solid Model.

Generalized Maxwell Model also known as the Maxwell-Wiechert Model is more general form for modeling the linear viscoelasticity (see Figure 2.8). [9]. Complex modulus expression for the Generalized Maxwell Model model is as follows:

$$\tilde{E}^*(i\omega) = \sum_{n=1}^N \frac{i\omega E_n \eta_n}{1 + i\omega \eta_n} \quad (2.10)$$

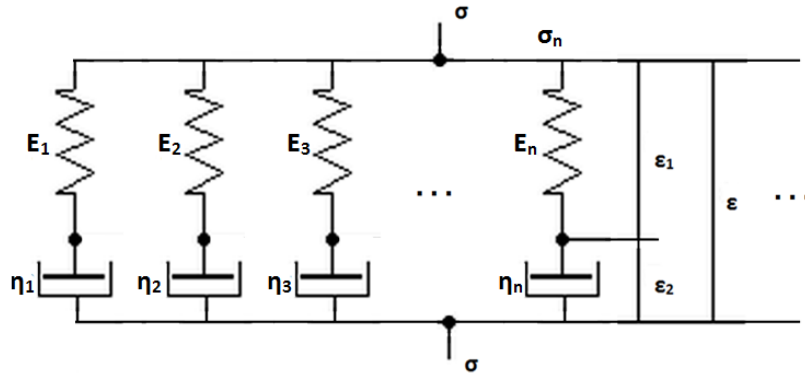


Figure 2.8 Generalized Maxwell Model or Maxwell-Wiechert Model

Using fractional derivative models in place of classical Calculus approach, offers a simplification in modeling viscoelastic material behavior in the frequency domain [1]. Use of fractional calculus enables the representation of actual complex modulus using less number of parameters and derivative terms compared to models like Generalized Maxwell Model which are based on ordinary differential equations to represent stress-strain relationship.

2.3 FAILURE CRITERIA OF ELASTOMERIC MATERIALS

The two types of failure models for polymers are isostate and evolving state models. In isostate failure model, loading history of the material does not contribute to the failure

characteristics. In evolving state models, failure is affected by the loading history of the material or the component (may also be called history-based models). Damage model is an example of an evolving model, while stress-based, strain-based and energy-based models are examples of isostate models [10].

An energy-based failure model is suggested by Volokh, where the increase in energy is limited by a critical value called material failure energy [11]. Another energy-based failure model is proposed by Gent and Chang [12]. In this approach, failure criterion is defined using the rate of release of strain energy instead of a limiting amount of stored energy. An alternative energy-based failure model is Maximum Energy theory [13].

Maximum principle stress, Von Mises stress, Tresca stress and Coulomb stress are also well known stress-based failure models. Von Mises and Coulomb stress terms are defined as follows [5]:

$$\sigma_{Mises} = \sqrt{\frac{1}{2}[(\sigma_1 - \sigma_2)^2 + (\sigma_2 - \sigma_3)^2 + (\sigma_3 - \sigma_1)^2]} \quad (2.11)$$

$$\sigma_{Coulomb} = (\sigma_1 - \sigma_2) + f(\sigma_1 - \sigma_3) \quad (2.12)$$

where σ_1 , σ_2 and σ_3 are principal stresses and f is the friction coefficient. According to these failure criteria, if the calculated values are higher than the yield strength of the material, designated as S_y , material fails.

Furthermore, some of the well-known strain-based failure models are Maximum Principal Strain and von Mises strain. [10]

$$\varepsilon_{Mises} = \sqrt{\frac{1}{2}[(\varepsilon_1 - \varepsilon_2)^2 + (\varepsilon_2 - \varepsilon_3)^2 + (\varepsilon_3 - \varepsilon_1)^2]} \quad (2.13)$$

where ε_1 , ε_2 and ε_3 are principle strains.

2.4 FINITE ELEMENT MODELING OF ISOLATORS

In his studies, R. C. Frampton gives very useful information on dynamic testing of elastomers [18]. In this thesis, dynamic properties of elastomeric materials will be found by dynamic characterization tests. Similar concepts are being used in dynamic characterization test system in Roketsan A.Ş. Dynamic properties of filled rubbers can be changed with different dynamic amplitude. This is called as the Fletcher-Gent effect or Payne effect. Negrete, Vinolas and Kari were developed a methodology to include this effect in a linear viscoelastic rubber material model to estimate the dynamic stiffness of filled rubber isolators using a finite element (FE) code [19]. In their studies, Beijers and de Boer modeled cylindrical vibration isolator with the Finite Element package ABAQUS. First they performed a nonlinear analysis for different pre-deformations of the mount and then a linear harmonic analysis on the pre-deformed isolator [20]. Mustafa and Kenan studied related to characterization of vibration isolators using vibration test data. They presented two approximate methods for the measurement of the dynamic properties of viscoelastic components. The first method is depend on linearizing the system. 'Estimation of Isolator Properties Using Log Decrement Method' aims to deliver amplitude-dependent parameters for the component under test [21]. The buckling of natural rubber bearings with finite element analysis were examined by Takayama and Morita. They studied how the material properties of the rubber (nonlinear properties) or the thickness of the interlayer steel plates affected the buckling load [22].

CHAPTER 3

TECHNICAL REQUIREMENTS OF THE ISOLATOR

Chapter 3 is about determination of technical requirements of vibration isolators for a sample application in ROKETSAN A.Ş. Vibration isolators are used to isolate electronic equipments used in products designed by ROKETSAN A.Ş. For a chosen sample application, geometric constraints, operating temperature range, maximum static load, etc. are determined in this part of the thesis work. This information is very important because vibration isolator will be designed according to these requirements. Performance of the designed elastomer vibration isolators will be first tried using a Matlab code, which can simulate the vibration isolation performance for a 6 DOF rigid body supported on multiple resilient elements for a given input random PSD (Power Spectral Density) profile.

3.1 AREA OF APPLICATION

Electronic equipment (i.e. missile computer, telemetry, IMU, power supply unit), mounted in missiles, are exposed to aerodynamic forces and random vibration in three axes during the free flight of the missiles, which are caused by the missile engine. In order for a missile to carry out its mission successfully, electronic equipment in the missile should carry on their functionality, that is, their performance should not be affected by vibration disturbances. For electronic equipment used in missiles, information related to environmental conditions (vibration, humidity, temperature, etc.) in which their functionality is not adversely affected is also supplied by the manufacturers. Environmental vibration condition that equipment performs its functions problem-free is generally supplied by the manufacturer as a limiting random vibration profile that the equipment can withstand (Power Spectral Density, PSD graph, etc.) and a maximum acceleration level in root-mean-square value (also called g_{rms} level where g refers to the gravitational acceleration) it can take under operational conditions. Vibration levels (profiles), electronic equipment designed by ROKETSAN A.Ş are subject to at their mounting locations or these equipment can withstand are determined by in-house tests.

If the vibration profile that will be transmitted to electronic equipment is above the vibration profile (level) at which the equipment can withstand, vibration isolators must be used to reduce the random vibrations transmitted to the equipment. Since random vibrations are existent in all directions, isolators to be used for vibration isolation should have similar isolation characteristics for all three principal axes. Besides, small vibration isolators should be preferred since the volume of the missile is pretty low. Lastly, vibration isolator that will be designed should have the desired vibration isolation performance for a temperature range of -30 – +65 °C.

3.2 DESIGN REQUIREMENTS OF THE VIBRATION ISOLATOR TO BE DESIGNED

Base surface diameter of the conical elastomer vibration isolator that will be designed should be minimum 40 and maximum 60 mm's. Additionally, height of the isolator (distance between bottom and top connecting surfaces) should be minimum 10 and maximum 20 mm's. Related geometrical parameters are shown in Figure 3.1 for generic conical vibration isolator. These geometrical requirements are on account of the connecting interface of equipment that will be isolated using the isolator to be designed as at the end of this thesis study.

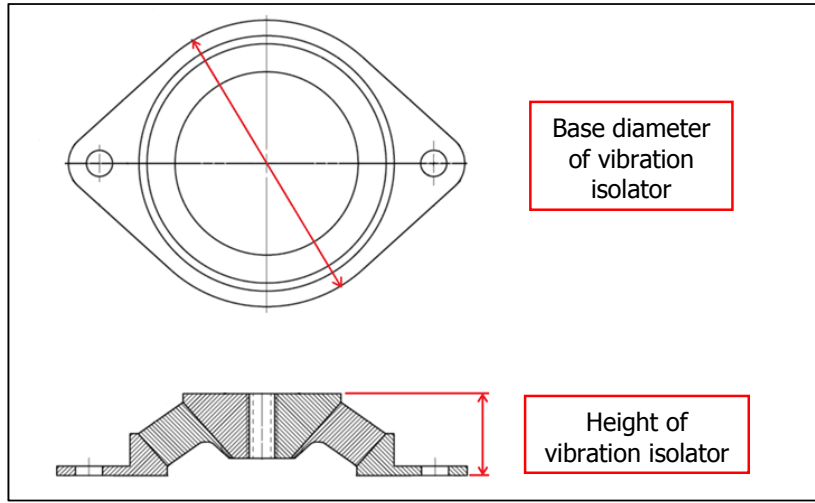


Figure 3.1 Height and base diameter of vibration isolator

Four vibration isolators that will be designed will be connected equipment with 10 kg mass. Natural frequency of this system (resonance frequency) should be below 200 Hz. Under operating conditions, vibration isolator's nominal stiffness in radial direction should be at least 90% of stiffness in axial radiation. Vibration isolator should function under static loads of maximum 375 N in axial (compression) and maximum 125 N in radial directions. Vibration isolator should statically support maximum 500 N in axial (compression) and maximum 200 N in radial directions. Isolation performance of vibration isolator should be kept -30 – +65 °C temperature range. Vibration isolators should isolate random vibration profile, shown in Figure 3.2, in axial direction. This vibration profile has 3.66 g_{rms} value.

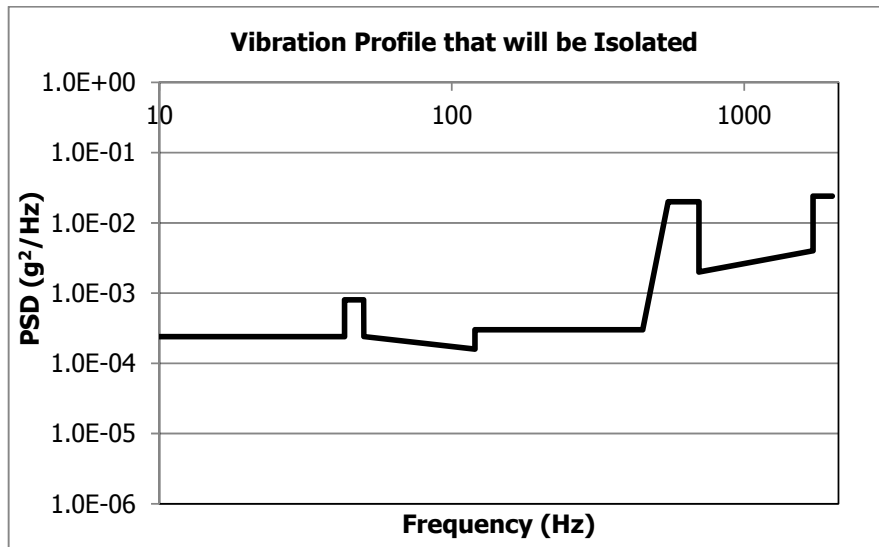


Figure 3.2 Random vibration profile in axial direction that will affect the equipment

Isolation performances of elastomer vibration isolators can be measured by a test set up designed by Sami Samet Özkan who is a senior engineer in ROKETSAN A.Ş. In Figure 3.3, configuration of test setup is shown. Sample mass that will be isolated is supported by two isolators (bottom and top) as demonstrated in figure.

Test set up has compatible interface with shaker and tests will be conducted when the shaker is in vertical position. Vibration profile, having a definite g_{rms} level, (and detail of which is given above) will be applied to the test set up. As a result of the test, output vibration profile measured from the mass and output g_{rms} value will be obtained. Output g_{rms} value is supposed to be below 1.

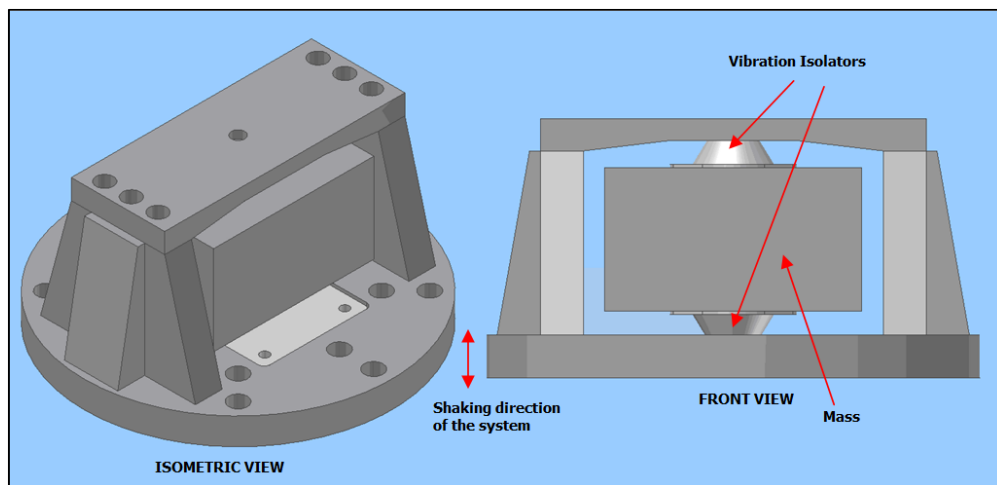


Figure 3.3 Test configuration for the vibration isolators

3.3 PERFORMANCE MEASUREMENTS OF VIBRATION ISOLATORS

Isolation performance of vibration isolators, design and production steps of which are accomplished, is achieved by different tests and approaches. At a definite temperature, frequency dependent dynamic stiffness and loss factors of vibration isolators both in axial and radial directions can be found using a commercial test system in the market. In Figure 3.4, test configurations of a sample vibration isolator at MTS test system. Static strength tests of vibration isolators in axial and radial directions can also be done using the same configuration.

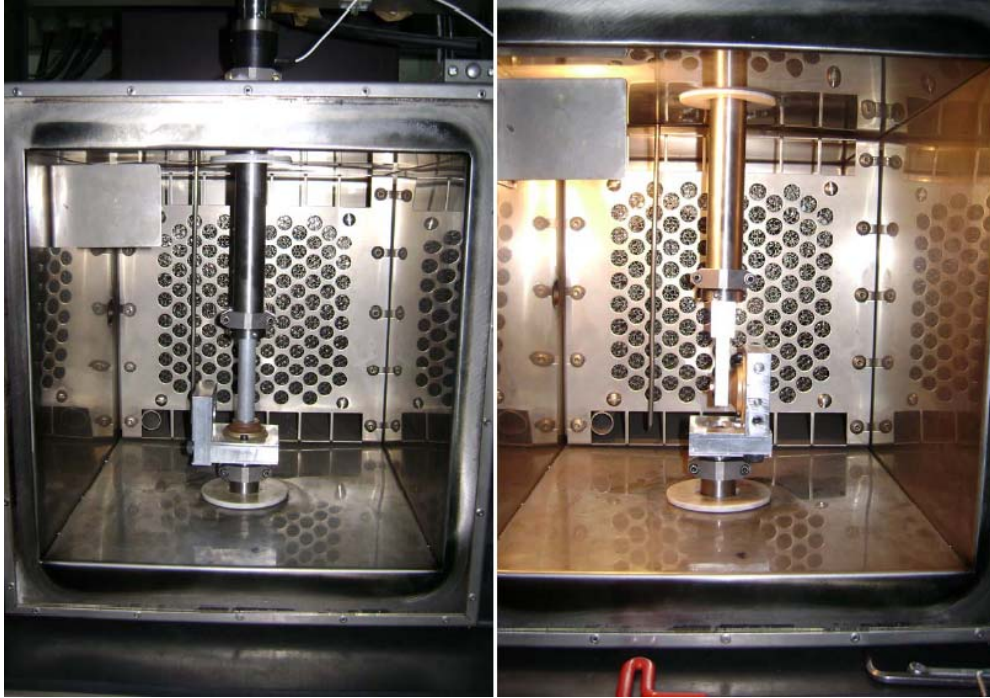


Figure 3.4 Axial (left) and radial (right) test configurations

Vibration isolation performance of elastomer isolators can be measured with two approaches. In the first approach, test system designed by Sami Samet Özkan can be used. In the second approach, this test is simulated analytically by a Matlab code. This code is originally developed by Bayındır Kuran who is System Design Administrator in ROKETSAN A.Ş. and modified in order to simulate isolation performance of vibration isolators supported by elastomer vibration isolators.

The response of the equipment under the random vibration environment can be expressed as [25]:

$$\{PSD_{equipment}(\omega)\} = [H(\omega)][H(\omega)]^* \{PSD_{input}(\omega)\} \quad (3.1)$$

where $[H(\omega)]^*$ is complex conjugate of the absolute displacement transmissibility function matrix for a six DOF supported on isolators connected to a moving foundation, $\{PSD_{equipment}(\omega)\}$ is the vibration (calculated as PSD) level on the equipment, and $\{PSD_{input}(\omega)\}$ is the vibration input (as PSD) of the support.

The Matlab code is written for the general case where the equipment is supported by 4 vibration isolators. In order to simulate the test mentioned before, 2 vibration isolators which support the specified mass are considered. Since the stiffness and loss factors of elastomer vibration isolators depend on frequency, these parameters are imported as frequency dependent into the code.

CHAPTER 4

CONCEPTUAL DESIGN OF VIBRATION ISOLATOR

According to technical requirements determined in *Chapter 3* for a sample application, conceptual design of vibration isolator will be determined in this chapter. In order to decide on the conceptual design, vibration isolators found in the catalog of commercial companies like Lord, Barry and Laspar will be investigated first. Existing vibration isolators which are the candidate for the similar vibration isolation applications in ROKETSAN A.Ş. will also be investigated thoroughly. Dynamic and static tests at which the dynamic characteristics of these vibration isolators found will be given to get an idea on target values for isolator properties. According to all these investigations conceptual design of the elastomeric vibration isolator will be decided. Conceptual design of the vibration isolator will be used to comprise geometric parameters and to create parametric finite element model of the isolator.

4.1 VIBRATION ISOLATORS USED IN LITERATURE

Many aerospace equipment isolators are of the conical type because they are iso-elastic, that is, their stiffness and damping properties are almost the same in all translational directions. Since vibration isolator to be designed will be used in products designed in ROKETSAN A.Ş., random vibration excitation will be exerted on equipment supported by vibrations isolators in three axes. Therefore, vibration isolator that will be designed in this thesis is chosen to be of conical shape. Figure 4.1 shows the generic structure of a conical vibration isolator. Standard elastomeric vibration isolators from catalogs of known commercial companies have been investigated. In the coming sections details related to these products are given.

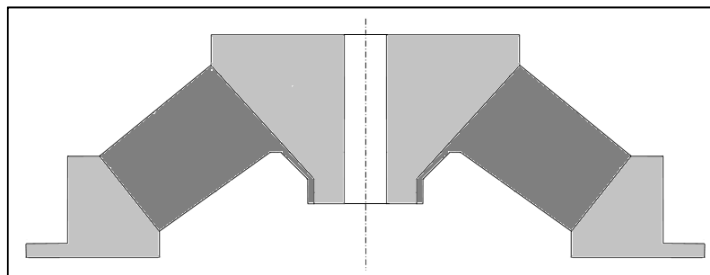


Figure 4.1 Generic structure of a conical vibration isolator

4.1.1 Lord Brand Isolators

Low profile Avionics Mounts (AM series) of Lord Corporation can be used to isolate electronic equipment and other sensitive components in aerospace applications in all

directions (axial and radial) [3]. In Figure 4.2, a sample Lord vibration isolator is given. In addition to compact design, these vibration isolators have high load carrying capacity.

AM series vibration isolators can be used in a temperature range of -50°C to $+150^{\circ}\text{C}$ and they have high damping and linear deflection characteristics. In the catalog of AM series vibration isolators of Lord Corporation [3], axial and radial stiffness values, static load capacities, maximum dynamic amplitudes, typical transmissibility plots and other useful performance data are presented. Temperature and frequency dependent stiffness and damping information is not given in the catalog. If needed, frequency and temperature dependencies of Lord brand vibration isolators must be obtained through in-house experiments performed on sample isolators.

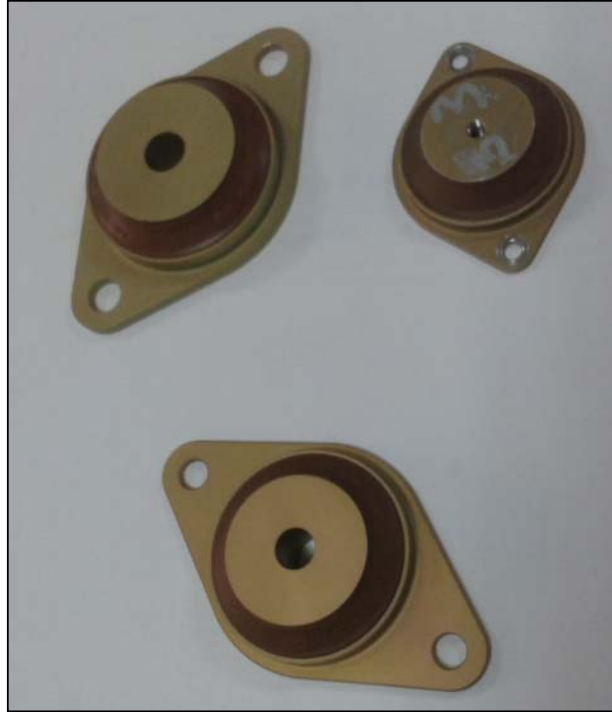


Figure 4.2 A sample conical vibration isolator by Lord Company

4.1.2 Barry Brand Isolators

For Barry brand vibration isolators, their types and properties are given in its product catalog [16]. Looking at the catalog, it can be seen that, 6300/6550 series isolators have properties that can be used for applications of ROKETSAN A.Ş. (carrying static loads in all directions and the ratio of radial to axial stiffness being close to 1). Isolator properties for Barry brand isolators are given in a similar fashion compared to the isolator catalog for Lord products. Temperature and frequency dependent stiffness and damping information of Barry brand isolators are also not given in the company catalog.

4.1.3 Laspar Brand Isolators

Sample catalog information of Laspar Company's conical vibration isolator is given in [17]. There is not any information related to properties in radial direction, but axial stiffness, maximum load force and deflection at maximum load are given.

4.2 VIBRATION ISOLATORS USED IN SIMILAR APPLICATIONS

Lord brand AM type vibration isolators are used for similar applications in ROKETSAN A.Ş. These vibration isolators are used to isolate electronic equipment and sensitive parts used for aerospace applications from low profile vibrations in both radial and axial directions.

An AM005 series low profile elastomer vibration isolator is cut from its center axis in order to better investigate its geometrical details (see Figure 4.3). Since conical vibration isolator will be designed within the scope of this thesis study, it will be benefitted from this geometry while constituting the conceptual design of the isolator.



Figure 4.3 Section view of AM005 series vibration isolator

4.2.1 Properties of Vibration Isolator

From the catalog of Lord Company, properties of AM-005-2 isolator can be obtained which are the maximum static load per mount (2.7 kg), maximum dynamic input at resonance (0.91 mm), weight (7.7 g). As performance characteristics, axial natural frequency, axial and radial dynamic spring rate are also given. Nominal properties of AM-005-2 vibration isolators are also obtained from characterization tests of which are done in Bayrak Plastik.

4.2.2 Tests Conducted on Vibration Isolators

Axial-radial dynamic characterization and static tests of low profile AM-005-2 vibration isolator were also conducted. These tests are done by Bayrak Plastik, a rubber company located in Bursa. Test system present in Bayrak Plastik contains "MTS 831.50 Elastomer Test System" and "MTS 651 Environmental Chamber". It has a maximum testing frequency of 1000 Hz and 10 kN load capacity (Figure 4.4).



Figure 4.4 MTS test system in Bayrak Plastik

Dynamic tests were conducted at -40, -20, 25, 40 and 70 °C temperatures, 0 – 200 Hz frequency range in both axial and radial directions. Static tests were also done with the same temperatures in axial and radial directions. Axial and radial test configurations are shown in Figure 4.5. Frequency dependent test results (axial dynamic stiffness, axial loss factor, radial dynamic stiffness, and radial loss factor) at various temperatures are given in Figure 4.6, Figure 4.7, Figure 4.8 and Figure 4.9, respectively.

When the test results are investigated, it can be easily seen that the change in the stiffness in both axial and radial directions between the temperatures -40 °C and +70 °C at a specified frequency is less than %100 which is a pretty good value. Additionally, loss factor is in the range of 0.35 – 0.55 for the temperatures at which tests were done. Radial and axial stiffness values are also very close to each other, which is a desired property for conical isolators. Additionally, when the test results are examined, it can be realized that there is very limited information about dynamic properties of isolators in their catalog.

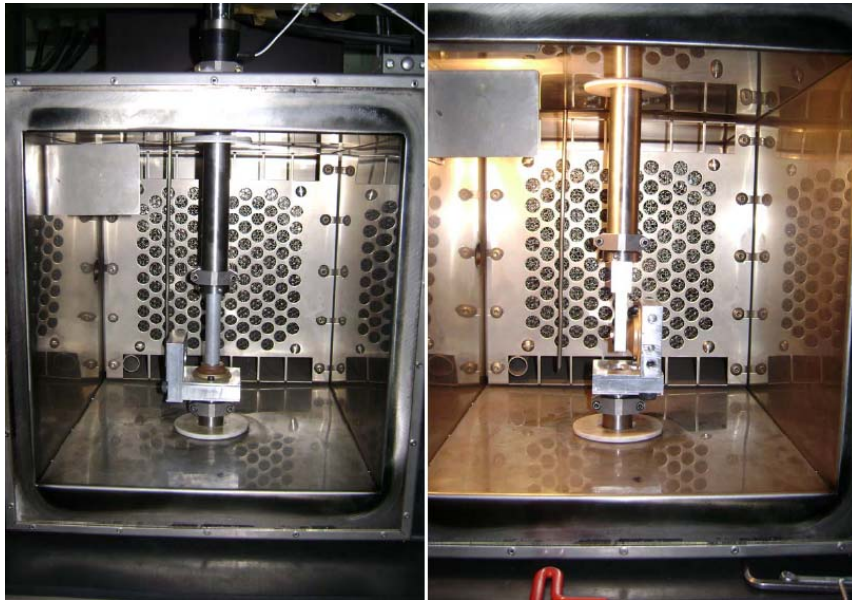


Figure 4.5 Axial (left) and radial (right) test configurations

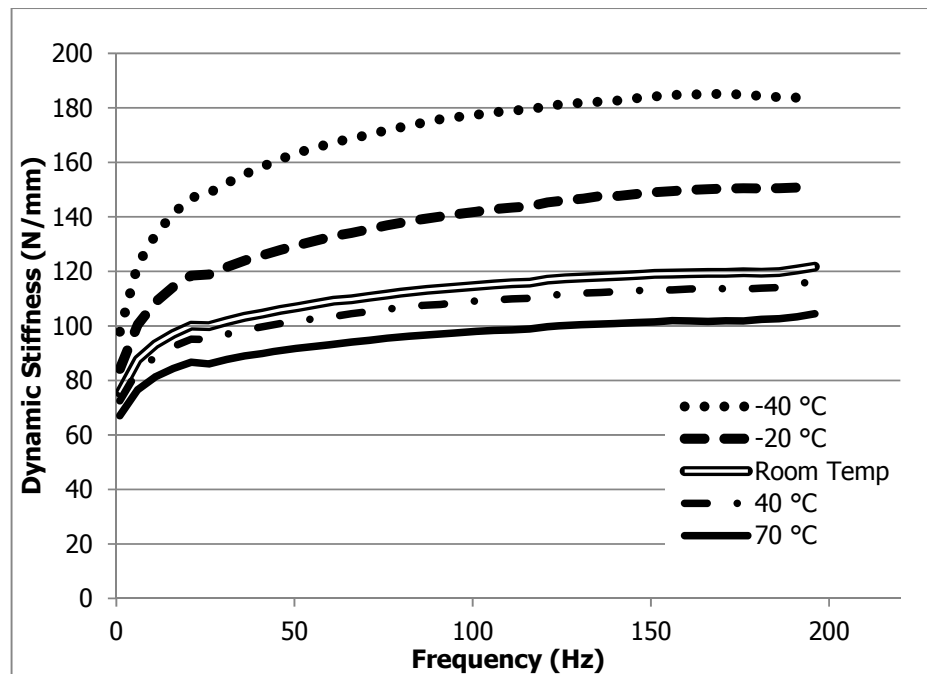


Figure 4.6 Frequency Dependent Axial Dynamic Stiffness of AM-005-2 Isolator

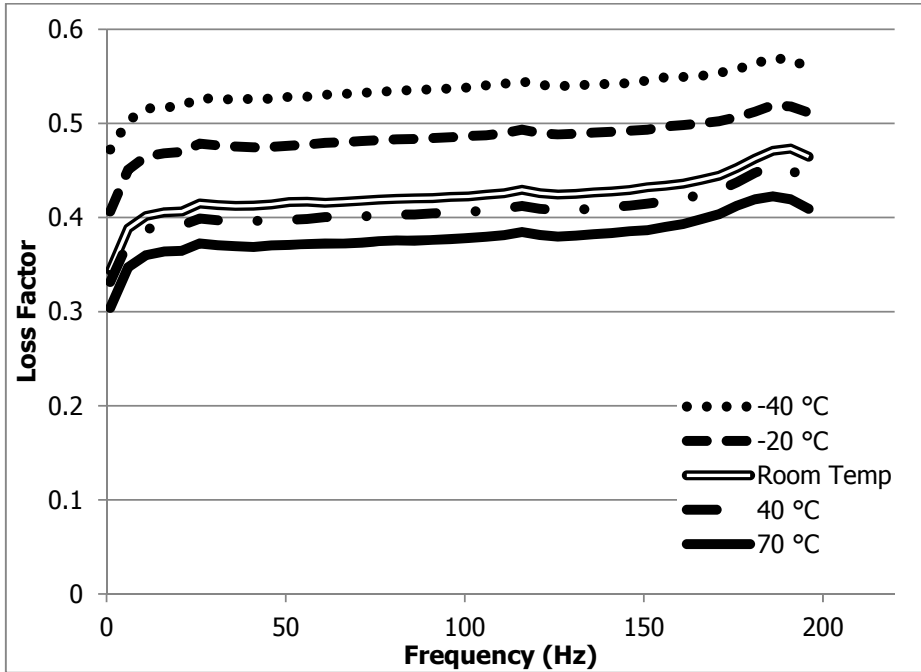


Figure 4.7 Frequency Dependent Axial Loss Factor of AM-005-2 Isolator

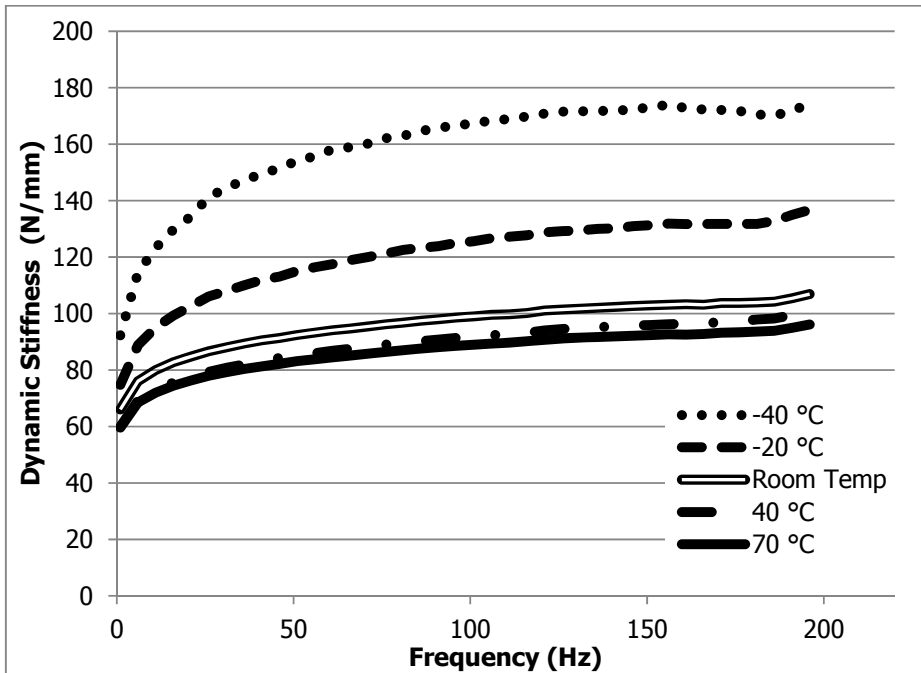


Figure 4.8 Frequency Dependent Radial Dynamic Stiffness of AM-005-2 Isolator

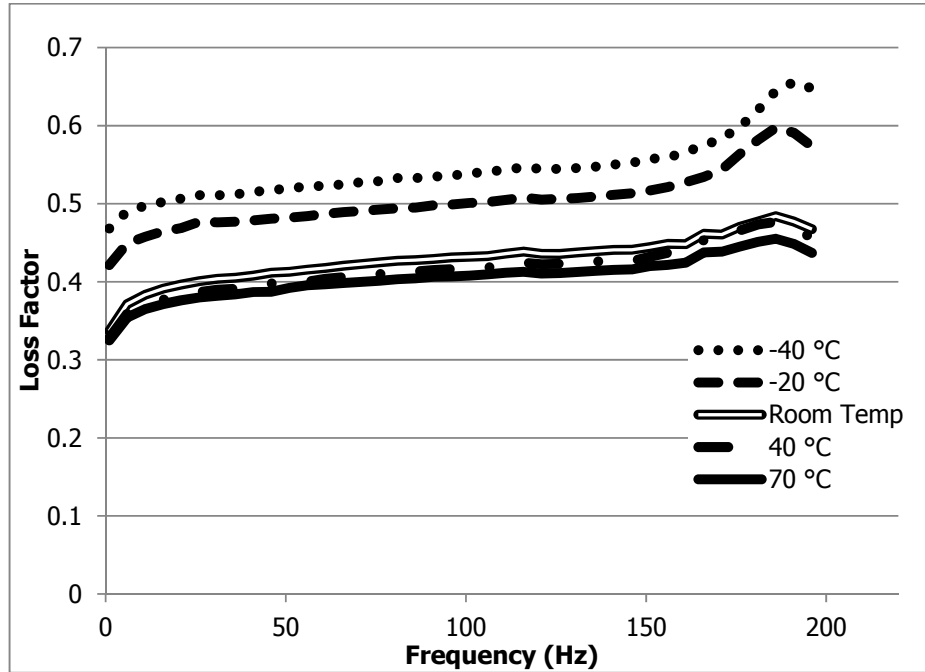


Figure 4.9 Frequency Dependent Radial Loss Factor of AM-005-2 Isolator

4.3 DETERMINATION OF ISOLATOR'S CONCEPTUAL DESIGN

Vibration isolators that are used to mount electronic equipments for applications of ROKETSAN A.Ş. should have sufficient isolation performance in all directions. Therefore, vibration isolators that will be designed in the scope of this thesis should have similar isolation behavior in both axial and radial directions. Elastomeric vibration isolators having this type of behavior are generally conical in geometry (as discussed in previous sections of this thesis), that is, dynamic stiffness in axial and radial direction is close to each other. Thus, vibration isolator to be designed in this thesis will be in conical structure to satisfy similar isolation performance in axial and radial directions.

According to all these investigations, final conceptual design of the vibration isolator is determined as shown in Figure 4.10. In this figure, 2D section view of the isolator is demonstrated. Parametric finite element model will be constituted to model this generic geometry.

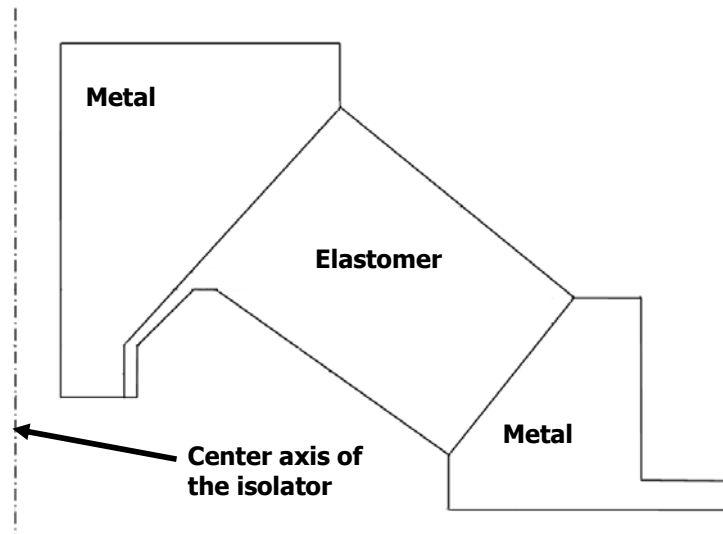


Figure 4.10 Generic geometry (conceptual design) of the isolator

CHAPTER 5

ELASTOMERIC MATERIALS AND CHARACTERIZATION TESTS

Vibration isolator that will be designed in this thesis is of elastomeric conical type isolator. Elastomeric vibration isolators that are being used in aerospace applications have many advantages compared to others. Pouring in any kind of shape, having different stiffness values from low to high, damping behavior higher than metals, fulfilling the minimum mass and volume requirements, binding to metals effectively are some of the reasons and properties of elastomers to be used in vibration isolators commonly. In this chapter, some common rubbers are selected in order to identify their dynamic characteristics. So as to do that, tensile and shear material specimens are manufactured and their dynamic modulus and loss factor properties are attained using the test system in ROKETSAN A.Ş. Dynamic properties that will be found will constitute input for analyses of vibration isolator to be designed.

5.1 DESIRED PROPERTIES OF ELASTOMERS IN THE ISOLATOR DESIGN

Elastomer material that will be used in a conical vibration isolator should have some desired properties in order to provide a good isolation performance for the isolator. One of the most important parameters for good isolation performance of an elastomer isolator is having high loss factor for the elastomer within the operational temperature range. If high loss factor is achieved for the elastomer being used in the isolator, vibration levels at resonant frequencies of transmissibility plots will be low. Another required property of an elastomer in order to improve the isolation performance is to have a glass transition temperature T_g as low as possible. This brings about less stiffening behavior at low temperatures of the operational temperature range compared to elastomers with higher T_g . In parallel with this, an elastomer material that will be used in the design of a vibration isolator is preferred to be in rubbery region within the operational temperature range for the isolator so that dynamic stiffness of isolator do not deviate from its nominal value with changing temperature [15].

In this study, as mentioned before, vibration isolator should operate effectively from -30 °C to +65 °C temperature range. Additionally, so as to give g_{rms} vibration output under a specified value (in this case under 1 g_{rms}), elastomer material should preserve its elasticity at low temperatures around -30 °C. Some standard materials in the market were investigated and their properties were given in the next subsection.

5.2 SELECTION OF ELASTOMER SPECIMENS FOR DYNAMIC CHARACTERIZATION

Some standard elastomeric materials with different hardness values were selected in order to do dynamic characterization. Output of dynamic characterization of an elastomer is frequency dependent complex modulus (E^*). Complex modulus can be expressed as:

$$E^* = E'(1 + \eta) \quad (5.1)$$

where E' is frequency dependent storage modulus and E'' is frequency dependent loss factor. Elastomeric materials of EPDM (Ethylene-Propylene Rubber) (50 and 80 Shore A), Neoprene (50 and 80 Shore A), and Silicone (50 and 80 Shore A) were selected for dynamic characterization. Note that Shore A is a hardness measure for viscoelastic materials and is also an indicator of static modulus of the elastomer [6]. For example, if an elastomer has a Shore A hardness value of 50, the static Young's Modulus of that elastomer is expected to be close to 2.5 MPa.

Material specimens for the selected elastomers were supplied from Bil-Plas, a rubber company in Ankara. Material specimens were obtained for both tension/compression (30x30x60 mm in dimension) and shear (5x5x50 mm in dimension) tests.

Dynamic characterization tests were conducted with the test system (shown in Figure 5.1) installed in ROKETSAN A.Ş. Since it is assumed that conical elastomer vibration isolator will operate in tension-compression mode, characterization tests were done mainly for tensile specimen. For a selected elastomeric material, shear tests were achieved in order to check the relation of $E = 3G$ with the incompressibility assumption of the material.

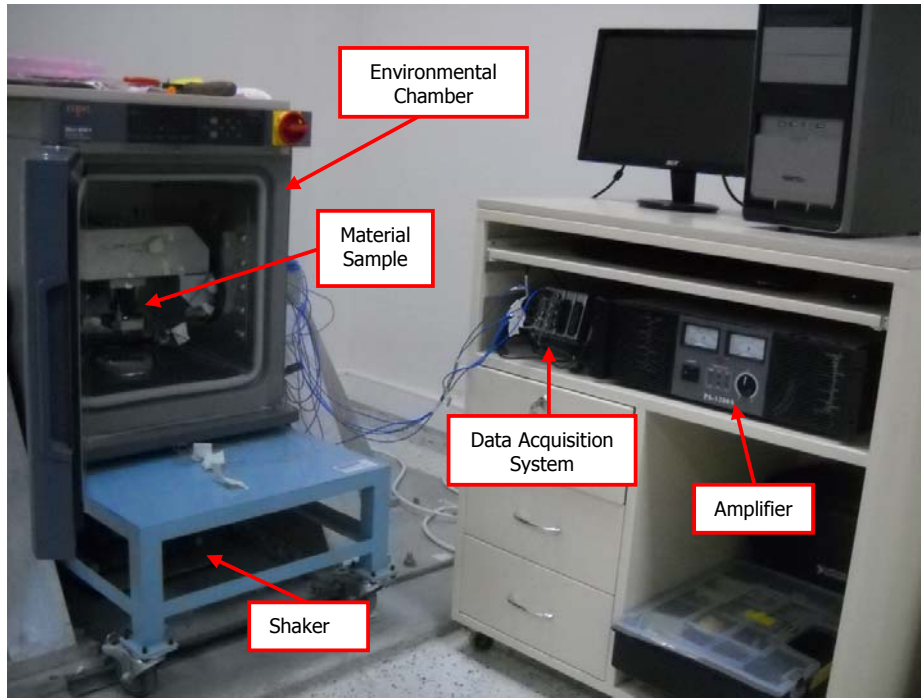


Figure 5.1 Elastomer material dynamic characterization test system

For temperature control, there is ESPEC SU-661 environmental chamber with temperature range of -60/+150 °C and 64 liters of internal volume. This chamber has two holes with maximum diameter of 100 mm at both sides (left and right) for entrance of supporting beams of the test system frame and sensor cables. Test set up contains DL Vibration ESD-045 shaker with maximum force amplitude for sinusoidal wave of 450 N. For response measurements, there are four PCB 352B piezoelectric accelerometers each with a sensitivity of 1000 mV/g. For force measurement, there is one PCB 208C02 piezoelectric force transducer with a sensitivity of 11.2 mV/kN. Since temperature dependent measurements on the elastomer sample and the test frame are required, T type thermocouples are present

within the test system. Locations of accelerometers, force transducer and thermocouples are given in Figure 5.2.

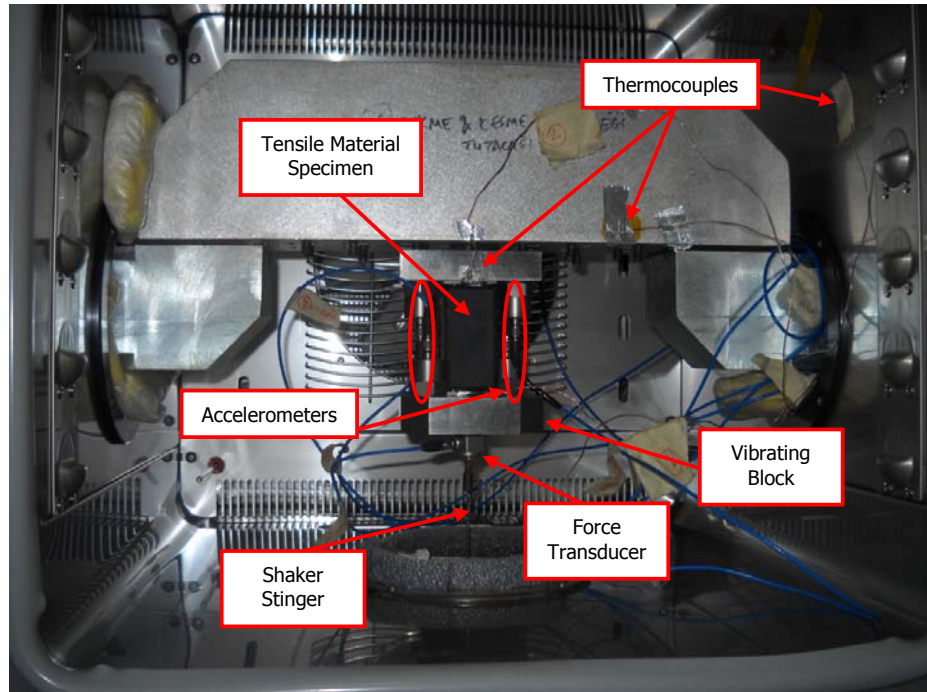


Figure 5.2 Tensile elastomer material specimen and force transducer, accelerometers, thermocouples locations

For data acquisition system, National Instruments LabVIEW™ is being used as software. For measurement of the signals coming from force transducers and accelerometers, there are two National Instruments NI 9234 analog voltage measurement cards. In order to send out force input to the shaker, test set up has one National Instruments NI 9263 analog voltage signal generator card. Additionally, there is one National Instruments NI 9211 thermocouple card with 4 channels for the measurement of thermocouples. There is also National Instruments cDAQ-9174 chassis for computer communication of these cards via one USB cable.

During the tests, elastomer material is excited by random vibration input generated by the shaker. Tests were conducted at each temperature in the range of -55 – +75 °C with 5 °C increment between 0 to 800 Hz. Frequency dependent storage modulus and loss factor were saved at the end of each test (at each temperature) in order to post process the data.

Assuming that elastomeric materials, that were tested, show thermo-rheologically simple behavior, master curves for elastic modulus and loss factor of elastomeric materials were obtained using different temperature data. For master curves, frequency-temperature shift factors, corresponding to each temperature were obtained using Arrhenius model. Arrhenius model is defined as **[1]**:

$$\log[\alpha(T)] = T_A \left(\frac{1}{T} - \frac{1}{T_0} \right) \quad (5.2)$$

where T_0 is the reference temperature and T_A is slope of $\log[\alpha(T)]$ vs. $1/T$ linear equation.

Master curves of elastomeric materials, obtained using Arrhenius model, contain frequency and temperature dependent modulus and loss factor. Mathematical models with 15 parameters were fitted to these curves for both elastic modulus and loss factor. By this way, complex modulus of elastomeric materials for all temperatures (T) and frequency (f) can be found. Master curves of related elastomeric materials are given in APPENDIX A. Mechanical properties of tested elastomers within the scope of this thesis are also given in APPENDIX A.

CHAPTER 6

PARAMETRIC FEM GENERATION OF THE ISOLATOR

In this chapter, it is explained how finite element model of elastomeric vibration isolator is generated parametrically. For parametric finite element model of vibration isolator, Parametric Design Language of ANSYS (APDL) is used. Dynamic properties (frequency and temperature dependent dynamic modulus and loss factor) of elastomeric materials that were tested are used as inputs (calculated from fitted mathematical models with 15 parameters) for the finite element model. Parametric finite element model is constituted for two configurations: axial and radial. For both configurations parametric models are generated with same geometric parameters. The only difference is in the dimension of the finite element model. For axial static and harmonic analysis, since boundary and loading conditions are symmetric with respect to center axis of the isolator, 2D axisymmetric finite element model is generated. However, 3D model is established for radial analyses because loading is not symmetric with respect to center axis. For modal analysis, 3D finite element model is used. For each analysis type (static, modal and harmonic analyses), geometric, material, analysis options, configuration, etc. variables are taken as parameters and they can be changed interactively. Boundary and loading conditions are described for each analysis in the other subsections. Finite element codes that have been generated in this part will be used for the design iterations of the vibration isolators.

6.1 INTRODUCTION

Elastomeric vibration isolators, of which technical requirements were determined, should be examined according to their isolation performance with different geometries and elastomeric materials. Therefore, in order to generate detailed design of vibration isolator, satisfying these requirements, many analyses should be conducted with different parameters (geometry, material, temperature, etc.). Since constituting analysis model from beginning again when the parameters change and getting the results are very time consuming, this process should be automated. Thus, a code should be written in a finite element program in order to constitute vibration isolator geometry parametrically and to enter frequency dependent properties of different elastomer material at any temperature. So as to do that "Parametric Design Language, APDL" of ANSYS [24] was used.

Different parametric finite element models of the vibration isolator should be established for different analyses configurations. For axial analysis, since the isolator geometry and boundary/loading conditions are symmetrical with respect to isolator axis, parametric model is created as 2-D axisymmetric. For radial analysis, however, loading condition is not symmetric with respect to axis of the isolator, so 3-D parametric analysis model was used. Using parametric model created for static analysis, static stiffness of the isolator both in axial and radial directions can be obtained. Additionally, stress values on the elastomeric materials should be checked whether they are critical or not. Parametric model that was established for modal analysis can be used to determine the natural frequencies and mode shapes of the isolator. In order to obtain frequency dependent dynamic stiffness and loss

factor of the isolator both in axial and radial directions, parametric finite element analysis code, generated for harmonic analysis, can be used.

While constituting analysis models with different geometrical parameters, geometric parameters should be within the geometric limits of the isolator. Besides, maximum variation of isolator stiffness within the temperature range, specified at technical requirements, should not exceed the limits at technical requirements. Technical requirements stated at previous sections were evaluated as a guide for final elastomeric isolator design. In this whole process, ANSYS APDL was used. Using APDL of ANSYS, analysis models can be created via commands. With this property, models whose geometry depends on too many parameters can be constructed in an APDL code by writing mathematical relationships between the parameters. The advantage of the code similar to this emerges if too many iterations with different parameters are required in design work.

6.2 GENERATION OF VIBRATION ISOLATOR PARAMETRIC MODEL

In Figure 6.1, geometrical parameters on the final vibration isolator conceptual design (constituted in *Chapter 4*) are shown. There are 21 parameters in this geometry. However, some parameters can be expressed as a function of the other parameters. Therefore, 3 dependent parameters (in this case g , p , and σ are assumed as dependent) were not used directly in APDL codes. Independent geometric parameters used in parametric model are a , b , c , d , e , f , h , k , m , n , t_1 , o , l , α_{up} , α_{low} and γ ; a total of 18. The angle of external surface of elastomer with vertical is named as "conical angle". Conical angle value is affecting the static and dynamic stiffness of the vibration isolator. Axial and radial stiffness can be tuned by changing the conical angle. Since it is required for conical vibration isolators to have axial and radial stiffness close to each other, this parameter can be used in order to ensure this case [3].

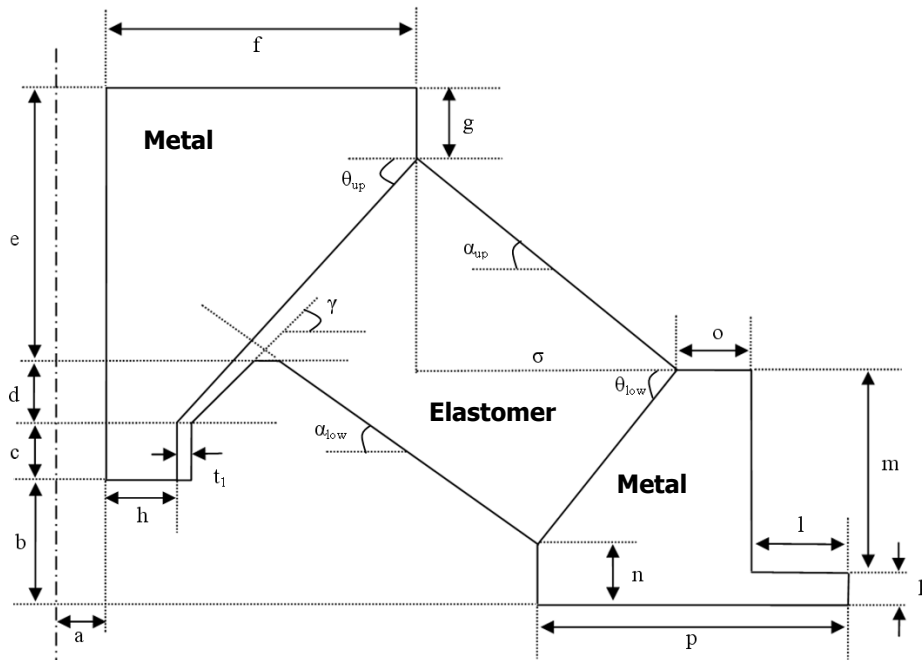


Figure 6.1 Geometrical parameters determined on the final conceptual design of the isolator

While generating finite element model of the isolator, at first, independent geometric parameters mentioned above were entered into ANSYS. Using command written in APDL, user defined values of the parameters were utilized in the finite analysis model. Sample data entrance window that was used for this purpose is shown in Figure 6.2.

Parameters	Default values
a	2
b	5
c	2.5
d	2.5
e	12
f	15
h	3
teta_up	45
alfa_up	40

Figure 6.2 Getting geometric parameters into the ANSYS

After getting geometric parameters into ANSYS, key-points were generated according to x and y coordinates calculated using parameter values. Then, using these points, lines were constructed using a command of APDL. At this point, radiuses were created at some intersection points. After that, areas were generated for each isolator's component. Figure 6.3 shows these generated areas. This geometry was used directly for 2-D axisymmetric analysis. For 3-D model, however, volumes were established by sweeping the areas about the center of isolator 360°. 2-D surface model and 3-D solid model are displayed in Figure 6.4. In both cases, components (surfaces for 2-D, volumes for 3-D) were glued in order to provide tracing of elements when meshes are constituted. Passing to the other steps was accomplished after this process.

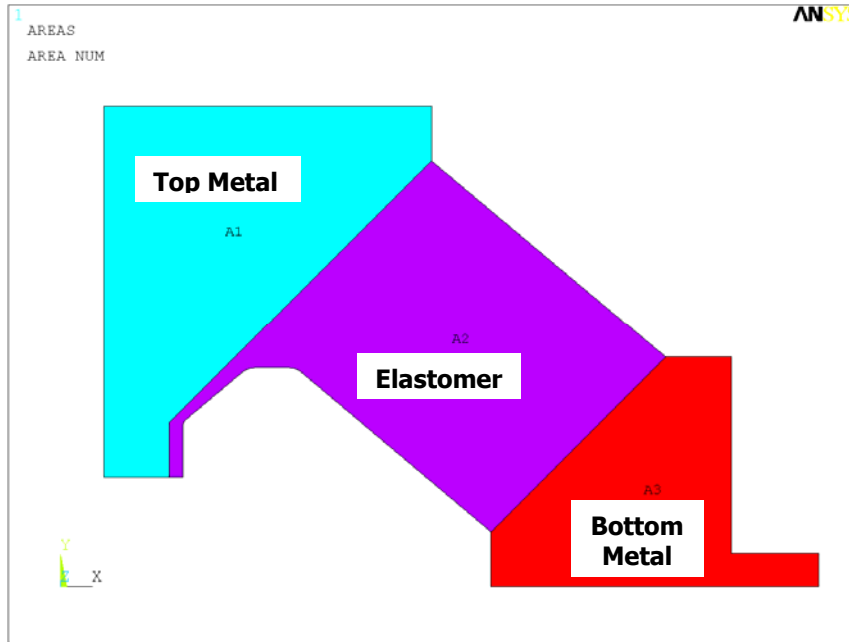


Figure 6.3 Areas for each component of the vibration isolator

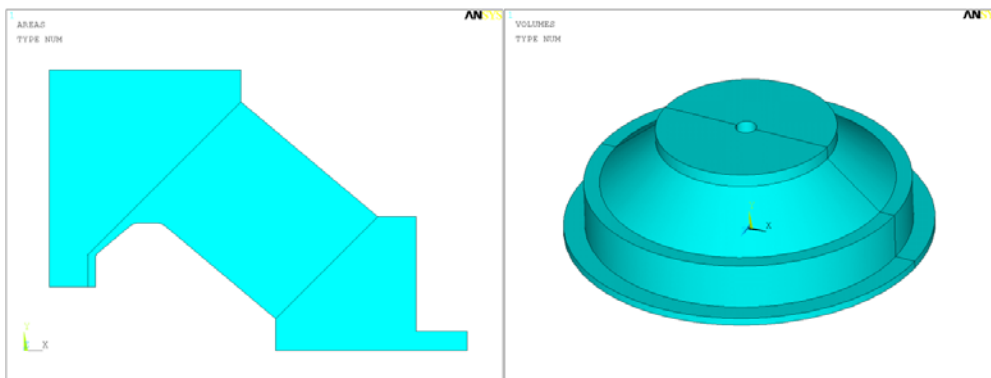


Figure 6.4 2-D surface model (left) and 3-D solid model (right)

Element size can also be tuned by a command and different mesh densities can be obtained using this element size parameter. Figure 6.5 displays finite element models with different element sizes for both 2-D and 3-D models.

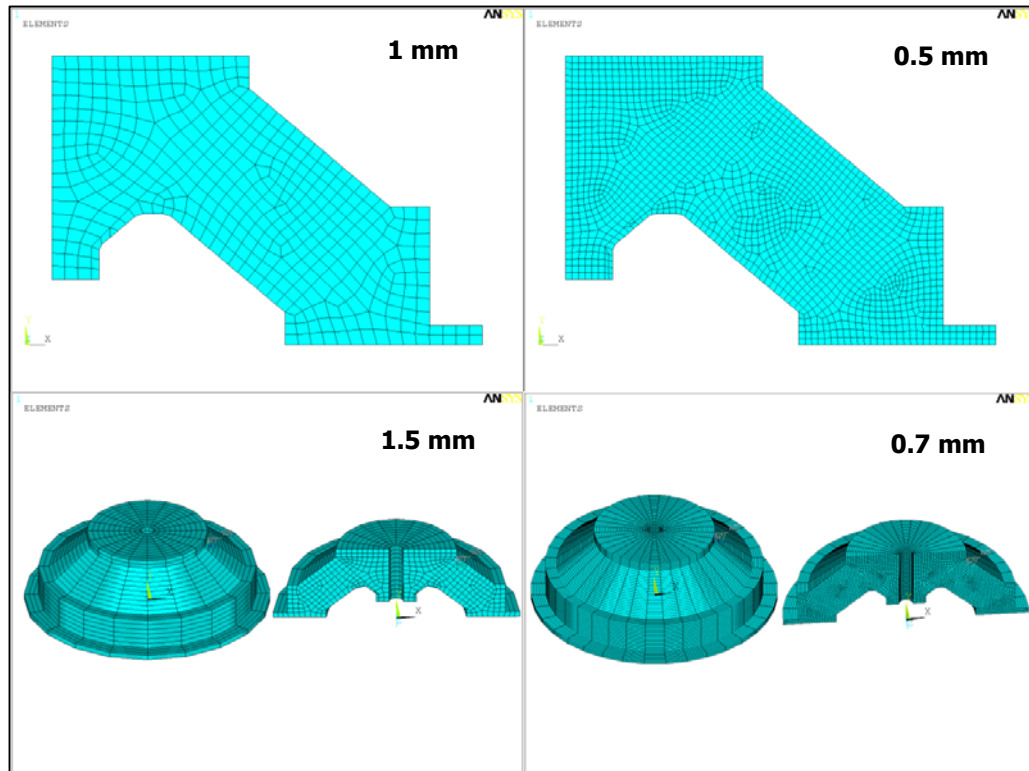


Figure 6.5 Finite element models with different element sizes

After generating the mesh, commands that will be related to material properties (elastic modulus, Poisson's ratio, and density) of top and bottom aluminum components were added to the code. Depending on the analysis type, material properties of elastomeric materials were supplemented to the code in two different ways. For static and modal analysis, elastic modulus value in rubbery region of the elastomeric materials was used. For harmonic analysis, however, frequency dependent elastic modulus and loss factor, obtained from characterization tests, were utilized.

As mentioned before, a mathematical model with 15 parameters was fitted to experimental data obtained from the material characterization tests of each elastomeric material. This model depends both on temperature and frequency. In other words, with this model, dynamic modulus and loss factor of an elastomer can be found for a specific temperature and in a specified frequency range. Thus, for harmonic analysis, temperature input and frequency information of harmonic analysis were used in order to calculate dynamic modulus and loss factor of each elastomeric material.

6.3 BOUNDARY/LOADING CONDITIONS OF THE ANALYSES

Using parametric model of the vibration isolator, static, modal and harmonic analyses of the isolator will be conducted. Separate APDL codes were prepared for each analysis. Boundary and loading conditions of modal, static and harmonic analyses are explained in the following sections, respectively.

6.3.1 Modal Analysis

3-D solid model was used for modal analysis of the vibration isolator. They were achieved with two different boundary conditions: free – free and fixed – free. Fixed – free boundary condition is represented in Figure 6.6.

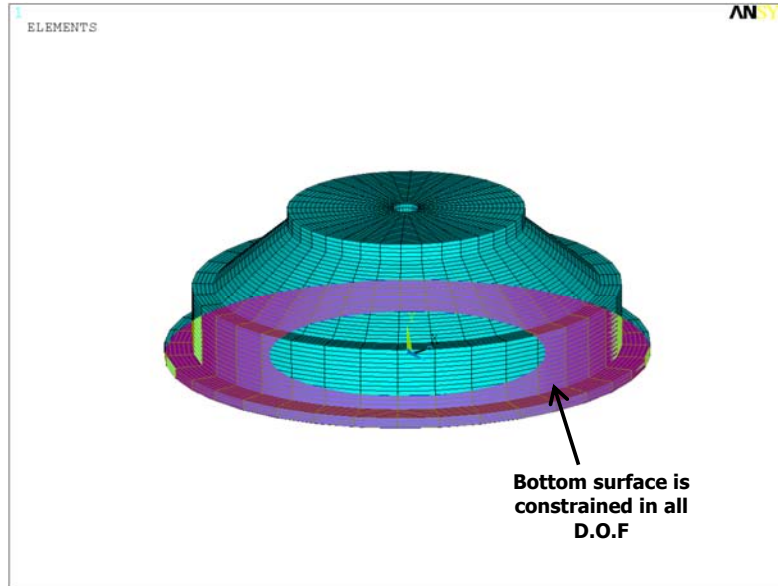


Figure 6.6 Fixed – free boundary condition for modal analysis

6.3.2 Static Analysis

Static analysis of the elastomeric vibration isolator was done both in axial and radial directions. Thus, two different analysis models (2-D and 3-D) were established in APDL code.

6.3.2.1 Axial Static Analysis

By axial static analysis of the isolator, axial static stiffness of the component and stress gradient in the elastomeric material will be obtained using 2-D axisymmetric analysis model. Boundary and loading conditions used in axial static analysis are displayed in Figure 6.7. Pressure corresponding to 50 N axial load is applied at the top region. Bottom region, shown in figure, was constrained in all D.O.F. In this case, axial static stiffness can be found by force – displacement ratio.

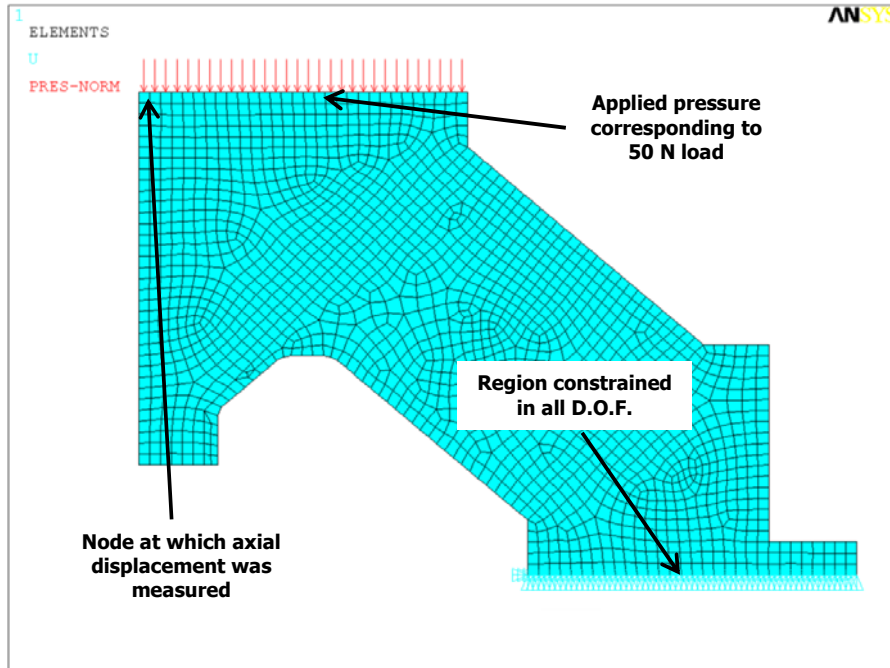


Figure 6.7 Boundary and loading conditions for axial static analysis

6.3.2.2 Radial Static Analysis

For radial static analysis, 3-D analysis model is used. Radial static stiffness and stress gradient for this loading case can be obtained by this analysis. Boundary and loading conditions used in radial static analysis are displayed in Figure 6.8. RBE2 connection was applied between the cylinder surface and a point at the center of this cylinder shown in Figure 6.8. Then, 50 N radial force is applied at that point. Surface, shown in figure, of bottom aluminum component is constrained in all D.O.F. In this case, radial static stiffness can be found in a similar way.

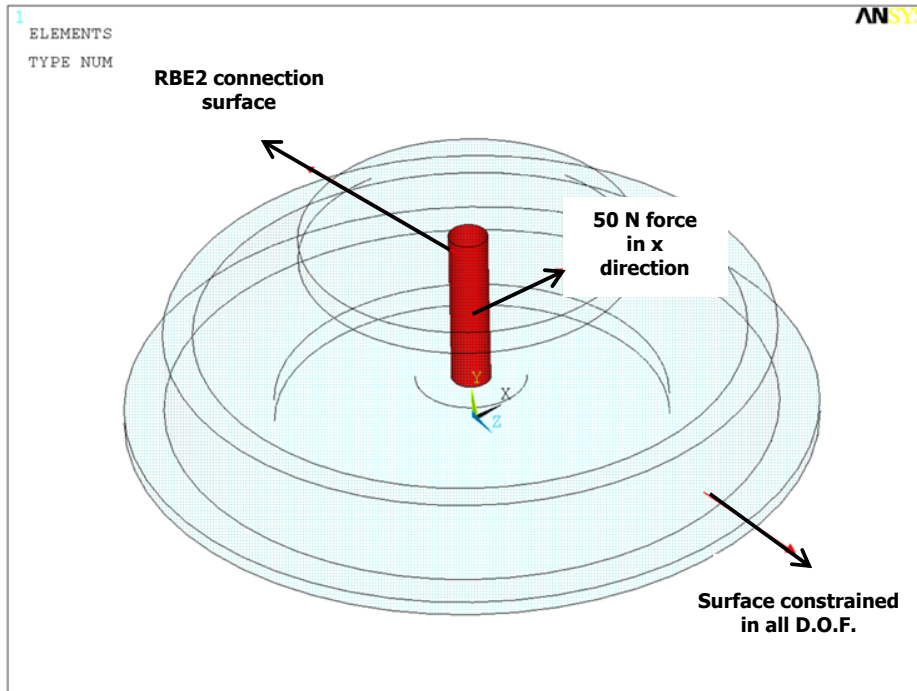


Figure 6.8 Boundary and loading conditions for radial static analysis

6.3.3 Harmonic Analysis

Similar to static analysis, in order to find dynamic properties of the isolator two different analyses model are utilized. For axial harmonic analysis, 2-D axisymmetric analysis model and for radial harmonic analysis, 3-D analysis model are used.

6.3.3.1 Axial Harmonic Analysis

Boundary and loading conditions for axial harmonic analysis is given in Figure 6.9. Point 1 and point 2 are connected to bottom and top lines displayed in Figure 6.9 with RBE2, respectively. Point 1 is constrained in all D.O.F. and harmonic force is applied at point 2 in axial direction. After achieving steady-state frequency response analysis, harmonic reaction force at point 1 and harmonic displacement response at point 2 will be measured. Both of them have real and imaginary parts because of damping properties of the elastomer. Then, axial complex stiffness of the vibration isolator can be obtained by dividing harmonic reaction force with harmonic displacement response in complex numbers. Real part of complex stiffness gives the frequency dependent dynamic stiffness and the ratio of imaginary part to real part gives the frequency dependent loss factor.

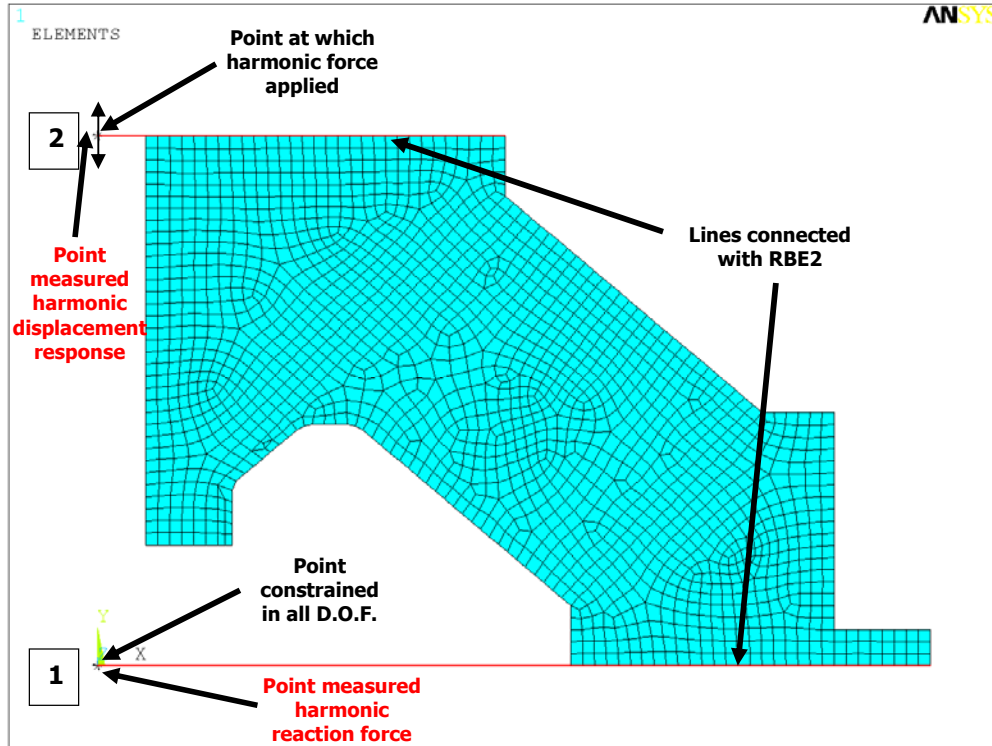


Figure 6.9 RBE2 connections, boundary and loading conditions for 2-D axisymmetric model

6.3.3.2 Radial Harmonic Analysis

Boundary and loading conditions for radial harmonic analysis is given in Figure 6.10. Point 1 and point 2 are connected to bottom and cylinder surfaces displayed in figure with RBE2, respectively. Point 1 is constrained in all D.O.F. and harmonic force is applied at point 2 in radial direction. Likewise, radial complex stiffness of the vibration isolator can be obtained by dividing harmonic reaction force (obtained at point 1) with harmonic displacement response (obtained at point 2) in complex numbers. Finally, radial frequency dependent dynamic stiffness and loss factor can be obtained from the complex stiffness.

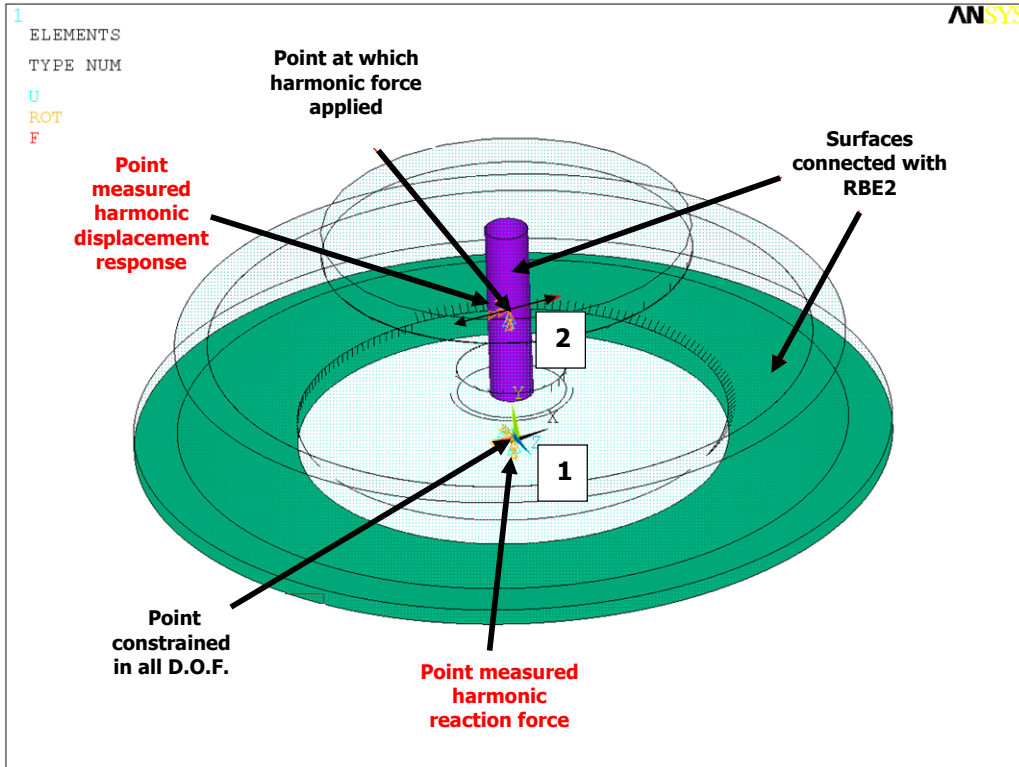


Figure 6.10 RBE2 connections, boundary and loading conditions for 3-D model

CHAPTER 7

CONVERGENCE STUDIES AND ANALYSES RESULTS

In this chapter, studies related to convergence of all analyses results are explained. Analysis results with different element sizes are given for static, modal and harmonic analysis for each configuration (axial and radial) for a specific geometric parameter set. EPDM 50 Shore A elastomeric material is utilized for the elastomeric material inputs. Convergence studies of static analyses are done according to static stiffness and maximum stress values for axial and radial configurations separately. For convergence of dynamic analysis, natural frequency results of the vibration isolators for 2-D and 3-D are taken into account. Optimum element sizes which make possible to obtain pretty good results in a short time are determined for all analyses. Design iterations, details of which will be given in *Chapter 8*, will be accomplished with these element sizes. During the design iterations all inputs and outputs of the analyses will be saved. Details about this subject are also given in this last subsection of this chapter

7.1 CONVERGENCE ANALYSES

Convergence analyses are done on the axisymmetric and full analyses models separately. In these analyses a specific parameters set are used with EPDM 50 Shore A elastomer material properties. Convergence studies are accomplished both for static and dynamic analyses. For dynamic analyses, modal analyses of the isolator are done with fixed – free boundary conditions and values of first 3 natural frequencies are taken into account for the convergence. For static analyses, static stiffnesses in axial and radial directions are calculated with different element sizes and it is investigated whether stiffness values has converged or not. In order to have a high quality mesh within the volumes, glue contact between them in 3-D model were defined and analyses (static and dynamic) are carried out with this model. Results are then compared with the others obtained by APDL codes for 3-D models. This is achieved for 2-D axisymmetric analyses with the model having 0.05 mm element size. Optimum element sizes for all analyses are determined after that.

7.1.1 Convergence of Axial Analyses

Convergence analyses for axial finite element models are studied with 4 different element sizes. These are shown in Figure 7.1. Load and boundary conditions (for both static and dynamic analyses) mentioned in *Chapter 3* will be applied to the models.

Axial static stiffness values and their differences with the stiffness value obtained with 0.05 mm element size are given in Table 7.1. Additionally, von Mises stresses are compared using the results of each axial static analysis. First, path at which stresses are critical are determined and stress values are noted at specific regions (head, middle, and end) on the path. In Figure 7.2, von Mises stress gradient is shown for EPDM 50 Shore A. Besides, von Mises stress values at these regions and their differences with the stress values obtained

with 0.05 mm element size are given in Table 7.2. At regions 1 and 3 there is a stress singularity. Therefore, differences are a bit high as expected. Region 2 can be gotten into account for stress convergence.

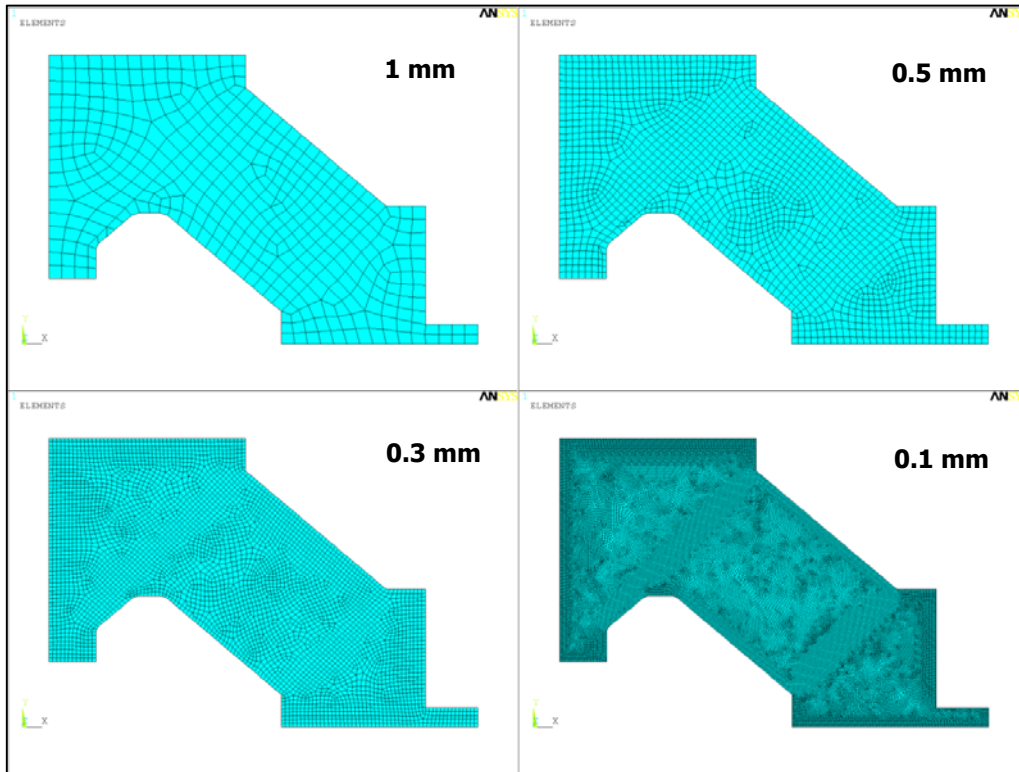


Figure 7.1 2-D axisymmetric models with different element sizes

Table 7.1 Stiffness values with different element sizes and percentage differences with the stiffness value obtained with 0.05 element size

1 mm element size		0.5 mm element size		0.3 mm element size		0.1 mm element size	
Stiffness value (N/mm)	Diff. (%)	Stiffness value (N/mm)	Diff. (%)	Stiffness value (N/mm)	Diff. (%)	Stiffness value (N/mm)	Diff. (%)
793.6	2	785.1	0.9	781.8	0.5	778.7	0.09

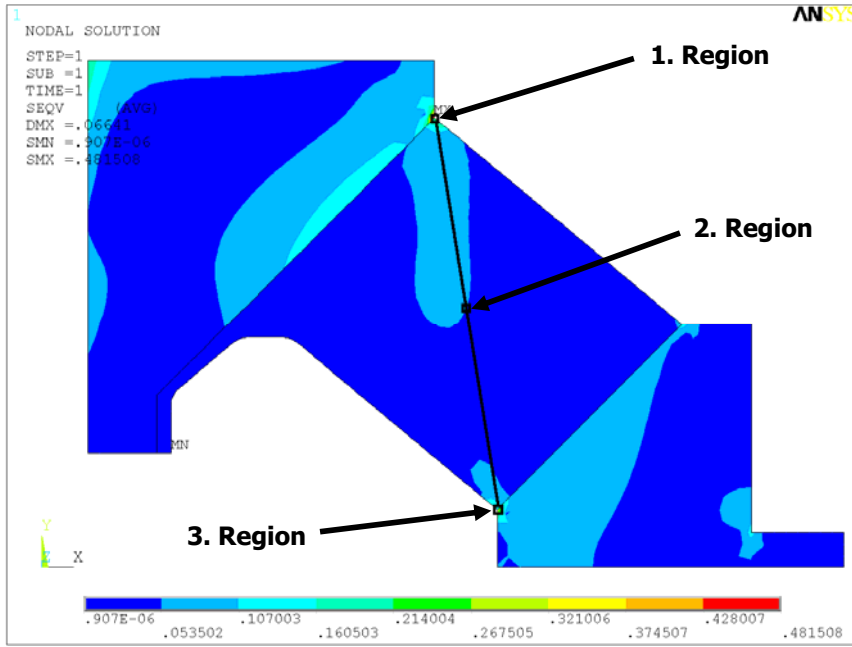


Figure 7.2 Von Mises stress distribution of the EPDM 50 ShA (2-D)

Table 7.2 von Mises stress values with different element sizes and percentage differences with the stress values obtained with 0.05 element size

	1 mm element size		0.5 mm element size		0.3 mm element size		0.1 mm element size	
	Stress (Mpa)	Diff. (%)	Stress (Mpa)	Diff. (%)	Stress (Mpa)	Diff. (%)	Stress (Mpa)	Diff. (%)
1. region	0.116	70.8	0.153	61.5	0.188	52.6	0.297	25.2
2. region	0.53E-1	0.9	0.53E-1	0.4	0.54E-1	0.2	0.535	0
3. region	0.17	71	0.224	61.8	0.276	52.9	0.4374	25.4

Isolator's first 3 axial modes, obtained by modal analyses, are shown in Figure 7.3. Related natural frequencies and their differences with the natural frequencies obtained using the model having 0.05 mm element size is represented in Table 7.3.

When all results are investigated, it could be concluded that 2-D axisymmetric finite element models with 0.5 mm element size give sufficiently good results for both static and dynamic analyses.

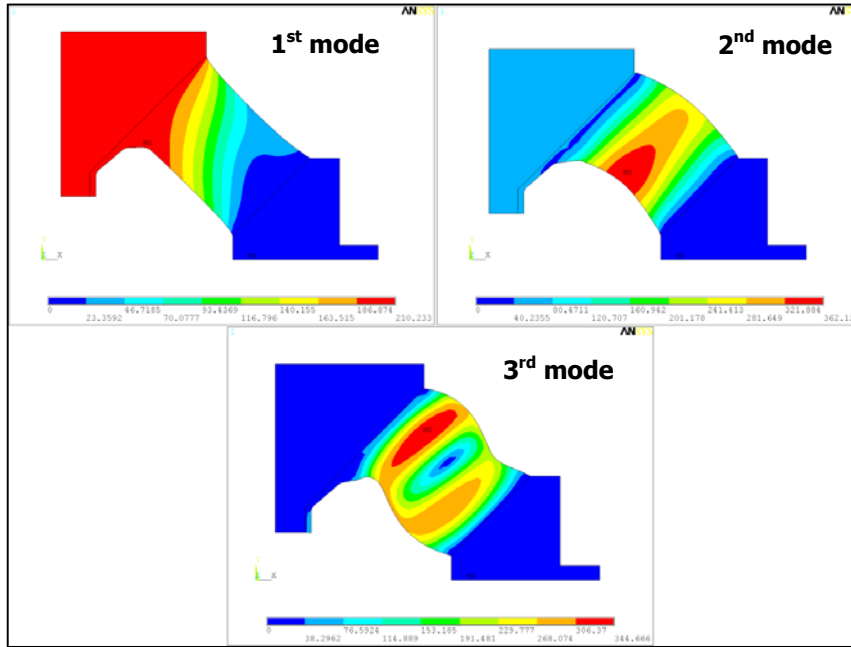


Figure 7.3 First 3 mode shapes of 2-D axisymmetric analysis model

Table 7.3 First 3 axial natural frequencies with different element sizes and percentage differences with the natural frequencies obtained with 0.05 element size

	1 mm element size		0.5 mm element size		0.3 mm element size		0.1 mm element size	
	Natural Frequency (Hz)	Diff. (%)	Natural Frequency (Hz)	Diff. (%)	Natural Frequency (Hz)	Diff. (%)	Natural Frequency (Hz)	Diff. (%)
1. Axial Mode	889.2	0.9	884.9	0.41	883.2	0.22	881.7	0.05
2. Axial Mode	2017.9	0.71	2009.6	0.29	2006.8	0.15	2004.3	0.03
3. Axial Mode	3615.2	0.14	3611.8	0.05	3610.8	0.02	3610.1	0

7.1.2 Convergence of Radial Analyses

Convergence analyses for radial finite element models (3-D model) are done for using 4 different element sizes. These meshes are shown in Figure 7.4. Load and boundary conditions (for both static and dynamic analyses) discussed in *Chapter 3* are applied to the models. As mentioned before, volumes with a high density mesh are combined to each other using glue contact. This model is given in Figure 7.5. Analysis results, obtained by this model, will be taken as reference for the convergence analyses.

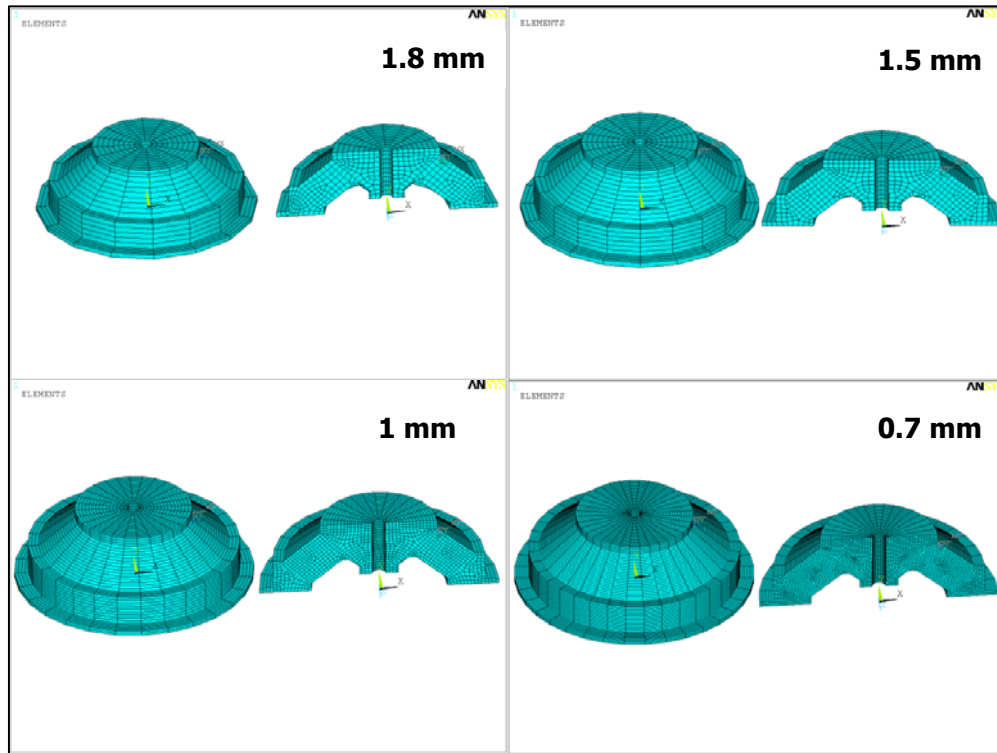


Figure 7.4 3-D models with different element sizes

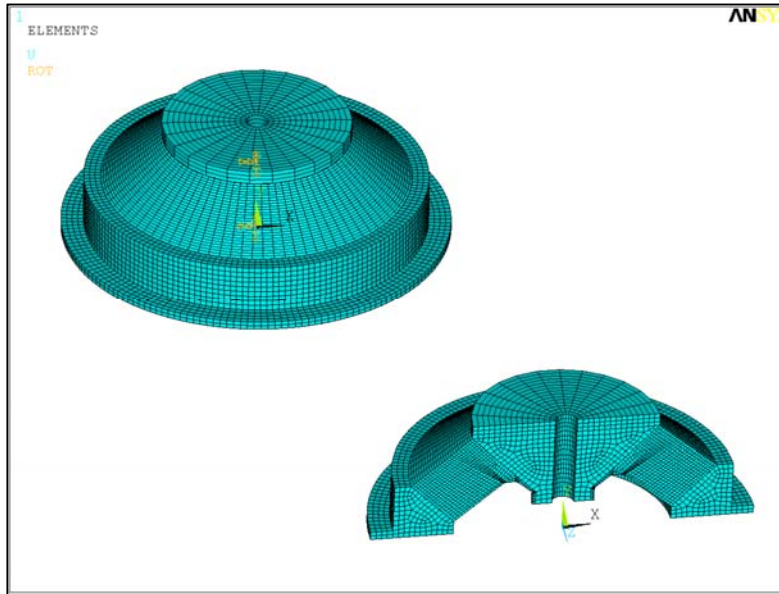


Figure 7.5 3-D finite element model with high density mesh (Reference model)

Radial stiffness values obtained from trial models and their differences with the stiffness value obtained using the reference finite element model with high density mesh are given in Table 7.4. Similar to axial static analyses, von Mises stresses were compared using the results of each radial static analysis. Path at which stresses are critical was decided and stress values were noted at specific regions on the path. Von Mises stress gradient for EPDM 50 Shore A is shown in Figure 7.6. Additionally, von Mises stress values at these regions and their differences with the stress values obtained with higher quality mesh are given in Table 7.5. Like the case for axial static analysis, at regions 1 and 3 there is a stress singularity. Therefore, differences are a bit high as expected. Region 2 can be gotten into account for stress convergence.

Table 7.4 Stiffness values with different element sizes and percentage differences with the stiffness value obtained with high quality mesh

1.8 mm element size		1.5 mm element size		1 mm element size		0.7 mm element size	
Stiffness value (N/mm)	Diff. (%)	Stiffness value (N/mm)	Diff. (%)	Stiffness value (N/mm)	Diff. (%)	Stiffness value (N/mm)	Diff. (%)
573.4	1.04	572.7	0.92	570.8	0.58	569.5	0.35

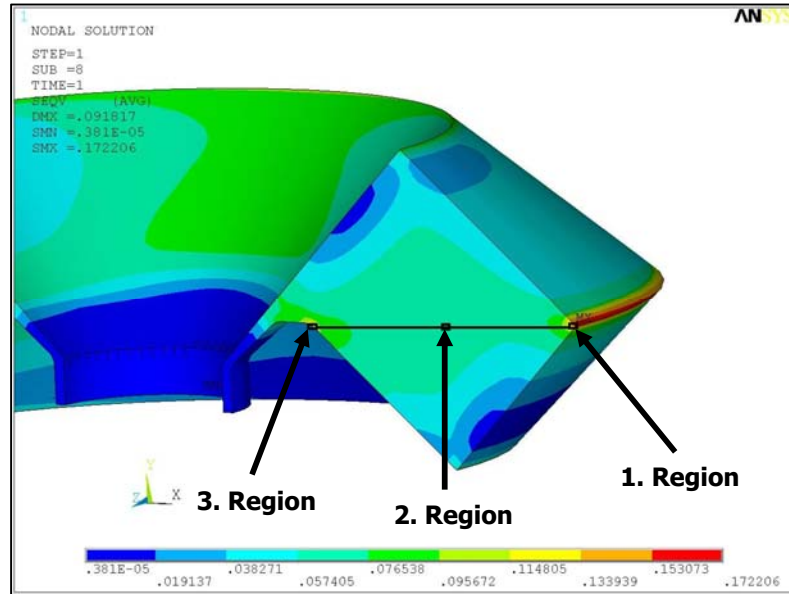


Figure 7.6 Von Mises stress distribution of the EPDM 50 ShA (3-D)

Table 7.5 Von Mises stress values with different element sizes and percentage differences with the stress values obtained with higher quality mesh

	1.8 mm element size		1.5 mm element size		1 mm element size		0.7 mm element size	
	Stress (Mpa)	Diff. (%)	Stress (Mpa)	Diff. (%)	Stress (Mpa)	Diff. (%)	Stress (Mpa)	Diff. (%)
1. region	0.111	38.3	0.118	34.4	0.136	24.4	0.153	15
2. region	0.725E-1	1.1	0.719E-1	0.3	0.719E-1	0.3	0.721E-1	0.6
3. region	0.996E-1	20.3	0.108	13.6	0.113	9.6	0.118	5.6

First 5 axial modes for 3-D analysis model with fixed – free boundary condition are given in Figure 7.7. Related natural frequencies and their differences with the natural frequencies obtained using the model having high quality mesh is given in Table 7.6.

To conclude, it could be said that 3-D analysis models with 1.5 mm element size give sufficiently good results in a short time compared to others. Therefore, 3-D models (both static and dynamic) can be prepared with this element size.

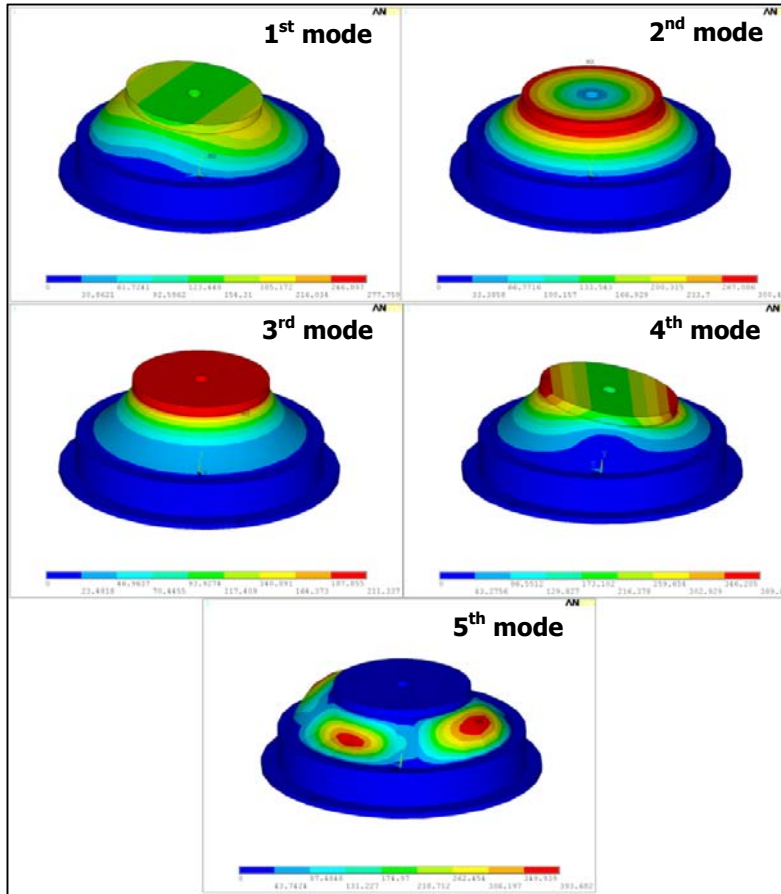


Figure 7.7 First 5 mode shapes of 3-D analysis model

Table 7.6 First 5 axial natural frequencies with different element sizes and percentage differences with the natural frequencies obtained with high quality mesh

	1.8 mm element size		1.5 mm element size		1 mm element size		0.7 mm element size	
	Natural Frequency (Hz)	Diff. (%)	Natural Frequency (Hz)	Diff. (%)	Natural Frequency (Hz)	Diff. (%)	Natural Frequency (Hz)	Diff. (%)
1. Mode	697.6	2.12	693.3	1.49	687.9	0.70	685.6	0.37
2. Mode	886.1	0.76	883.3	0.44	880.2	0.09	877.9	0.17
3. Mode	905.3	2.76	898.6	2.00	891.5	1.19	887.8	0.77
4. Mode	1149.9	1.83	1143.9	1.30	1137.1	0.70	1133.3	0.36
5. Mode	2003.4	3.56	1981.6	2.43	1959.8	1.31	1949.2	0.76

7.2 SAVING INPUTS AND OUTPUTS OF ANALYSES

Inputs and outputs of each analysis are and can be saved during design iterations. Related parameters like geometric dimensions, material, temperature, frequency range used in static, modal and harmonic analyses for each parameter set are saved at the end of the analyses by command written at analyses codes. For axial and radial static analyses, axial and radial static stiffness are calculated within the codes and assigned to a parameter in order to get directly from the file that is saved. For modal analysis natural frequencies are saved in a similar way. In harmonic analyses, getting frequency dependent reaction force and displacement, calculating complex stiffness using these parameters and obtaining dynamic stiffness and loss factor are all done in ANSYS APDL using the commands. Additionally, frequency dependent dynamic stiffness and loss factor are automatically saved in “.csv” file format.

CHAPTER 8

FINALIZATION OF THE DETAILED DESIGN

After constituting analyses file inputs and accomplishing convergence studies, in this chapter, design iterations are carried out. In the first iteration, for a set of parameters static analysis is performed. Radial and axial static stiffness values for all materials are calculated. For free-free and fixed-free boundary conditions, modal analyses are obtained. By axial and radial harmonic analyses, frequency dependent dynamic stiffness and loss factor of vibration isolator are obtained for three temperature values (-30, 25 and 65 °C). Performances of vibration isolators with different elastomeric materials at each temperature are evaluated by a Matlab code and the best elastomeric material that can be used in vibration isolator design is selected as EPDM 50 Shore A. In the second iteration, static and modal analyses are done with this material with different parameter set which would bring isolator performance closer to a point satisfying design requirements. One of the criteria in the vibration isolator design is to be the axial and radial dynamic stiffness values as close to each other as possible. In the third iteration this is achieved. Additionally, the performance characteristics of the vibration isolator are improved by the third parameter set. After design iterations had been completed, technical drawings of the final vibration isolator design are prepared. Prototypes of the isolator are manufactured according to these drawings by a local rubber company using the elastomer material (EPDM 50 ShA) selected. Dynamic characterization tests of manufactured prototypes are conducted in Bayrak Plastik. Finally, frequency-dependent dynamic stiffness and loss factor are compared with analysis results.

8.1 DESIGN ITERATIONS

In order to determine the detailed design of the isolator, analyses are accomplished with 3 different parameter sets. In Figure 8.1, geometric parameters of the isolator are shown again. Related geometric parameter values are represented in Table 8.1, for each parameter set.

Table 8.1 Geometric parameter values for 3 iterations

Parameters	Iteration1	Iteration2	Iteration3
a (mm)	2	2	2
b (mm)	5	2.7	2.7
c (mm)	2.5	0	0
d (mm)	2.5	2.2	2.5
e (mm)	12	7.8	7.5
f (mm)	15	10.3	10.3
h (mm)	3	2.5	2.5

Table 8.1 (continued)

\square_{up} (°)	45	48	48
α_{up} (°)	40	40	35
k (mm)	1.5	1.5	1.5
m (mm)	9	5	5
n (mm)	2.5	1.5	1.5
\square_{low} (°)	45	48	48
α_{low} (°)	40	40	35
t1 (mm)	0.6	0.6	0.6
γ (°)	40	40	42
o (mm)	3	1.3	1.3
l (mm)	4	2.5	2.5

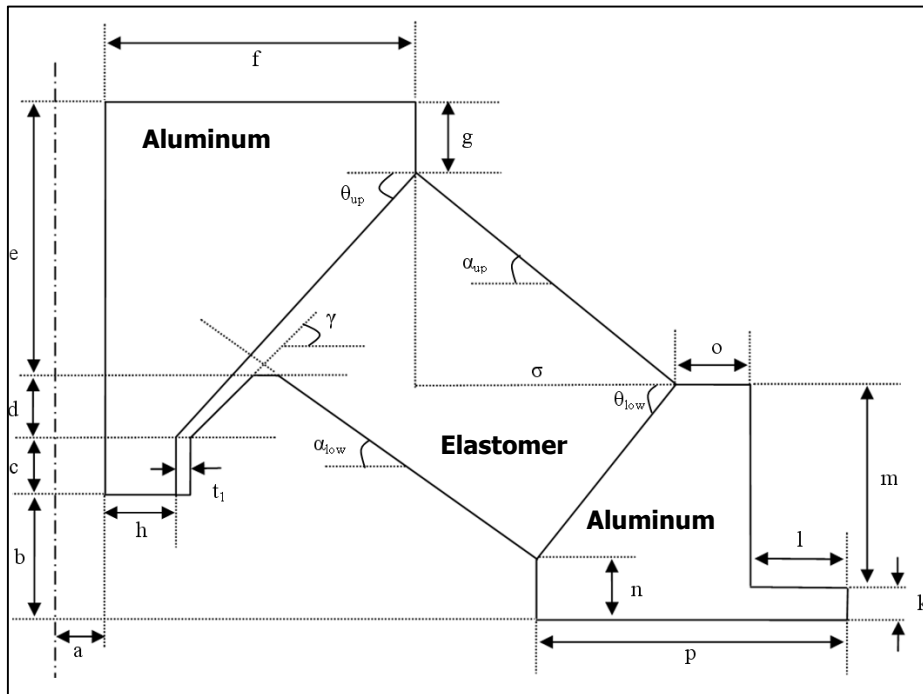


Figure 8.1 Geometrical parameters of the isolator, detailed design of which was be determined

Static, modal, and harmonic analyses, explained in *Chapter 7*, were done with the element sizes determined before. Related boundary and loading conditions, mentioned in *Chapter 6*, were applied to each analysis. Static elastic modulus of each material was taken as the smallest value from their master curves. Although it is a dynamic value, since the frequency is nearly 0, this assumption is not bad. Modal analyses were achieved with the same elastomeric material property.

Harmonic analyses were conducted at temperatures -30, 25 and 65 °C, within the frequency range of 0 – 500 Hz, with different elastomeric materials. Frequency dependent dynamic modulus and loss factor, obtained at the end of the analyses, provided inputs to Matlab code. By running this code, isolation performance of the system was interpreted with respect to technical requirements.

8.1.1 First Design Iteration

Geometric structure of the isolator with first parameter set is given in Figure 8.2. Static, modal and harmonic analyses were done with these parameters set for the first iteration.

8.1.1.1 Static Analysis

Axial and radial static stiffness values (as a result of static analysis) of the isolator with different elastomeric materials are given in Table 8.2. By static analyses, von Mises stress distributions on different elastomeric materials as a result of maximum axial static loading (500 N), defined in the technical requirements, are given in Figure 8.3. When the results were examined, tensile strength (given in APPENDIX A) of each material is about twice of the maximum stresses. Therefore, it can be concluded that stresses on the elastomeric materials of the isolators are not critical.

Von Mises stress distributions on the elastomeric materials as a result of a maximum radial static loading (200 N), are given in Figure 8.4. For radial static analysis, tensile strength of each material is about ten times of the maximum stresses. Thus, stresses on the elastomeric materials of the isolators are not critical.

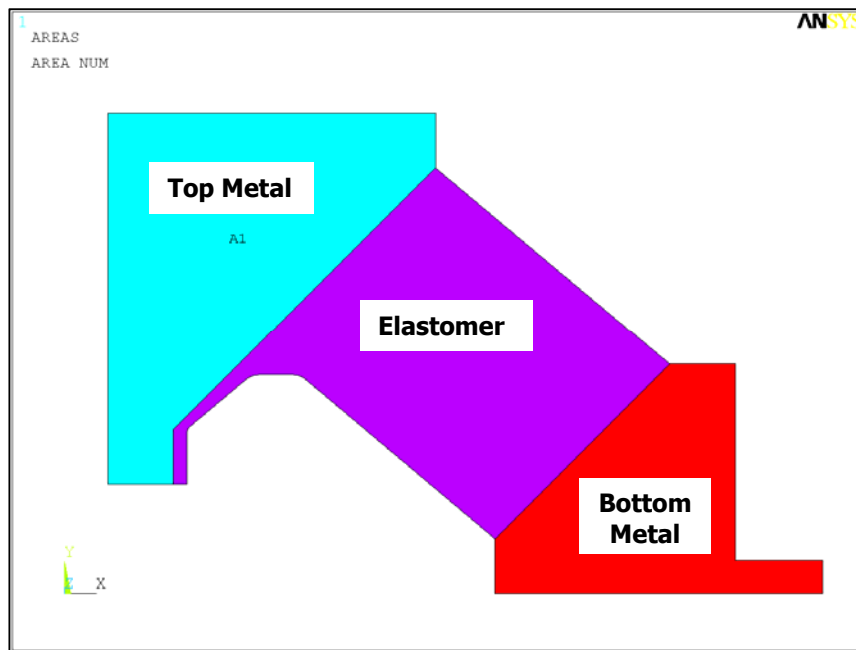


Figure 8.2 Geometric structure of the isolator at the first iteration

Table 8.2 Axial and radial static stiffness values with different materials (1st parameter set)

Materials	EPDM 50ShA	EPDM 80ShA	Silicone 50ShA	Silicone 80ShA	Neoprene 50ShA
Axial Static Stiffness (N/mm)	328.7	1584.5	408.2	801.6	248.1
Radial Static Stiffness (N/mm)	228.3	1140.1	285.4	570.6	171.2

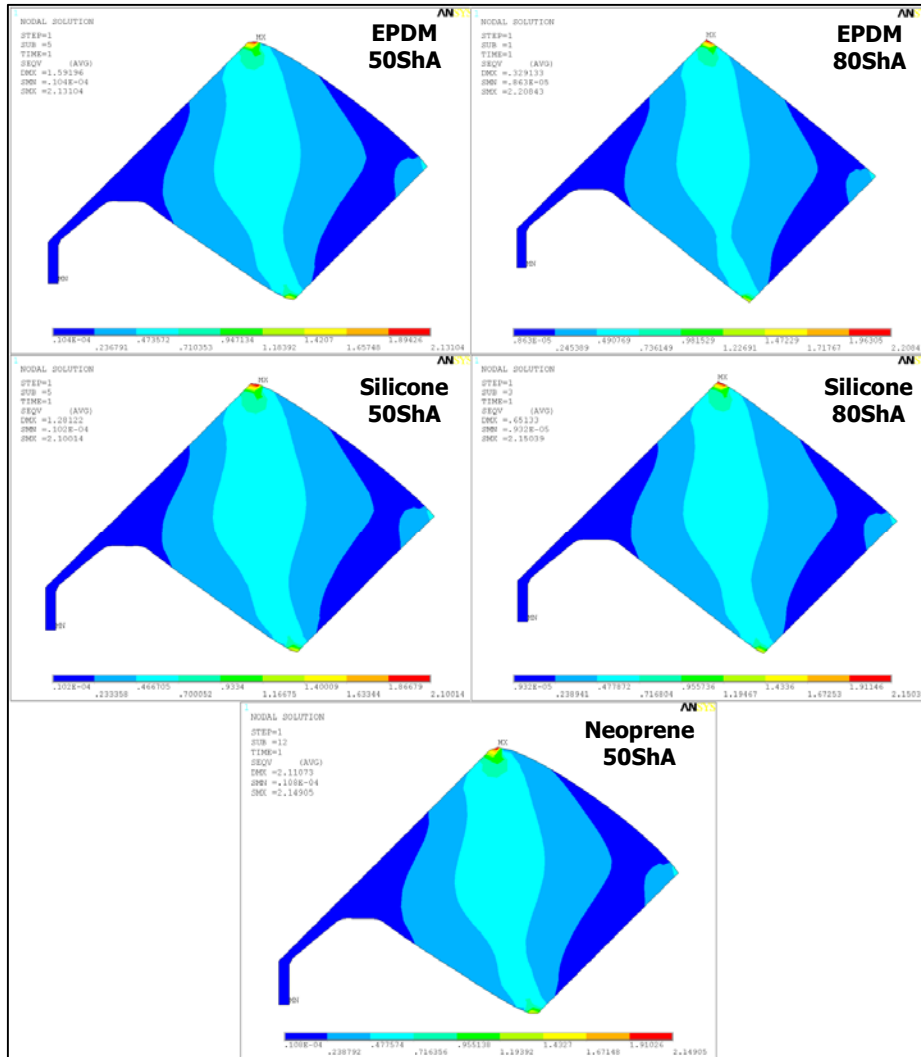


Figure 8.3 Von Mises stress distributions on different elastomeric materials as a result of maximum axial static loading

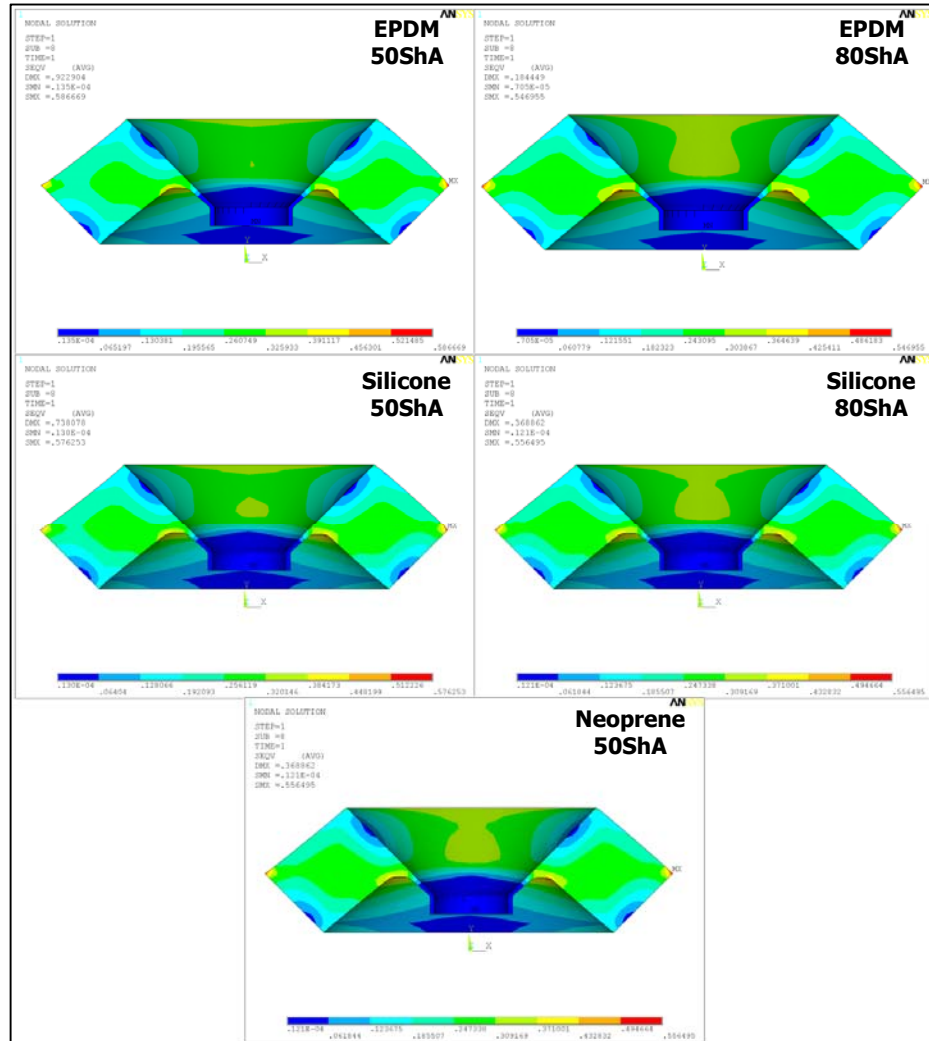


Figure 8.4 Von Mises stress distributions on different elastomeric materials as a result of maximum radial static loading

8.1.1.2 Modal Analysis

As a result of modal analyses, modes and modal frequencies of the isolator with different materials for fixed – free and free – free boundary conditions were obtained. First 5 mode shapes of the isolator are the same with the others given in Figure 7.7 of *Chapter 7*. First 5 natural frequencies with fixed – free and free – free boundary conditions are given in Table 8.3 and in Table 8.4 , respectively.

Table 8.3 First five natural frequencies of the isolator with fixed – free boundary condition

Natural Frequencies (Hz)	EPDM 50ShA	EPDM 80ShA	Silicone 50ShA	Silicone 80ShA	Neoprene 50ShA
1. Mode	432.4	946.6	482.1	675.5	367.0
2. Mode	432.4	946.6	482.1	675.5	367.0
3. Mode	553.8	1206.3	617.0	862.5	467.7
4. Mode	562.4	1235.3	627.3	880.2	478.9
5. Mode	718.1	1567.8	800.2	1119.9	607.9

Table 8.4 First five natural frequencies of the isolator with free – free boundary condition

Natural Frequencies (Hz)	EPDM 50ShA	EPDM 80ShA	Silicone 50ShA	Silicone 80ShA	Neoprene 50ShA
1. Mode	530.1	1162.9	591.2	829.1	451.1
2. Mode	530.1	1162.9	591.2	829.1	451.1
3. Mode	598.7	1312.9	667.6	936.0	508.9
4. Mode	706.6	1557.3	788.5	1108.2	604.1
5. Mode	834.8	1831.2	930.9	1305.5	710.1

8.1.1.3 Harmonic Analysis

Axial and radial harmonic analyses of the isolator are achieved using the 1st parameter set (1st design iteration). As a result of these analyses, vibration isolators' dynamic stiffness and loss factors are obtained in both axial and radial directions. In Figure 8.5 and Figure 8.14 , axial dynamic stiffness and loss factors of the isolator with different materials at temperatures -30, 25 and 65 °C and within 0 – 500 Hz frequency range are given.

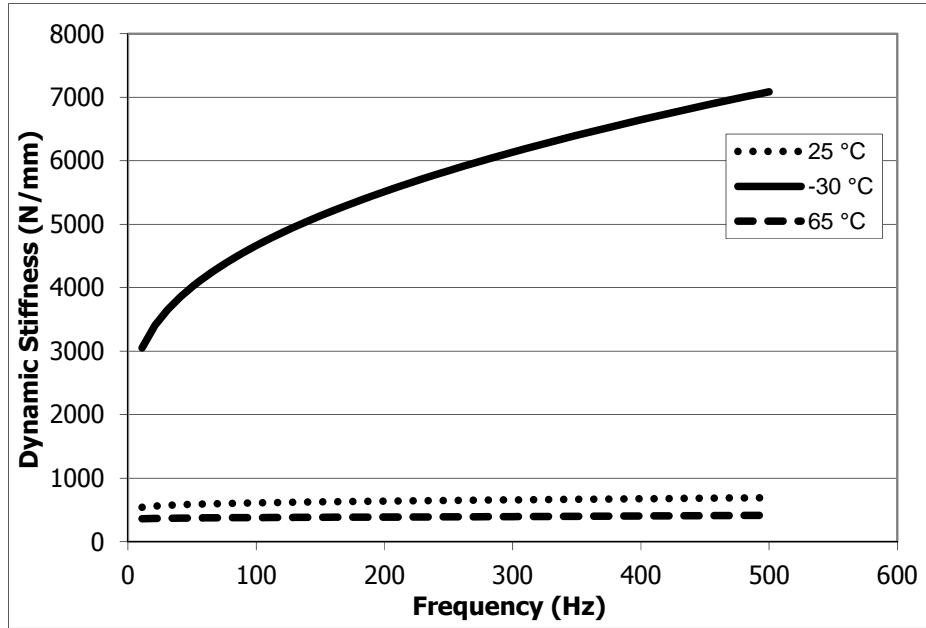


Figure 8.5 Frequency dependent dynamic stiffness of the isolator with EPDM 50ShA at different temperatures (1st design iteration)

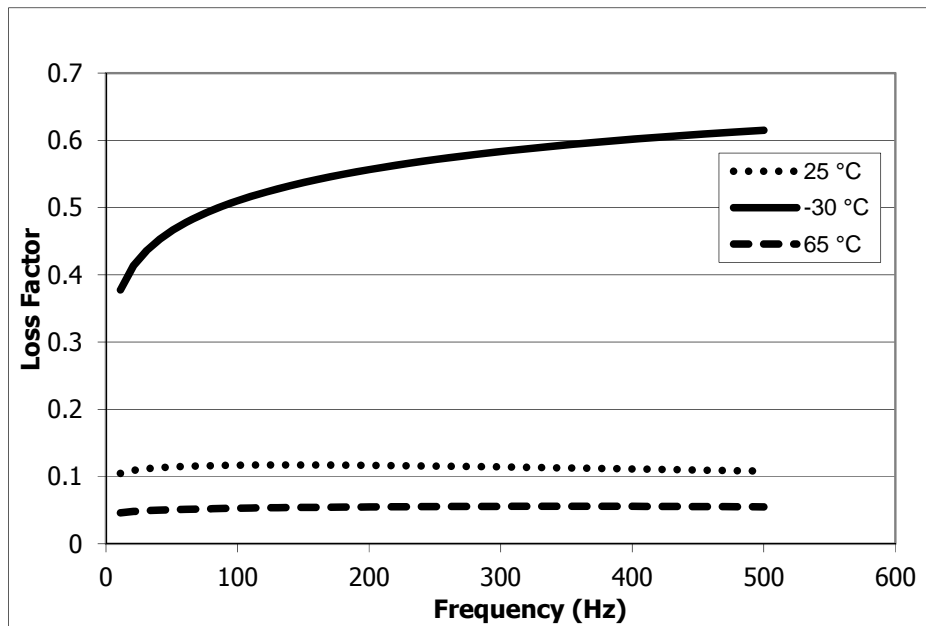


Figure 8.6 Frequency dependent loss factor of the isolator with EPDM 50ShA at different temperatures (1st design iteration)

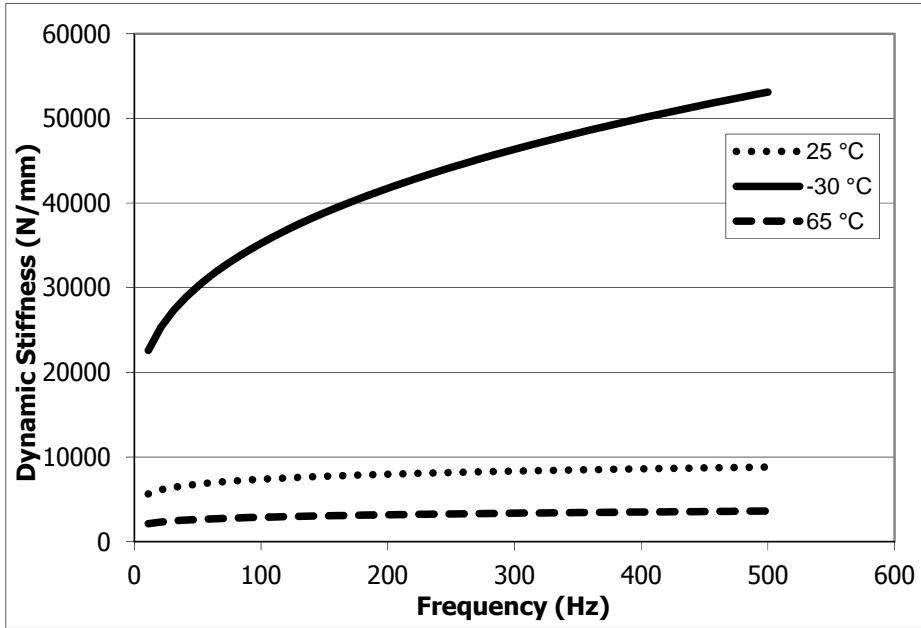


Figure 8.7 Frequency dependent dynamic stiffness of the isolator with EPDM 80ShA at different temperatures (1st design iteration)

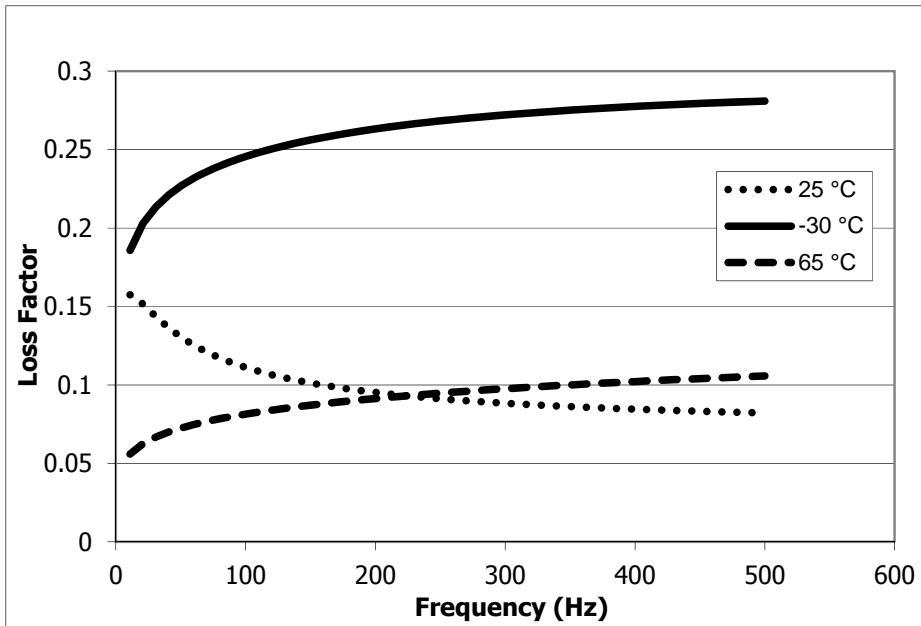


Figure 8.8 Frequency dependent loss factor of the isolator with EPDM 80ShA at different temperatures (1st design iteration)

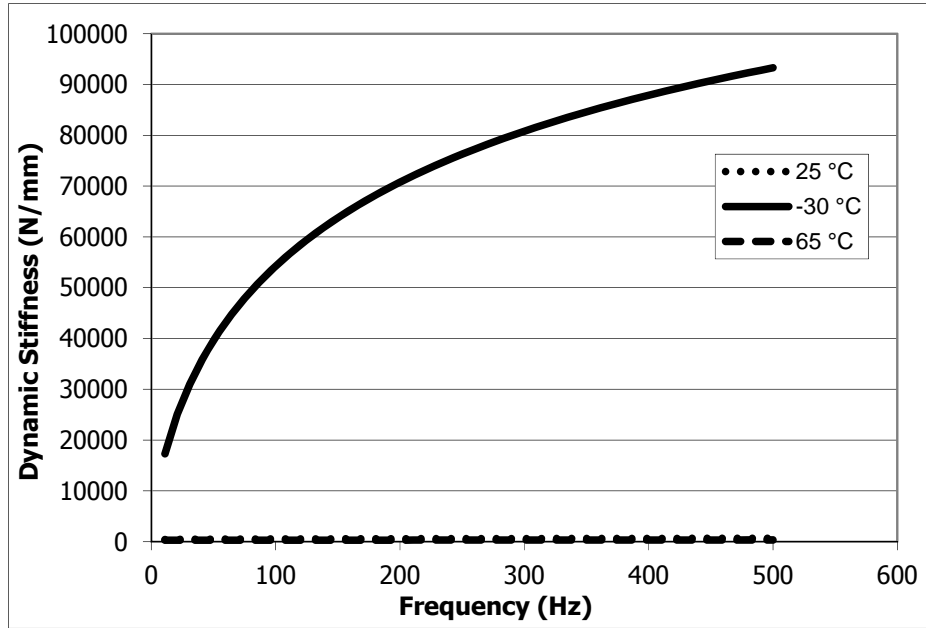


Figure 8.9 Frequency dependent dynamic stiffness of the isolator with Neoprene 50ShA at different temperatures (1st design iteration)

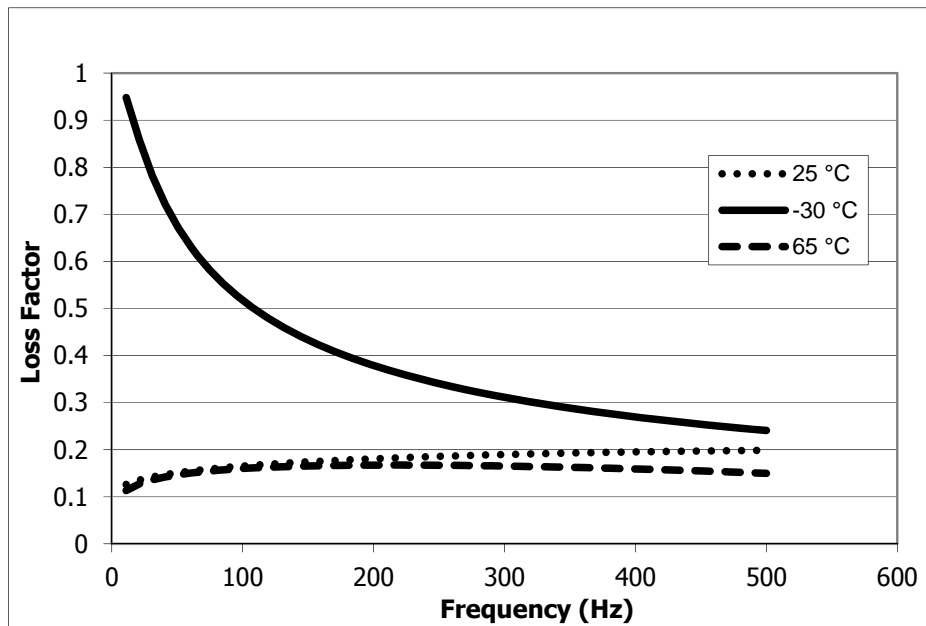


Figure 8.10 Frequency dependent loss factor of the isolator with Neoprene 50ShA at different temperatures (1st design iteration)

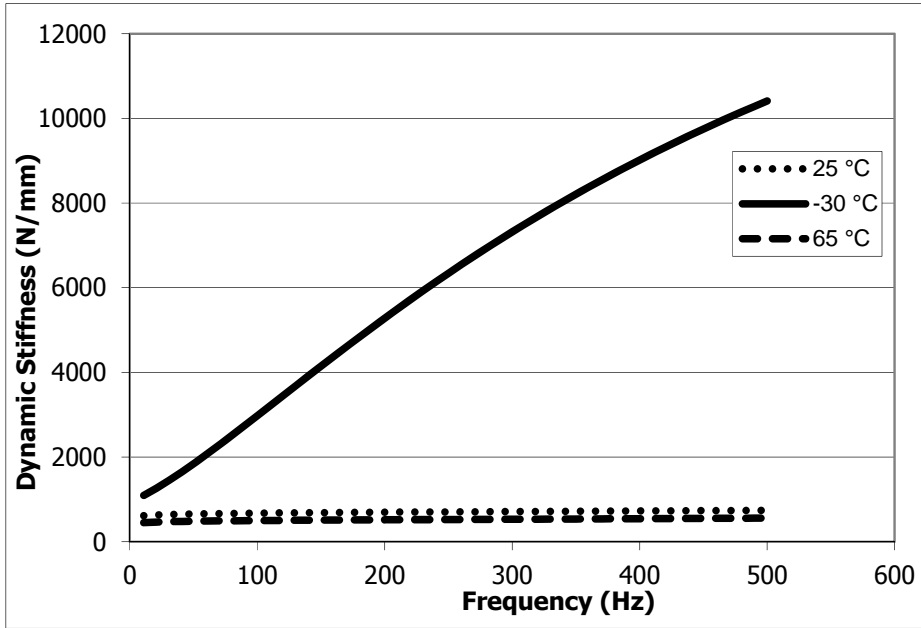


Figure 8.11 Frequency dependent dynamic stiffness of the isolator with Silicone 50ShA at different temperatures (1st design iteration)

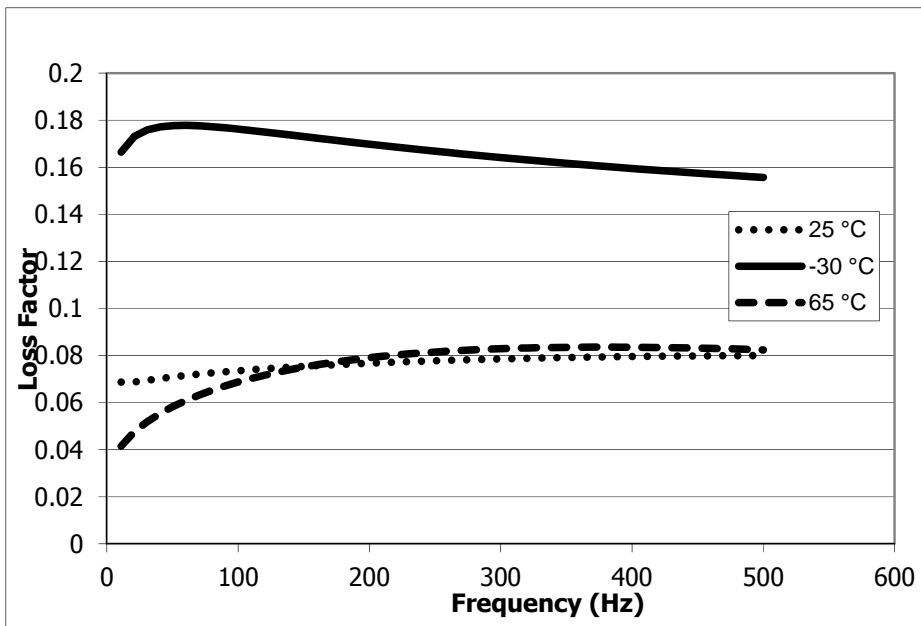


Figure 8.12 Frequency dependent loss factor of the isolator with Silicone 50ShA at different temperatures (1st design iteration)

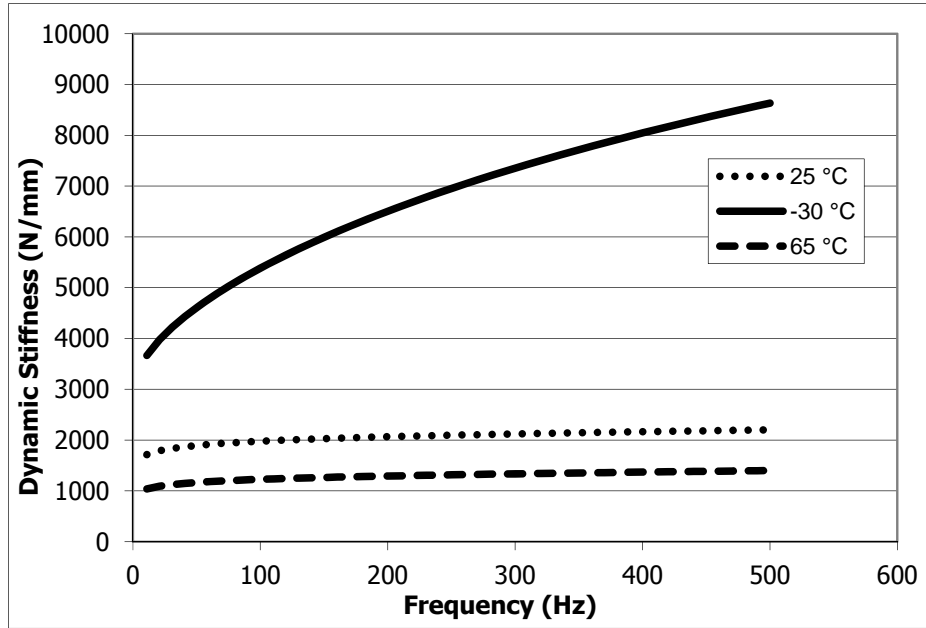


Figure 8.13 Frequency dependent dynamic stiffness of the isolator with Silicone 80ShA at different temperatures (1st design iteration)

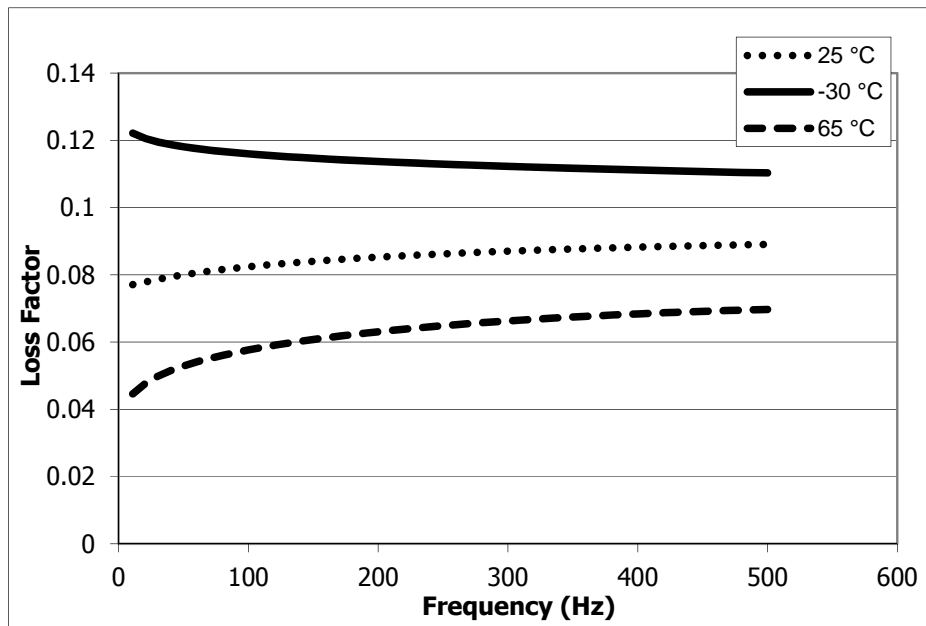


Figure 8.14 Frequency dependent loss factor of the isolator with Silicone 80ShA at different temperatures (1st design iteration)

When these graphs are examined, dynamic stiffness values of all materials get very high at -30 °C. The reason is that, all materials at this temperature and frequency range pass from rubbery region to transition region. It is a design requirement that dynamic stiffness of the isolator should not be affected by temperature as much as possible. Therefore, which material

satisfies this condition was determined by using the Matlab code. Frequency dependent dynamic stiffness and loss factor results can be get into the code as an input. Vibration profile, given in *Chapter 3*, was applied to the system having these properties in order to find system natural frequency and output g_{rms} values. Using dynamic stiffness and loss factor of EPDM 50ShA at 25 °C, obtained PSD graph is given in Figure 8.15.

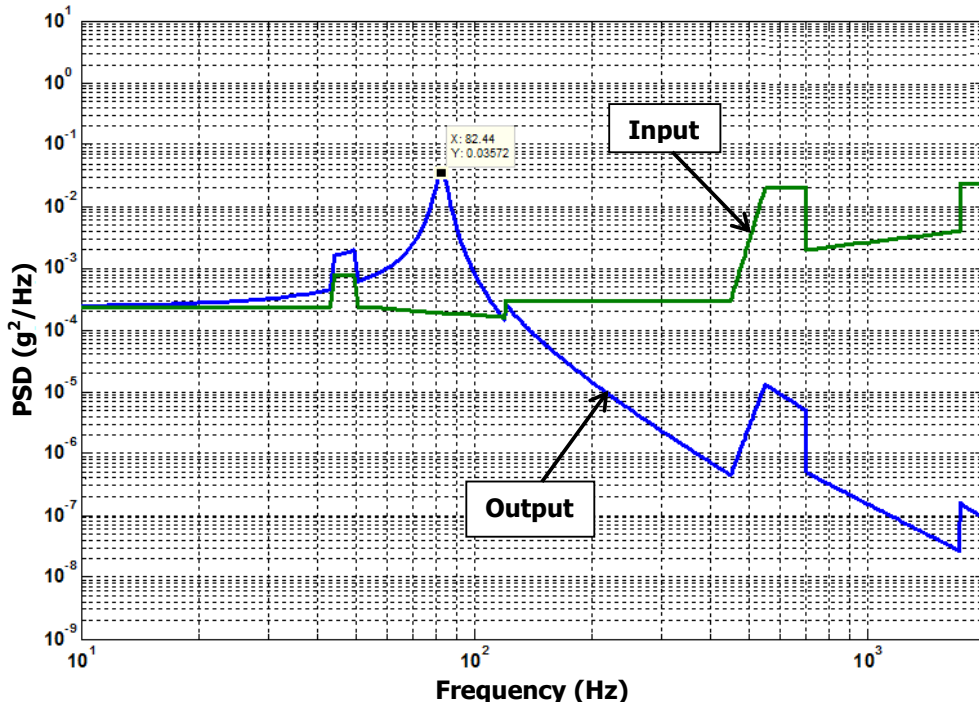


Figure 8.15 Output PSD using EPDM 50ShA dynamic properties at 25 °C

Isolation performances of the elastomeric vibration isolators with different materials were simulated using the Matlab code. In Table 8.5, Table 8.6 and Table 8.7 , system natural frequencies and output g_{rms} values are provided at 25, -30 and 65 °C, respectively.

Table 8.5 System natural frequency and output g_{rms} value at 25 °C

Materials	EPDM 50ShA	EPDM 80ShA	Silicone 50ShA	Silicone 80ShA	Neoprene 50ShA
System Natural Frequency (Hz)	78.6	291	82	143	73.5
Output g_{rms} (g)	0.48	1.43	0.60	0.91	0.41

Table 8.6 System natural frequency and output g_{rms} value at -30 °C

Materials	EPDM 50ShA	EPDM 80ShA	Silicone 50ShA	Silicone 80ShA	Neoprene 50ShA
System Natural Frequency (Hz)	240	700	258	270	982
Output g_{rms} (g)	0.76	5.42	1.35	1.31	4.93

Table 8.7 System natural frequency and output g_{rms} value at 65 °C

Materials	EPDM 50ShA	EPDM 80ShA	Silicone 50ShA	Silicone 80ShA	Neoprene 50ShA
System Natural Frequency (Hz)	62	179	71	113	54.4
Output g_{rms} (g)	0.66	1.02	0.62	0.77	0.42

If system natural frequency and output g_{rms} in technical requirements are considered, condition related to system natural frequency not being over 200 Hz was not satisfied at all 3 temperatures. However, output g_{rms} values at all 3 temperatures stayed under 1. In order to step back system natural frequency less than 200 Hz, geometrical dimensions of the isolator can be decreased provided that limits are not exceeded. Additionally, since EPDM 50 ShA is better than the others with respect to isolation performance at especially -30 °C, other iterations will be achieved with only this material.

8.1.2 Second Design Iteration

Geometric structure of the elastomeric vibration isolator with second parameter set is shown in Figure 8.16.

8.1.2.1 Static Analysis

Axial and radial static stiffness values of the isolator with EPDM 50ShA are given in Table 8.7 using the 2nd parameter set (2nd design iteration). Von Mises stress distributions on EPDM 50ShA as a result of maximum axial (500 N) and radial (200 N) static loading are given in Figure 8.17. According to the results, tensile strength of EPDM 50ShA is about twice of the maximum stress in axial and four times of the maximum stress in radial directions. Thus, it can be inferred that stresses on EPDM are not critical for both configuration.

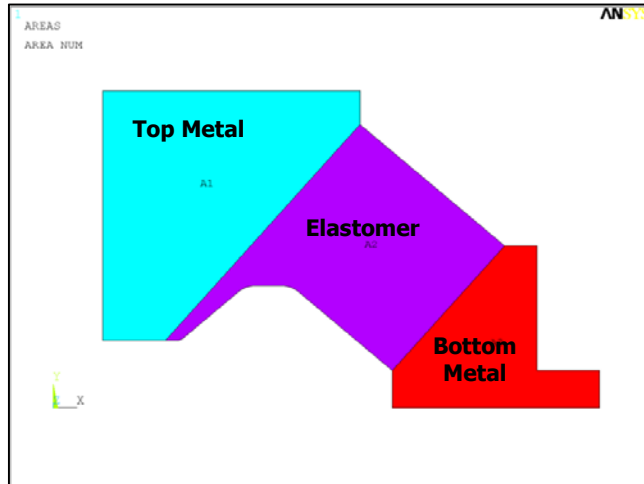


Figure 8.16 Geometric structure of the isolator at the second iteration

Table 8.8 Axial and radial static stiffness values with EPDM 50 ShA (2nd parameter set)

	EPDM 50ShA
Axial Static Stiffness (N/mm)	282.3
Radial Static Stiffness (N/mm)	206.7

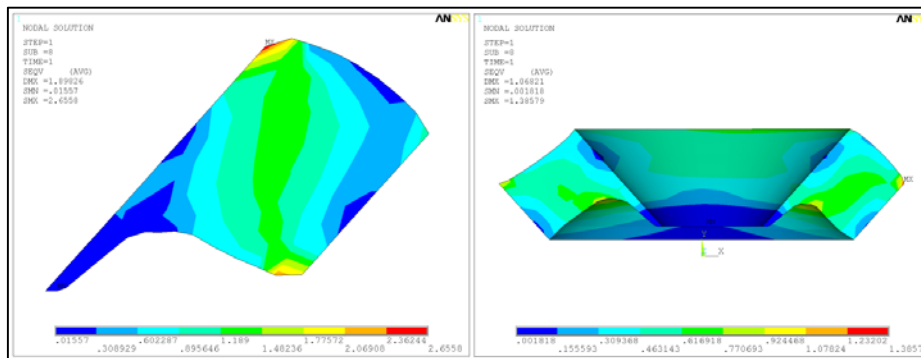


Figure 8.17 Von Mises stress distributions on EPDM 50ShA due to axial (left) and radial (right) static loadings with 2nd parameter set

8.1.2.2 Modal Analysis

Using 2nd parameter set, first five Modes and modal frequencies of the isolator with EPDM 50ShA for fixed – free and free – free boundary conditions are given in Table 8.9.

Table 8.9 First five natural frequencies of the isolator with EPDM 50ShA for fixed – free and free – free boundary conditions (2nd parameter set)

Natural Frequencies (Hz)	EPDM 50ShA	
	Fixed – free	Free – free
1. Mode	663.7	841.5
2. Mode	663.7	841.5
3. Mode	848.6	950.6
4. Mode	872.1	1179.2
5. Mode	1184.2	1473.0

8.1.2.3 Harmonic Analysis

Axial and radial harmonic analyses of the isolator were achieved using the 2nd parameter set. Dynamic stiffness and loss factor of the vibration isolator in both axial and radial directions were attained. Axial dynamic stiffness and loss factors of the isolator with EPDM 50ShA at temperatures -30, 25 and 65 °C and within 0 – 500 Hz frequency range are given in Figure 8.18, and Figure 8.19. Isolation performance of the isolator with EPDM 50ShA was simulated using Matlab code. In Table 8.10, system natural frequencies and output g_{rms} values are given at 25, -30 and 65 °C. As seen from the table, vibration isolator satisfies both maximum 1 g_{rms} output and maximum system natural frequency of 200 Hz. Additionally, it should be checked whether the axial and radial dynamic stiffness are close sufficiently to each other not (difference should be maximum 10%). Axial and radial dynamic stiffness of the isolator with EPDM 50ShA at 25 °C are shown together in Figure 8.20. The ratio of axial dynamic stiffness to radial one is about 1.2. In the 3rd iteration this ratio will be tried to be improved.

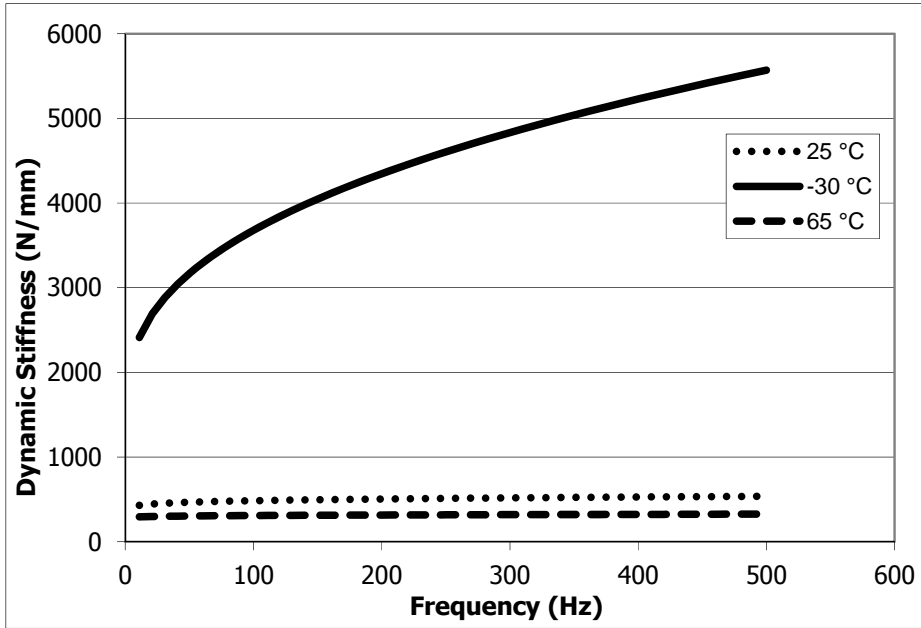


Figure 8.18 Frequency dependent dynamic stiffness of the isolator with EPDM 50ShA at different temperatures (2nd design iteration)

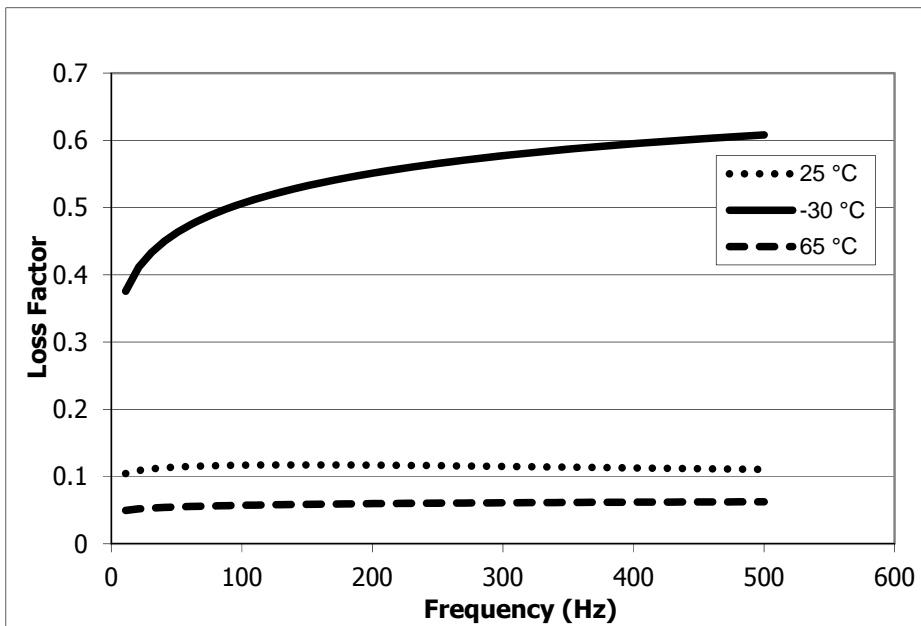


Figure 8.19 Frequency dependent loss factor of the isolator with EPDM 50ShA at different temperatures (2nd design iteration)

Table 8.10 System natural frequencies and output grms values at -30, 25 and 65 °C (2nd iteration)

Temperatures (°C)	EPDM 50ShA		
	-30	25	65
System Natural Frequency (Hz)	200	70	55
Output g_{rms} (g^2/Hz)	0.64	0.46	0.64

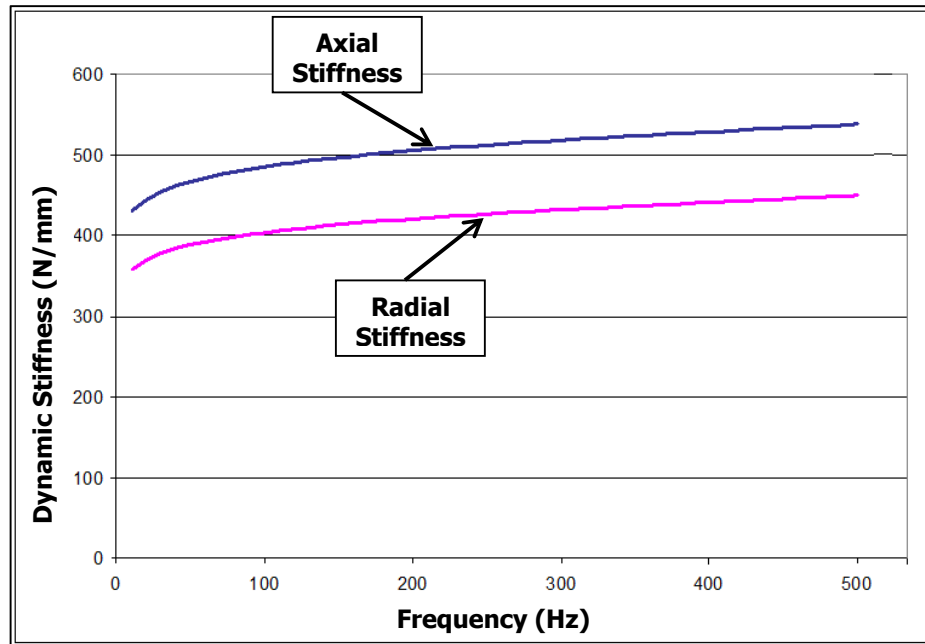


Figure 8.20 Using 2nd parameter set, axial and radial stiffness of the isolator with EPDM 50ShA at 25 °C

8.1.3 Third Iteration

Geometric structure of the elastomeric vibration isolator with third parameter set is shown in Figure 8.21.

8.1.3.1 Static Analysis

Axial and radial static stiffness values of the isolator with EPDM 50ShA are given in Table 8.11 using the 3rd parameter set. Von Mises stress distributions on EPDM 50ShA as a result of maximum axial (500 N) and radial (200 N) static loading are given in Figure 8.22. According to the results, tensile strength of EPDM 50ShA is about three times of the maximum stress in axial and six times of the maximum stress in radial directions. Thus, it can be inferred that stresses on EPDM are not critical for both configurations.

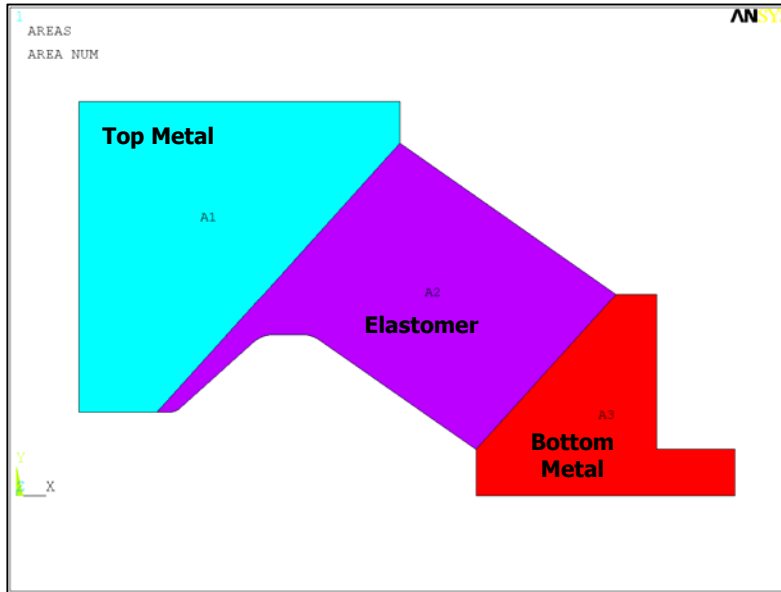


Figure 8.21 Geometric structure of the isolator at the third iteration

Table 8.11 Axial and radial static stiffness values with EPDM 50 ShA (3rd parameter set)

	EPDM 50ShA
Axial Static Stiffness (N/mm)	219.6
Radial Static Stiffness (N/mm)	189.1

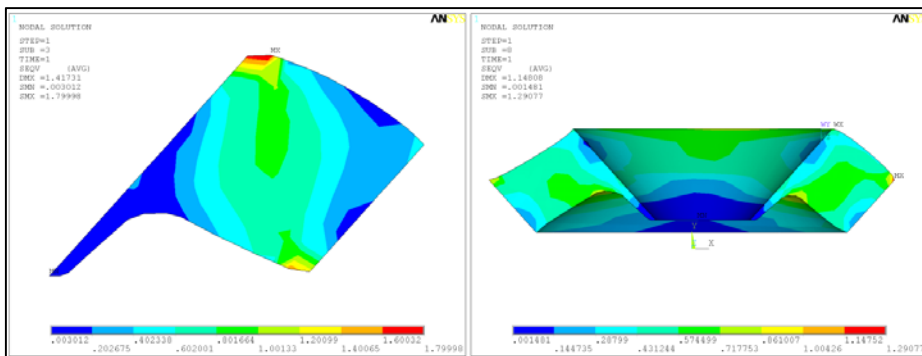


Figure 8.22 Von Mises stress distributions on EPDM 50ShA due to axial (left) and radial (right) static loadings with 3rd parameter set

8.1.3.2 Modal Analysis

Using 3rd parameter set, first five Modes and modal frequencies of the isolator with EPDM 50ShA for fixed – free and free – free boundary conditions are given in Table 8.12.

Table 8.12 First five natural frequencies of the isolator with EPDM 50ShA for fixed – free and free – free boundary conditions (3rd parameter set)

Natural Frequencies (Hz)	EPDM 50ShA	
	Fixed – free	Free – free
1. Mode	625.69	782.30
2. Mode	625.69	782.30
3. Mode	779.41	917.65
4. Mode	826.92	1044.5
5. Mode	1098.9	1349.3

8.1.3.3 Harmonic Analysis

Axial and radial harmonic analyses of the isolator are achieved using the 3rd parameter set. Dynamic stiffness and loss factor of the vibration isolator in both axial and radial directions are obtained. Axial dynamic stiffness and loss factors of the isolator with EPDM 50ShA at temperatures -30, 25 and 65 °C and within 0 – 500 Hz frequency range are given in Figure 8.23 and Figure 8.24, respectively.

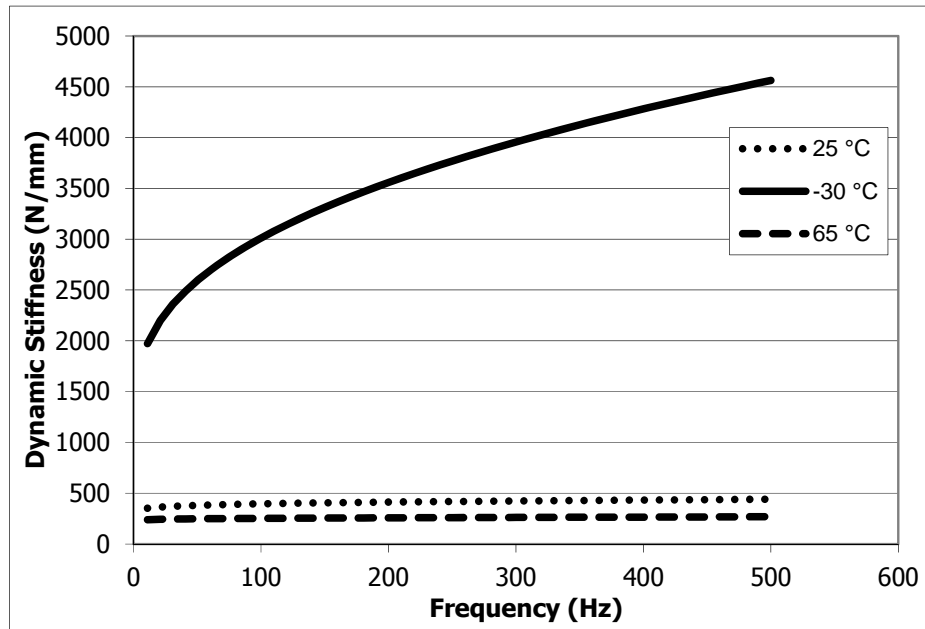


Figure 8.23 Frequency dependent dynamic stiffness of the isolator with EPDM 50ShA at different temperatures (3rd design iteration)

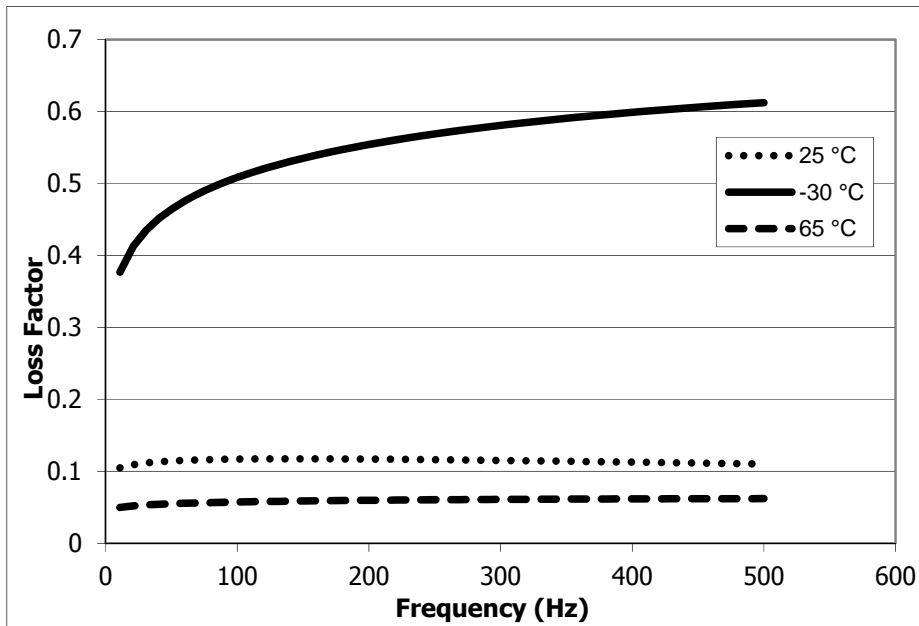


Figure 8.24 Frequency dependent loss factor of the isolator with EPDM 50ShA at different temperatures (3rd design iteration)

System natural frequencies and output g_{rms} values at temperatures of 25, -30 and 65 °C are given in Table 8.13. This reveals the isolation performance of the isolator, having EPDM 50ShA as an elastomeric material, with 3rd design iteration. When the results were examined, it can be seen that vibration isolator of the 3rd design iteration satisfies both maximum 1 g_{rms} output and maximum system natural frequency of 200 Hz at all temperatures. Besides, it was checked whether the improvement was achieved with respect to sufficient closeness between axial and radial dynamic stiffness. Axial and radial dynamic stiffness of the isolator with EPDM 50ShA at 25°C are shown together in Figure 8.25. While the ratio of axial dynamic stiffness to radial one was about 1.2 in 2nd parameter set, this ratio was decreased about 1.08, which satisfies the condition in technical requirements (difference being a maximum of 10%). Therefore, design iterations may end at this point. Final design of the vibration isolator will be generated with 3rd parameter set.

Table 8.13 System natural frequencies and output g_{rms} values at -30, 25 and 65 °C (3rd iteration)

Temperatures (°C)	EPDM 50ShA		
	-30	25	65
System Natural Frequency (Hz)	188	63	49.3
Output g_{rms} (g^2/Hz)	0.56	0.46	0.79

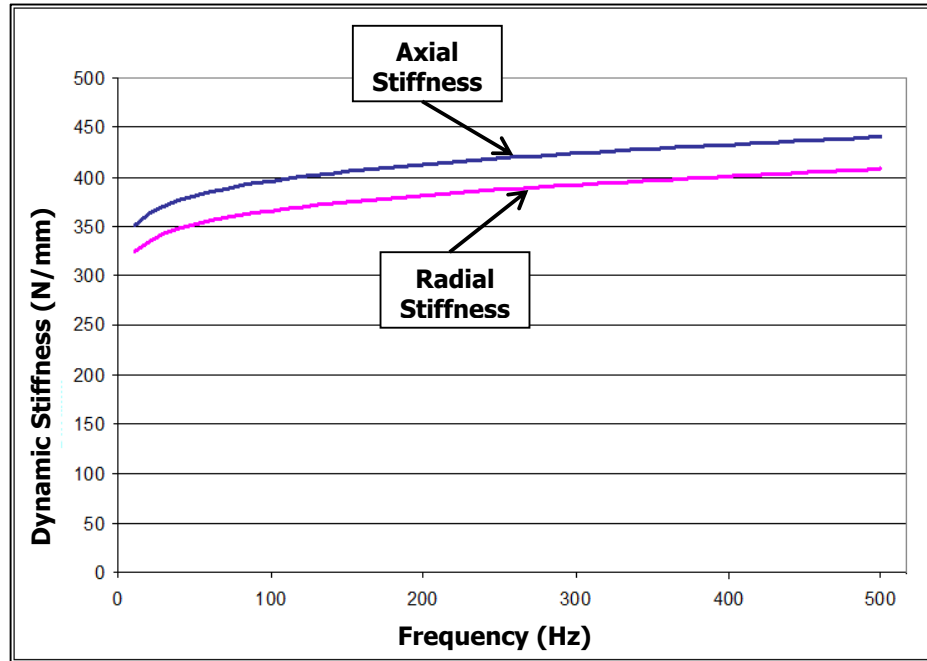


Figure 8.25 Using 3rd parameter set, axial and radial stiffness of the isolator with EPDM 50ShA at 25 °C

8.2 PRODUCTION OF THE PROTOTYPES AND VERIFICATION OF THE DESIGN PROCESS

It was revealed that design requirements were satisfied with 3rd geometric parameter set (3rd design iteration) at interested temperatures and frequency range and with the elastomer material of EPDM 50ShA. Geometric details (full and half solid models) of the final vibration isolator are shown in Figure 8.26. Additionally, solid model of the isolator with flanges (connection parts) is demonstrated in Figure 8.27.

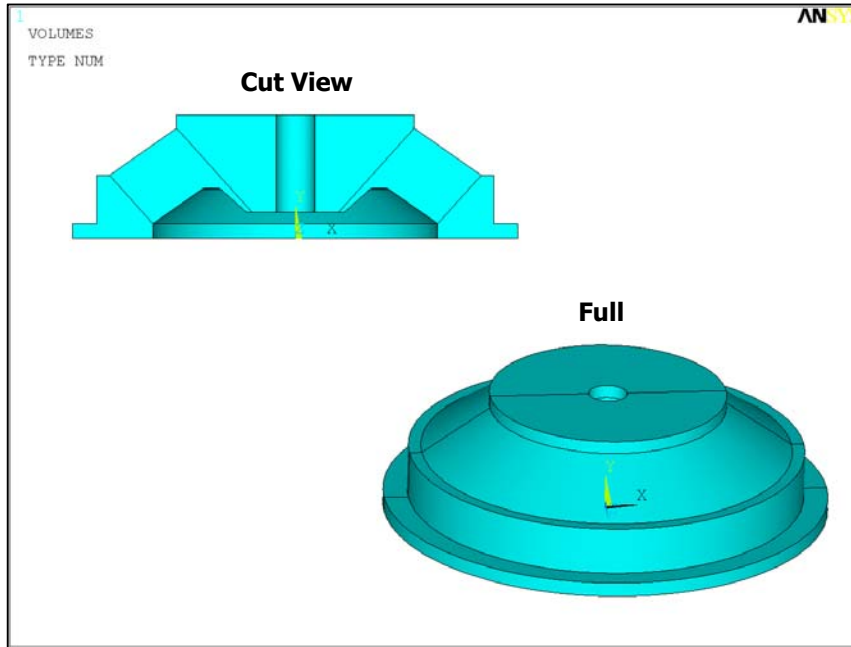


Figure 8.26 Solid model of final vibration isolator design

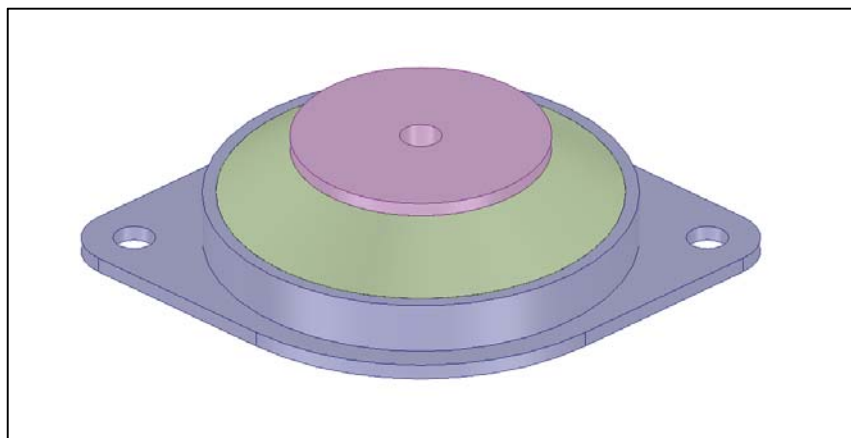


Figure 8.27 Final isolator design with flanges

Vibration isolator prototypes were produced using this geometry and with the same elastomeric material of EPDM 50ShA by BilPlas. As mentioned before, elastomeric material specimens, dynamic characterizations of which were achieved, were supplied again from BilPlas. Therefore, the formulas (recipes) of both materials are the same. In Figure 8.28, photograph of a prototype is given.



Figure 8.28 Photographs of a prototype

In order to verify the design process, dynamic characterization tests of the produced prototypes were conducted in Bayrak Plastik. These tests were done at room temperature and for 4 isolator prototypes. Both axial and radial dynamic stiffness and loss factors of the prototypes were found using the axial and radial test configurations as shown in Figure 8.29. These test results were used for comparison with the analysis results.

Axial and radial dynamic stiffness and loss factor from analysis and prototype tests were drawn on the same graphs between Figure 8.30 and Figure 8.33. Additionally, analysis and average test results (average values at each frequency) were shown in Figure 8.34 and Figure 8.37.



Figure 8.29 Axial (left) and radial (right) test configurations of the prototypes

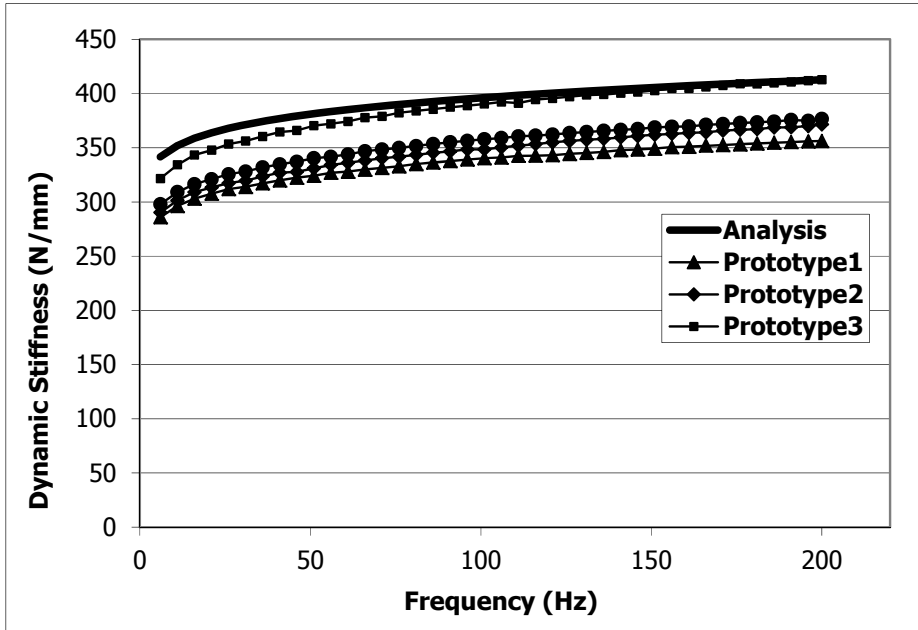


Figure 8.30 Tested axial dynamic stiffness of the prototypes and analysis result

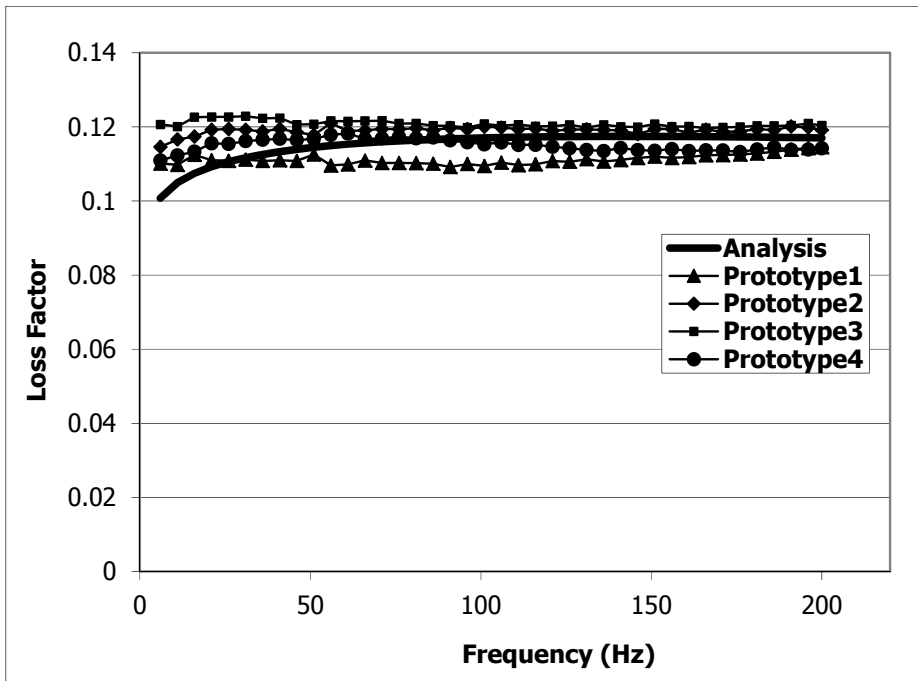


Figure 8.31 Tested axial loss factor of the prototypes and analysis result

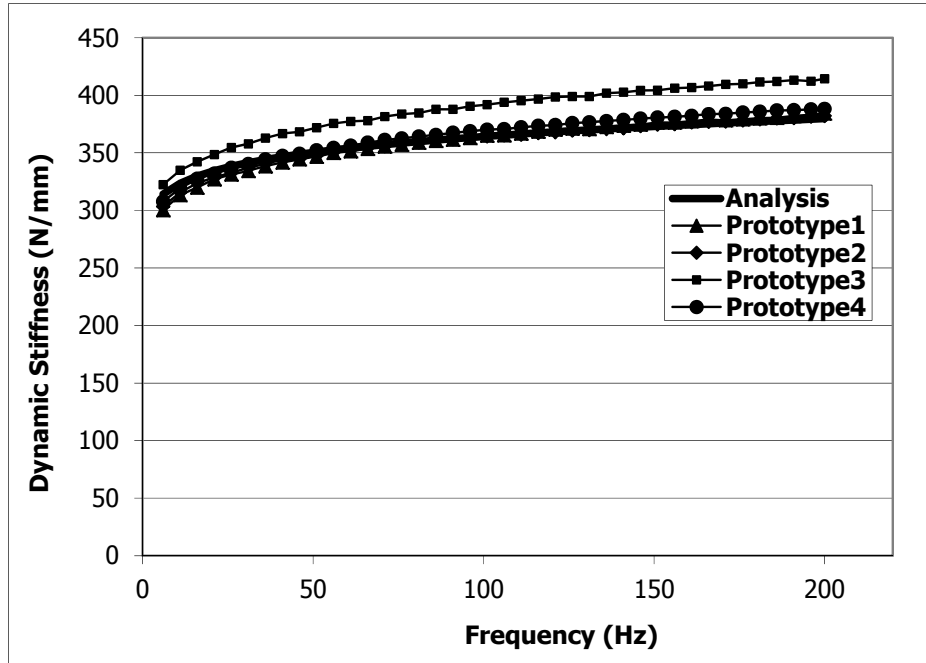


Figure 8.32 Tested radial dynamic stiffness of the prototypes and analysis result

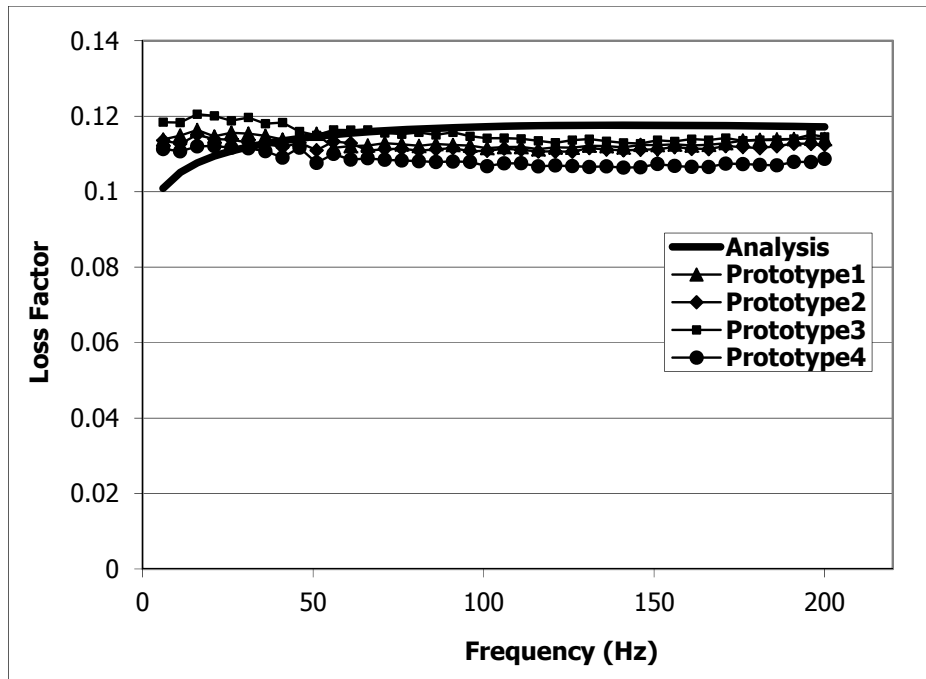


Figure 8.33 Tested radial loss factor of the prototypes and analysis result

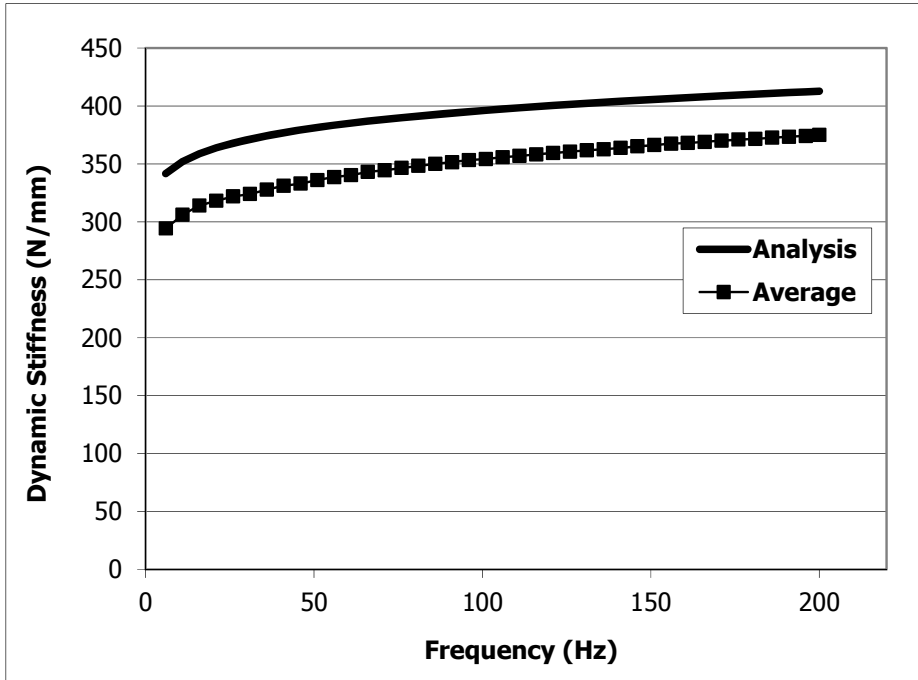


Figure 8.34 Axial dynamic stiffness average of the prototypes and analysis result

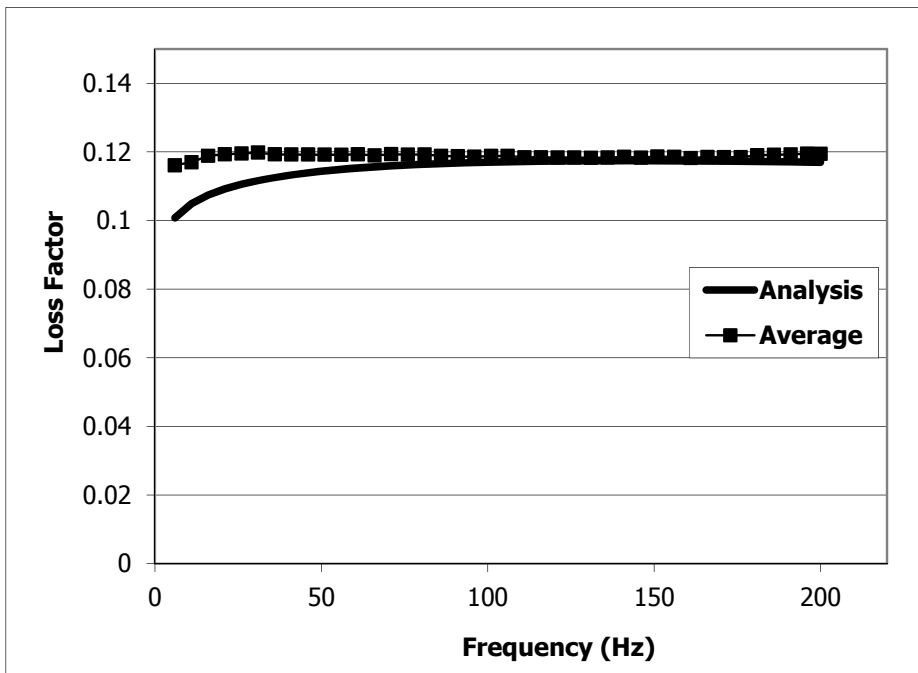


Figure 8.35 Axial loss factor average of the prototypes and analysis result

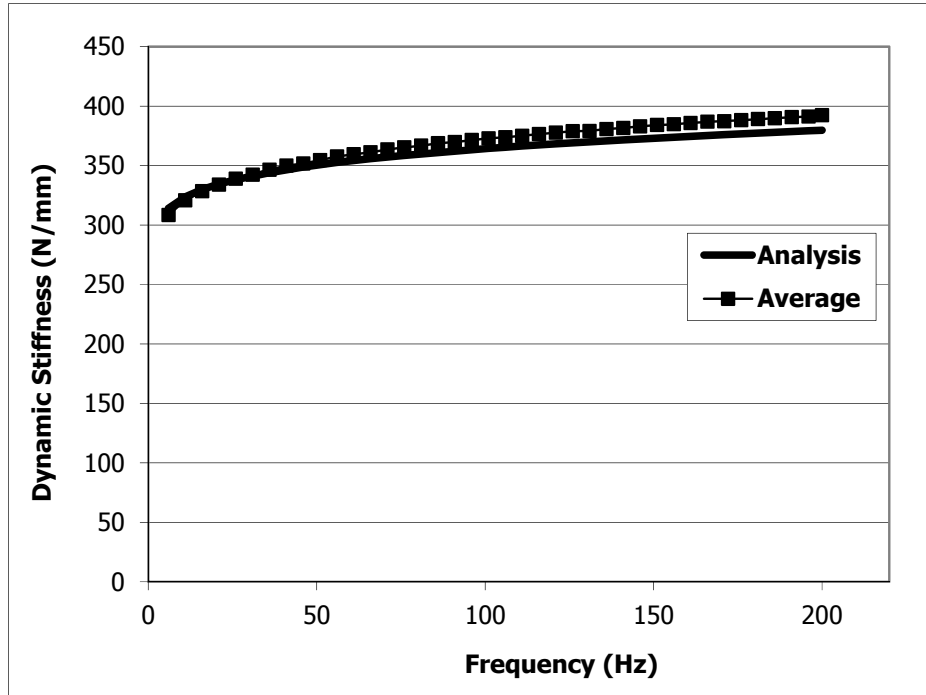


Figure 8.36 Radial dynamic stiffness average of the prototypes and analysis result

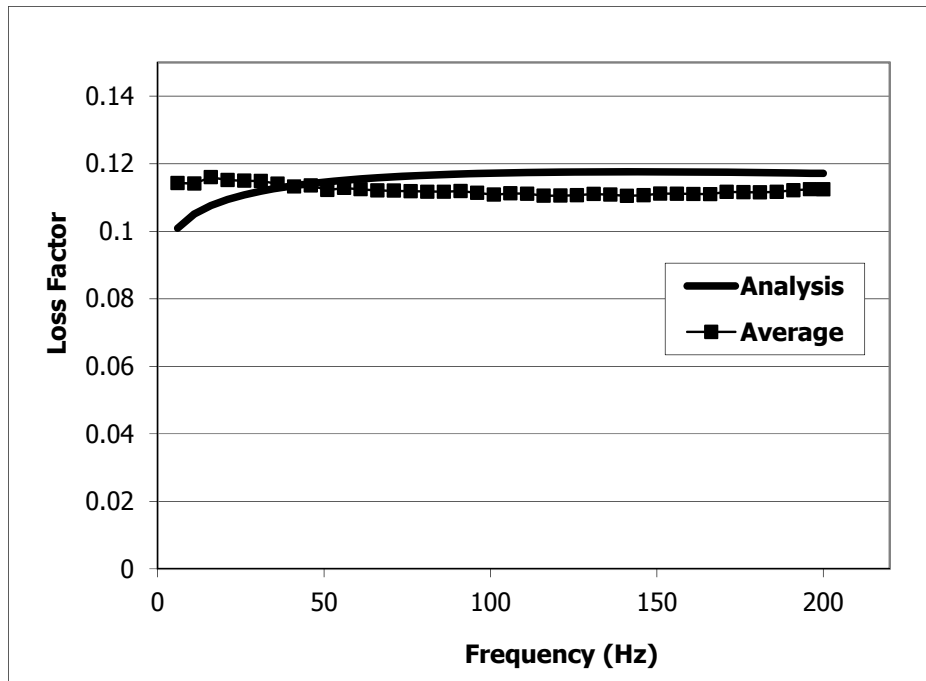


Figure 8.37 Radial loss factor average of the prototypes and analysis result

When the results are investigated, it is easily seen that average dynamic properties; both in axial and radial directions are in good agreement with the analysis results. There is approximately %10-15 differences between average axial dynamic stiffness values of prototypes and axial dynamic stiffness found using harmonic analysis throughout the frequency range. This difference is under the %5 within the major part of the frequency range (above 40 Hz) for axial loss factor. For radial dynamic stiffness values, average of the prototypes differs from analysis results only by %3 between 0 – 200 Hz frequency range. Average of the radial dynamic stiffness values measured from radial dynamic tests is about %5 different than the analysis results within the same frequency range.

Too many factors could cause this small difference between test and analysis results. One of them can be related to the compound of the EPDM 50ShA. Although the content of the EPDM material is same for both material specimen of EPDM, dynamic characterization of which was done, and material used in prototypes of the vibration isolators, there can be a small difference related to mixture preparation process since there was approximately 1.5 year between their productions.

While doing the dynamic characterization of the material specimens, mostly it was begun at low temperatures (-55 °C) and dynamic tests were accomplished for every 5 °C temperature increment. At low temperatures, however, crystallization of the elastomeric materials can be happened. This can change the dynamic properties of the elastomers a little bit unless they were held at room temperature for a while. During characterization tests, therefore, this situation might have been happened.

Dynamic properties of the elastomeric materials can change with the type of dynamic excitation. Dynamic characterizations of the selected elastomeric material specimens (including EPDM 50ShA) were done using a random vibration excitation input. However, dynamic tests of the prototypes were carried out using MTS test system in Bayrak Plastik. In this test system, sine sweep excitation was used as an input. Although it was paid attention to be dynamic strains below %0.1, especially during the material characterization test this might have not been satisfied. Additionally, in order to do tests, tensile elastomeric material specimens were glued between vibration and stationary steel blocks. Although the preload on the elastomeric specimen due to the weight of the vibrating block was low (approximately 10 N), this might have affected the dynamic properties of the material.

Elastomeric component of designed vibration isolator was assumed to deform predominantly in tensile and compression mode during the operation. Therefore, only dynamic characterization test results of tensile elastomeric material specimens were used during the design process. Nevertheless, this assumption cannot be completely true, since the vibration isolator is of conical shape and shear mode can be active a bit during the deformation of the isolator. Consequently, this might have created this deviation between tests and analyses results.

Lastly, in simulation environment all geometric dimensions were treated as exact. Nonetheless, this cannot be satisfied in real world. There was a tolerance band of each geometric dimension. Thus, this might have led to this deviance. Additionally, there might have had some errors related to test systems and their components. This uncontrollable phenomenon might have left out of count.

CHAPTER 9

SUMMARY AND CONCLUSIONS

9.1 GENERAL CONCLUSIONS

In this thesis, studies were carried out related to design of low profile elastomeric vibration isolators, used for vibration isolation of the electronic equipment in a missile or rocket. In order to do that, first of all, literature related to elastomeric vibration isolators was reviewed. Their general properties, types, functions, etc. were explained. Since isolation properties of a vibration isolator is supplied by the elastomeric component of that, researches related to elastomeric materials were done mainly. Leading factors like temperature, frequency etc. affecting the dynamic properties of these materials were clarified. Detailed explanation related to modeling and failure criteria of elastomeric materials were done in this chapter. Finally, important design parameters of vibration isolators were described. After that, studies related to determination of technical requirements of the vibration isolator for a sample application in ROKETSAN A.Ş. were achieved. Geometric constraints, operating temperature range, maximum static load, etc. were defined for the isolator. Additionally, vibration isolation target of the component and how it would be measured (with tests and Matlab simulation) were clarified. Then, in order to determine conceptual design of the vibration isolator according to technical requirements, vibration isolators found in the catalog of commercial companies like Lord, Barry and Laspar were looked over. Existing vibration isolators which are the candidate for the similar vibration isolation applications in ROKETSAN A.Ş. were investigated thoroughly. Conceptual design of conic and elastomeric vibration isolator was decided according to all these studies. After having determined the generic geometry of the isolator, various standard elastomers were searched and some of them were selected in order to get dynamic characteristics. In order to do that, tensile and shear material specimens were manufactured and their dynamic modulus and loss factor properties were attained using the test system in ROKETSAN A.Ş.

Next, finite element model of elastomeric vibration isolator was generated parametrically. To do so, Parametric Design Language of Ansys (APDL) was used. Dynamic properties (frequency and temperature dependent dynamic modulus and loss factor) of elastomeric materials that had been tested were used as inputs (i.e. mathematical models with 15 parameters) for the finite element model. Parametric finite element model was constituted for two configurations: axial and radial. For both configurations parametric models were generated with same geometric parameters. The only difference was in the dimension of the finite element model. For axial static and harmonic analysis, since boundary and loading conditions are symmetric with respect to center axis of the isolator, 2D axisymmetric finite element model was generated. However, 3D model was established for radial analyses because loading is not symmetric with respect to center axis. For modal analysis, 3D finite element model was used. For each analysis type (static, modal and harmonic analyses), geometric, material, analysis options, configuration, and similar variables were taken as parameters and be changed interactively. Besides, boundary and loading conditions were described for each analysis in this section.

After parametric finite element modeling, convergence studies for all analyses results were achieved. Optimum element sizes which make possible to obtain pretty good results in a short time were determined for all analyses.

After constituting analyses file inputs and accomplishing convergence studies, design iterations were carried out. In the first iteration, for a set of parameters, static analysis was performed. Radial and axial static stiffness values for all materials were calculated. For free-free and fixed-free boundary conditions, modal analyses were obtained. By axial and radial harmonic analyses, frequency dependent dynamic stiffness and loss factor of vibration isolator were attained for three temperature values (-30, 25 and 65 °C). Performances of vibration isolators with different elastomeric materials at each temperature were evaluated by a Matlab code and the best elastomeric material that can be used in vibration isolator design was selected as EPDM 50 ShA. In the second iteration, static and modal analyses were done with this material with different parameter set which would bring closer isolator performance to a point providing design requirements. One of the criteria in the vibration isolator design is to be the axial and radial dynamic stiffness values as close as to each other. In the third design iteration, this was achieved. Additionally, the performance characteristics of the vibration isolator were improved by the third parameter set. After design iterations had been completed, technical drawings of the final vibration isolator design were prepared. Prototypes of the isolator were manufactured according to these drawings at a rubber company with the elastomer material (EPDM 50 ShA) selected. Dynamic characterization tests of manufactured prototypes were conducted in Bayrak Plastic. Finally, frequency dependent dynamic stiffness and loss factor were compared with the analysis results.

According to the results, dynamic properties, both in axial and radial directions were good agreement with the analyses results. There were approximate differences between average test values and analyses results for axial dynamic stiffness %10-15, for axial loss factor under %5, for radial dynamic stiffness %3, and for radial loss factor %5 within the 0 – 200 Hz frequency range. Factors that could lead to these small differences between test and analysis results were explained comprehensively in the last part of the *Chapter 8*. To summarize, differences between mixture preparations of EPDM 50ShA tensile specimen and same material used in the isolator, crystallization of the elastomeric materials at low temperatures, different excitation types during the material characterization and isolator tests, preload effect of vibration block in material characterization, assumption of tensile deformation mode during the isolator's operation and lastly manufacturing errors might have caused the small variances between the test and analyses results.

9.2 FUTURE WORK

In this thesis, a methodology was developed for designing conical elastomeric vibration isolators in desired dynamic properties. In this way, after accomplishing dynamic characterization of any elastomeric material, using similar approach, any elastomeric vibration isolator can be designed with this material. This methodology can be improved with respect to some issues.

In this design process, dynamic characterizations of the elastomeric material specimens were done using a random excitation input. However, dynamic properties of the elastomeric materials can change with dynamic operating amplitude causing strains higher than %0.1. Therefore, in order to satisfy strain values below this, sine sweep excitation can be better. Using sine sweep excitation with an amplitude below a certain value (maximum amplitude which makes the strain values of the specimen %0.1), desired stable dynamic properties of the elastomeric material specimen can be accomplished. If design process of the vibration isolator is achieved with these properties of the elastomeric material and manufactured,

dynamic characterization of the isolator should be done with sine sweep in order to compare test and analyses results effectively.

Dynamic properties of the elastomeric materials change with static preload. In this design method, elastomeric vibration isolator design was done without preload. In order to add the effect of preload, material characterization tests should be conducted according to that. For this purpose, a different material characterization test system should be designed. Additionally, to do that, studies related to relationship between preload values of the material characterization and vibration isolator tests.

REFERENCES

- [1] Handbook of Viscoelastic Vibration Damping, David I. G. Jones, D/Tech Systems, Chandler, John Wiley & Sons, LTD, Arizona, USA, 2001.
- [2] METU, Mechanical Engineering Department, "ME708 - Techniques for Vibration Control and Isolation" lecture notes, 2010 – 2011 first semester.
- [3] Lord User's Guide, Lord Corporation, 2000, USA
- [4] Roylance, David (2001). Engineering Viscoelasticity. Cambridge, MA 02139: Massachusetts Institute of Technology. 8-11.
- [5] Li, Q.M. (2001), Strain energy density failure criterion, International Journal of Solids and Structures 38, pp. 6997–7013.
- [6] Alan N. Gent, "Engineering with rubber – how to design rubber components", Hanser Verlag, 2001.
- [7] Marc A. Meyers and Krishan Kumar Chawla, "Mechanical Behavior of Materials," 98-103, Prentice Hall, (1999).
- [8] McCrum, Buckley, and Bucknell (2003): "Principles of Polymer Engineering," 117-176, Oxford University Press, USA; 2 edition (November 27, 1997)
- [9] Roylance, David (2001); "Engineering Viscoelasticity", 14-15, Department of Materials Science and Engineering, Massachusetts Institute of Technology, Cambridge.
- [10] Bergström, J., Rimnac, C., & Kurtz, S. (2005). Molecular Chain Stretch is a Multiaxial Failure Criterion for Conventional and Highly Crosslinked UHMWPE. Journal of Orthopaedic Research, Volume 23, issue 2, 367-375.
- [11] Volokh, K. Y. (2007). Hyperelasticity with Softening for Modeling Materials Failure. Journal of the Mechanics and Solids, Volume 55, issue 10, 2237-2264.
- [12] Gent, A. N., & Chang, T. Y. (1993). Fracture and Fatigue of Bonded Rubber Blocks Under Compression. Engineering Fracture Mechanics, Volume 44, issue 6, 843-855.

- [13] Srinath, L. S. (2009). *Advanced Mechanics of Solids* (p. 114). Delhi: Tata McGraw-Hill Publishing Company Limited.
- [14] Fatt, M. S., & Bekar, I. (2004). High Speed Testing and Material Modeling of Unfilled Styrene Butadiene Vulcanizates at Impact Rates. *Journal of Materials Science*, Volume 39, issue 23, 6885-6899.
- [15] Rivin, I. Eugene (2003). *Passive Vibration Isolation*. New York, ASME Press.
- [16] Low Profile Mounts, 6300/6550 Mounts Catalog, Barry Controls. Retrieved May 10, 2012, from <http://www.barrycontrols.com/>
- [17] Industrial Catalog, Conical Vibration Isolator, Laspar. Retrieved May 10, 2012 <http://www.laspar.com.tr/>
- [18] R. C. Frampton, *The Dynamic Testing of Elastomers*. Retrieved June 5, 2012 <http://www.alphatestingsystems.com/>
- [19] N. Gil-Negrete, J. Vinolas, L. Kari (2006). A simplified methodology to predict the dynamic stiffness of carbon-black filled rubber isolators using a finite element code. *Journal of Sound and Vibration* 296 (2006) 757-776.
- [20] Clemens A. J. Beijers & Andre de Boer (2003). *Numerical Modeling of Rubber Vibration Isolators*. Tenth International Congress on Sound and Vibration.
- [21] Mustafa E. Levent & Kenan Y. Sanliturk (2003). *Characterization of Vibration Isolators Using Vibration Test Data*. Tenth International Congress on Sound and Vibration.
- [22] Mineo Takayama & Keiko Morita (2000). *Finite Element Analysis of Natural Rubber Isolators*, Department of Architecture, Fukuoka University, Japan.
- [23] Anders K. Olsson (2007). *Finite Element Procedures in Modeling the Dynamic Properties of Rubber*, Doctoral Thesis, Department of Construction Sciences, Lund University, Sweden.
- [24] ANSYS Mechanical APDL Programmer's Manuel, ANSYS, Inc. 2008.
- [25] D.E. Newland, "An Introduction to Random Vibrations, Spectral Analysis and Wavelet Analysis", 3rd Edition, Prentice-Hall, 1993

APPENDIX A

ELASTOMER MATERIAL PROPERTIES

A.1 PROPERTIES OF THE TESTED ELASTOMERS FOUND IN THE LITERATURE

Table A.1 Silicone rubber sheet mechanical properties [6]

Durometer (Shore A)	50	80
Tensile strength (MPa)	5.5	5.0
Ultimate elongation (%)	310	225

Table A.2 Commercial EPDM sheet mechanical properties [6]

Durometer (Shore A)	50	70
Tensile strength (MPa)	4.1	5.5
Ultimate elongation (%)	250	200

Table A.3 Commercial Neoprene sheet mechanical properties [6]

Durometer (Shore A)	50	80
Tensile strength (MPa)	5.5	6.9
Ultimate elongation (%)	300	100

A.2 MASTER CURVES OF SELECTED ELASTOMERS

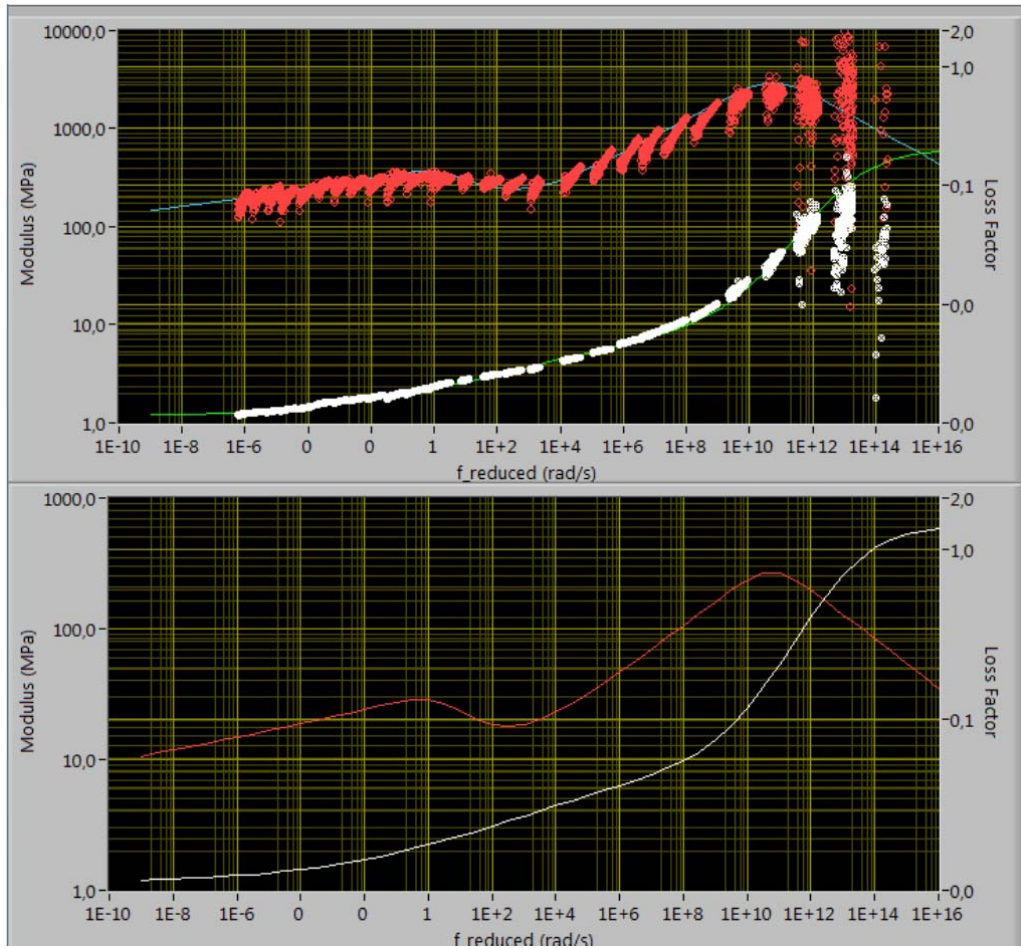


Figure A.1 Master curves of EPDM 50ShA shear sample

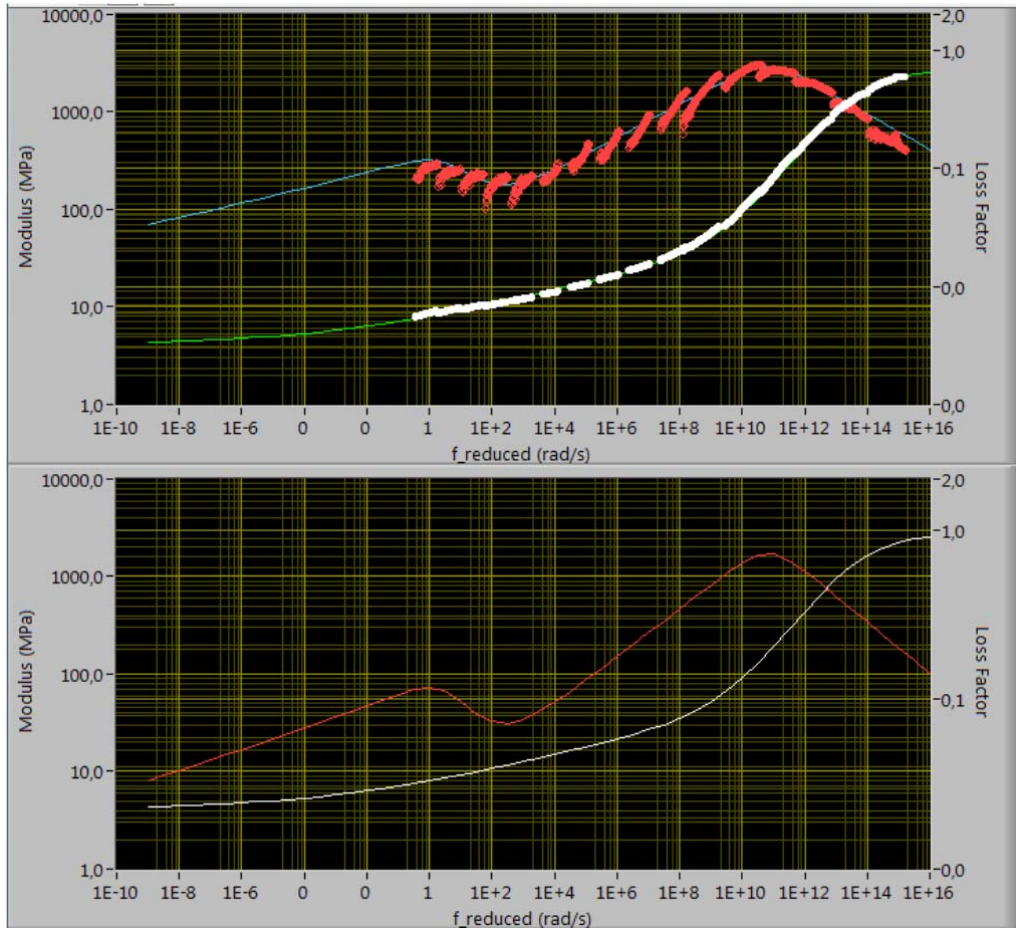


Figure A.2 Master curves of EPDM 50ShA tensile sample

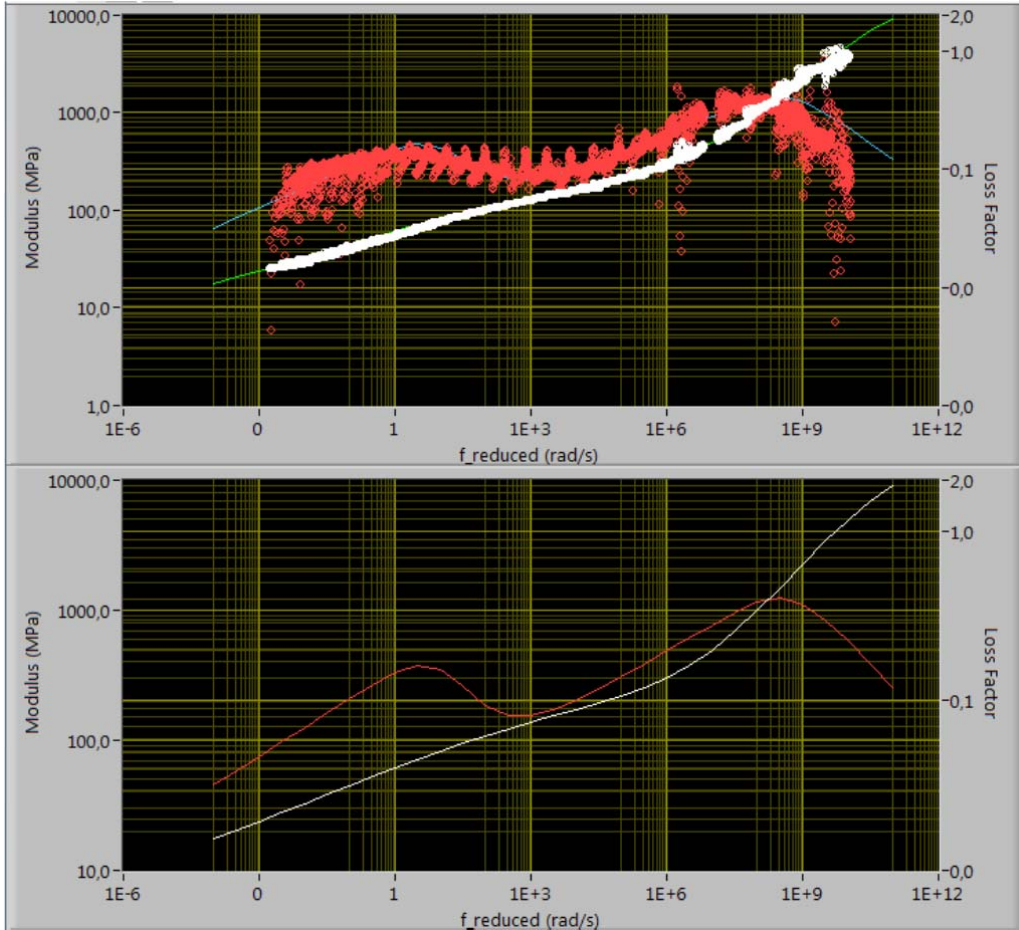


Figure A.3 Master curves of EPDM 80ShA tensile sample

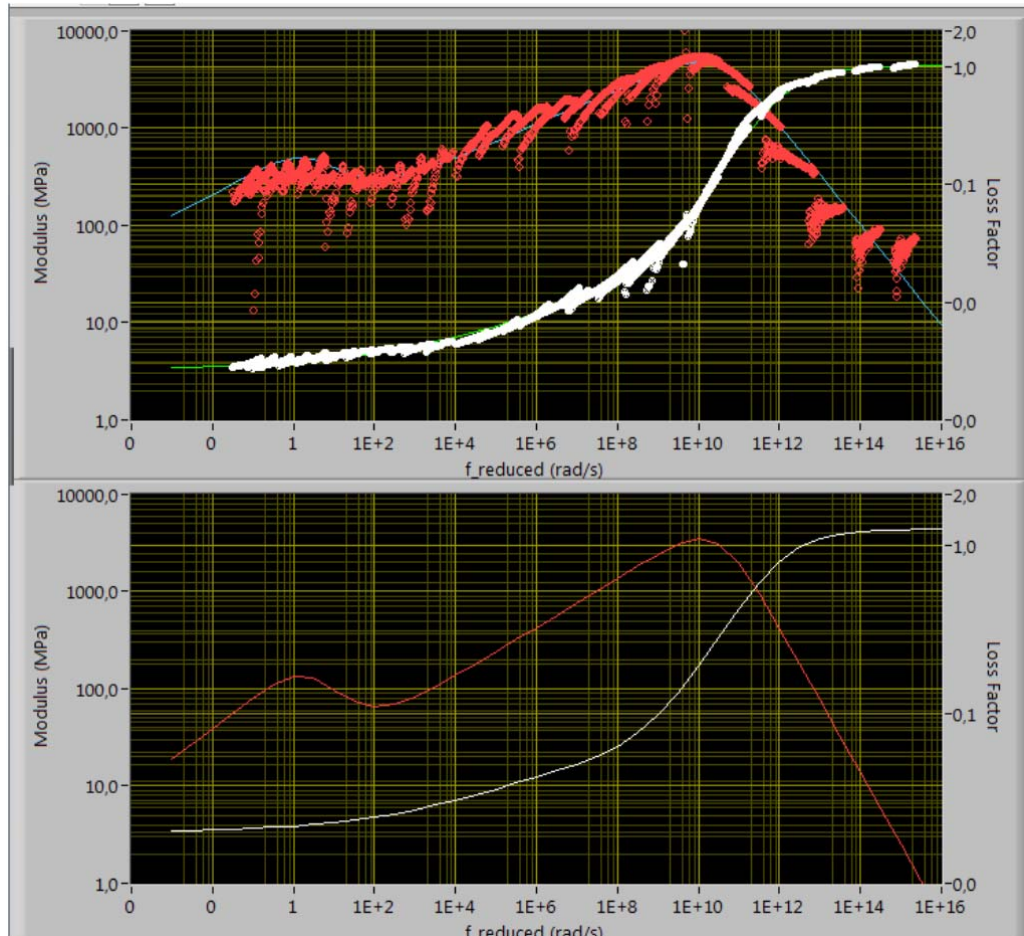


Figure A.4 Master curves of Neoprene 50ShA tensile sample

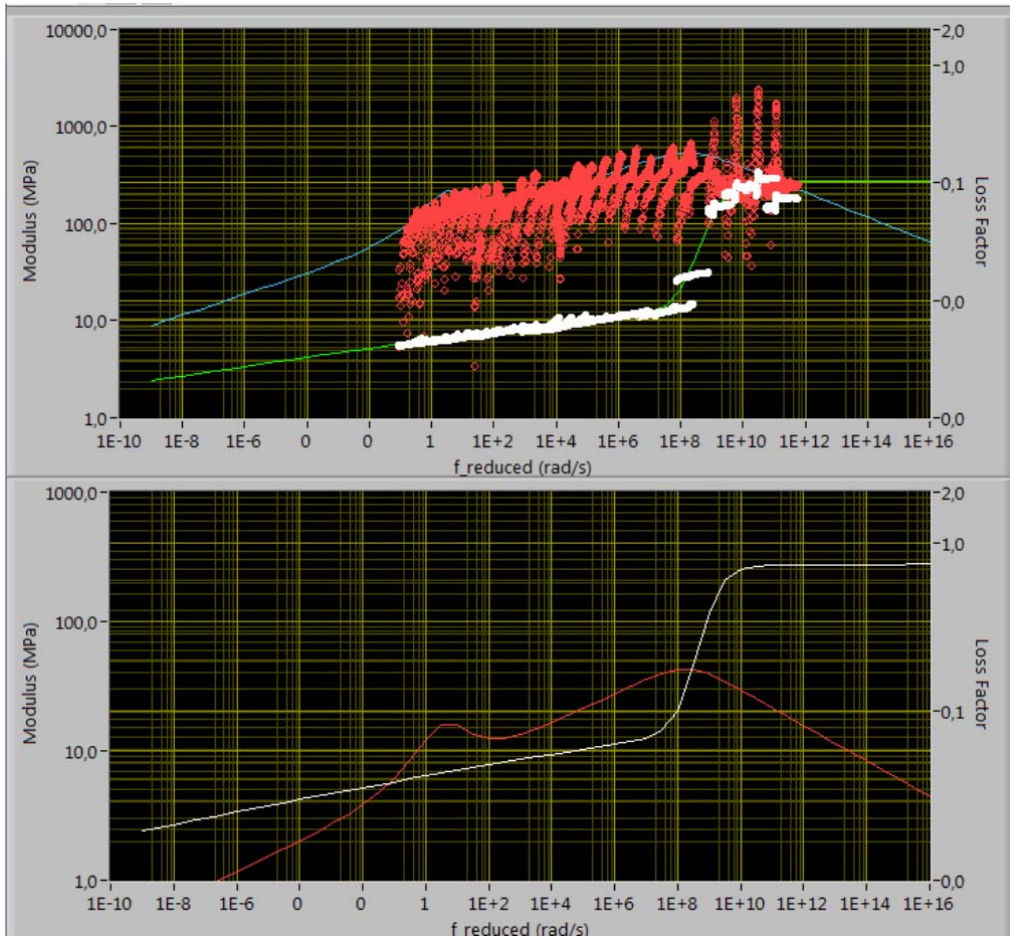


Figure A.5 Master curves of Silicone 50ShA tensile sample

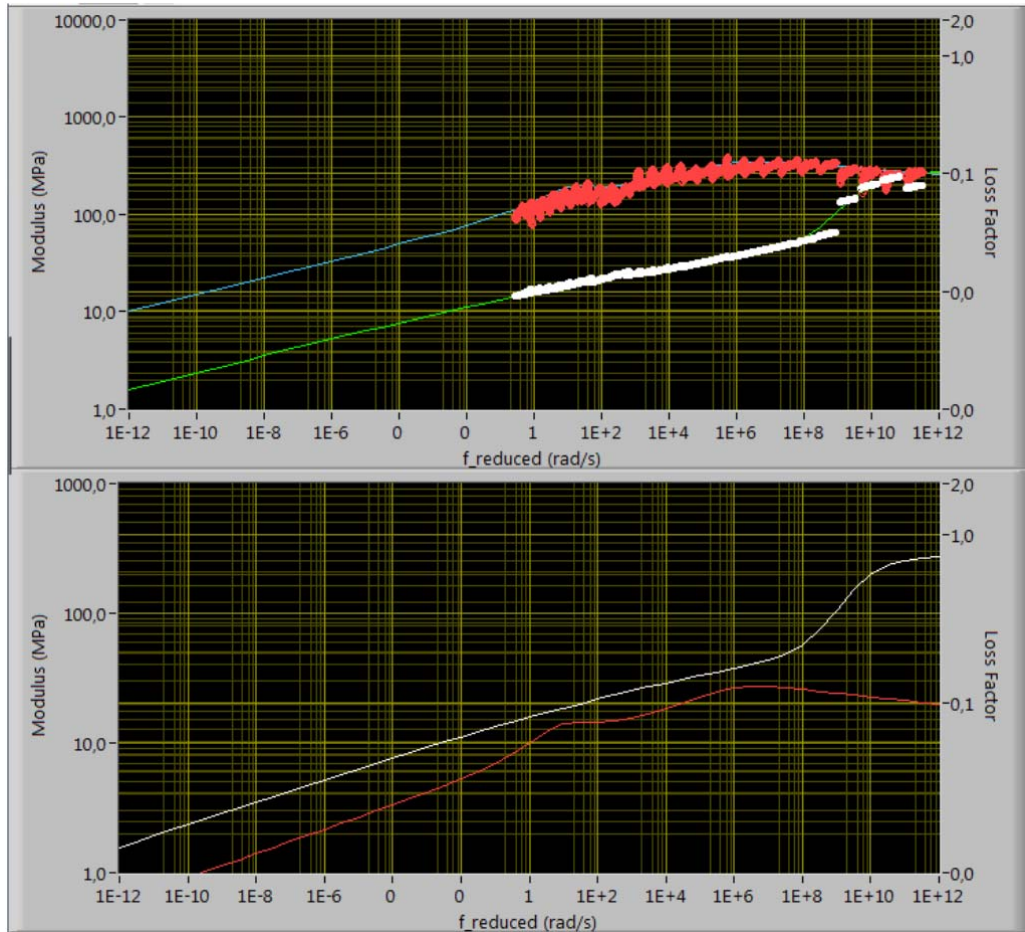


Figure A.6 Master curves of Silicone 80 ShA tensile sample